PHASE II BIOTRANSFORMATION OF XENOBIOTICS IN POLAR BEAR (*Ursus maritimus*) AND CHANNEL CATFISH (*Ictalurus punctatus*)

By

JAMES C. SACCO

A DISSERTATION PRESENTED TO THE GRADUATE SCHOOL
OF THE UNIVERSITY OF FLORIDA IN PARTIAL FULFILLMENT
OF THE REQUIREMENTS FOR THE DEGREE OF
DOCTOR OF PHILOSOPHY

UNIVERSITY OF FLORIDA

2006

This document is dedicated to Denise and my parents.

ACKNOWLEDGMENTS

First and foremost, I would like to thank my mentor, Dr. Margaret O. James, for her instruction, guidance, and support throughout my PhD program. Through her excellent scientific and mentoring skills I not only managed to complete several interesting studies but also rekindled my scientific curiosity with regards to biotransformation and biochemistry in general. I greatly appreciate the advice and instruction of Ms. Laura Faux, our laboratory manager, on enzyme assays, HPLC, and fish dissection. The assistance and advice of Dr. David S. Barber, Mr. Alex McNally, and Mr. Jason Blum at the Center for Human and Environmental Toxicology in walking me through the complexities of molecular cloning are much appreciated. Academic discussions with Dr. Liquan Wang, Dr. Ken Sloan, Dr. Joe Griffitt and Dr. Nancy Denslow also helped me to interpret my results and design better experiments accordingly.

Last but not least, I would like to thank my fiancée, Denise, and my parents, for their support and encouragement throughout my doctoral studies.

TABLE OF CONTENTS

LIST OF TABLES

LIST OF FIGURES

Abstract of Dissertation Presented to the Graduate School
of the University of Florida in Partial Fulfillment of the
Requirements for the Degree of Doctor of Philosophy

PHASE II BIOTRANSFORMATION OF XENOBIOTICS BY POLAR BEAR (*Ursus maritimus*) AND CHANNEL CATFISH (*Ictalurus punctatus*)

By

James C. Sacco

August 2006

Chair: Margaret O. James
Major Department: Medicinal Chemistry

Both polar bears and channel catfish are subject to bioaccumulation of persistent toxic environmental pollutants including hydroxylated compounds, which are potential substrates for detoxification via phase II conjugative processes such as sulfonation and glucuronidation. The objectives of this dissertation were to (a) study the capability of polar bear liver to sulfonate a structurally diverse group of environmental chemicals, and to study the glucuronidation of 3-OH-B[a]P; (b) study the effects of chlorine substitution pattern on the glucuronidation of polychlorinated biphenylols (OH-PCBs) by catfish liver and proximal intestine; (c) clone UDP-glucuronosyltransferase (UGT) from catfish liver and intestine; (d) develop a method to determine physiological concentrations of UDP-glucuronic acid (UDPGA) in catfish liver and intestine.

In the polar bear, the efficiency of sulfonation decreased in the order 3-OH-B[a]P>>>triclosan>>4′-OH-PCB79>OHMXC>4′-OH-PCB165>TCPM>4′-OH-PCB159 >PCP, all of which produced detectable sulfate conjugates. Substrate inhibition was

observed for the sulfonation of 3-OH-B[a]P and 4′-OH-PCB79. The hexachlorinated OH-PCBs, TCPM and PCP were poor substrates for sulfonation, suggesting that this may be one reason why these substances and structurally similar xenobiotics persist in polar bears.

OH-PCBs are glucuronidated with similar efficiency by channel catfish liver and proximal intestine. There were differences in the UGT activity profile in both organs. Both hepatic glucuronidation and intestinal glucuronidation were decreased with the addition of a second chlorine atom flanking the phenolic group, which is an arrangement typical of toxic OH-PCBs that persist in organisms.

One full length UGT from catfish liver, together with a full-length UGT (identical to the liver UGT), and a partial sequence of a different UGT from catfish intestine were cloned. The full-length catfish UGT clone appeared to be analogous to mammalian UGT1A1 or UGT1A6.

The anion-exchange HPLC method developed to determine UDPGA was sensitive, reproducible and displayed good resolution for the co-substrate. The hepatic UDPGA levels determined by this method were similar to those in other mammalian species and higher than reported for two other fish species. This was the first time intestinal UDPGA concentrations in any piscine species were determined; the values were similar to rat intestine, but significantly higher than in human small intestine.

CHAPTER 1
BIOTRANSFORMATION AND ITS IMPORTANCE IN THE DETOXIFICATION OF XENOBIOTICS

The exposure of biological systems to environmental compounds which may be potentially toxic to these systems has spurred the evolution of an elaborate, protective biochemical system whereby these xenobiotics are eliminated from cells and whole organisms, usually via chemical transformation (or biotransformation). This system is composed of a multitude of enzymes, which while being distributed in many tissues and organs, are principally located in organs such as liver, intestine and lungs. This is of physiological significance since these tissues represent major routes of xenobiotic entry into organisms. Within cells, biotransformation enzymes also display a level of organization in that while some are soluble and found in the cytosol (e.g. sulfotransferases (SULT), glutathione-S-transferases), others are relatively immobile and membrane-bound (e.g. UDP-glucuronosyltransferases (UGT) and cytochrome P450s (CYP) in the endoplasmic reticulum).

Since it is highly improbable that the organism has a substrate-specific enzyme for metabolizing every potential xenobiotic, biotransformation enzymes are generally non-specific, acting on a broad range of structurally unrelated substrates. In addition, several isoforms of the same enzyme (or more than one enzyme) may catalyze product formation from the same substrate, albeit at different rates and with different affinities. Enzymes in the same superfamily as those that act upon xenobiotics can also biotransform endogenous substances, indicating an equally important regulatory role for these

enzymes. This interrelationship between different enzymes and substrates can be illustrated by the metabolism of β-estradiol in humans, which can be biotransformed both via sulfonation (SULT1E1, which also acts on 7-hydroxymethyl-12-dimethylbenz-anthracene, the product of CYP450-catalyzed hydroxylation of 7,12-dimethyldibenz-anthracene (Glatt et al., 1995)) and glucuronidation (UGT1A1, which can also conjugate 1-naphthol (Radominska-Pandya et al., 1999)).

While these enzymes mainly represent a cellular defense mechanism against toxicity, occasionally procarcinogenic and protoxic xenobiotics are metabolized to active metabolites that attack macromolecules such as DNA, proteins and lipids.

In exposed organisms, metabolism is an important factor in determining the bioaccumulation, fate, toxicokinetics, and toxicity of contaminants. The majority of the compounds of interest to this study are derived from Phase I metabolism of environmental pollutants. These metabolites have been shown to have toxic effects both *in vitro* and *in vivo*, effects that can be eliminated by Phase II biotransformation (Chapter 2). In addition, contaminant exposure can result in the induction or inhibition of both Phase I and Phase II enzymes. For example, induction of CYP 1A (e.g., by polyaromatic hydrocarbons (PAHs) or co-planar polychlorinated biphenyls (PCBs)), CYP 2B and CYP3A (e.g., by *o*-chlorine substituted PCBs) will lead to increased formation of hydroxylated metabolites. Thus, a balance between the CYP and conjugative Phase II enzymes, sometimes directly mediated by the xenobiotic substrates and/or their metabolites, is responsible for either the detoxification or the accumulation of toxic metabolites in the body. The final removal of these metabolites from the cell is brought about by several different groups of membrane proteins (e.g., organic anion transport

protein (OATP), multidrug-resistance associated protein (MRP)), a process sometimes referred to as Phase III biotransformation (Figure 1-1).

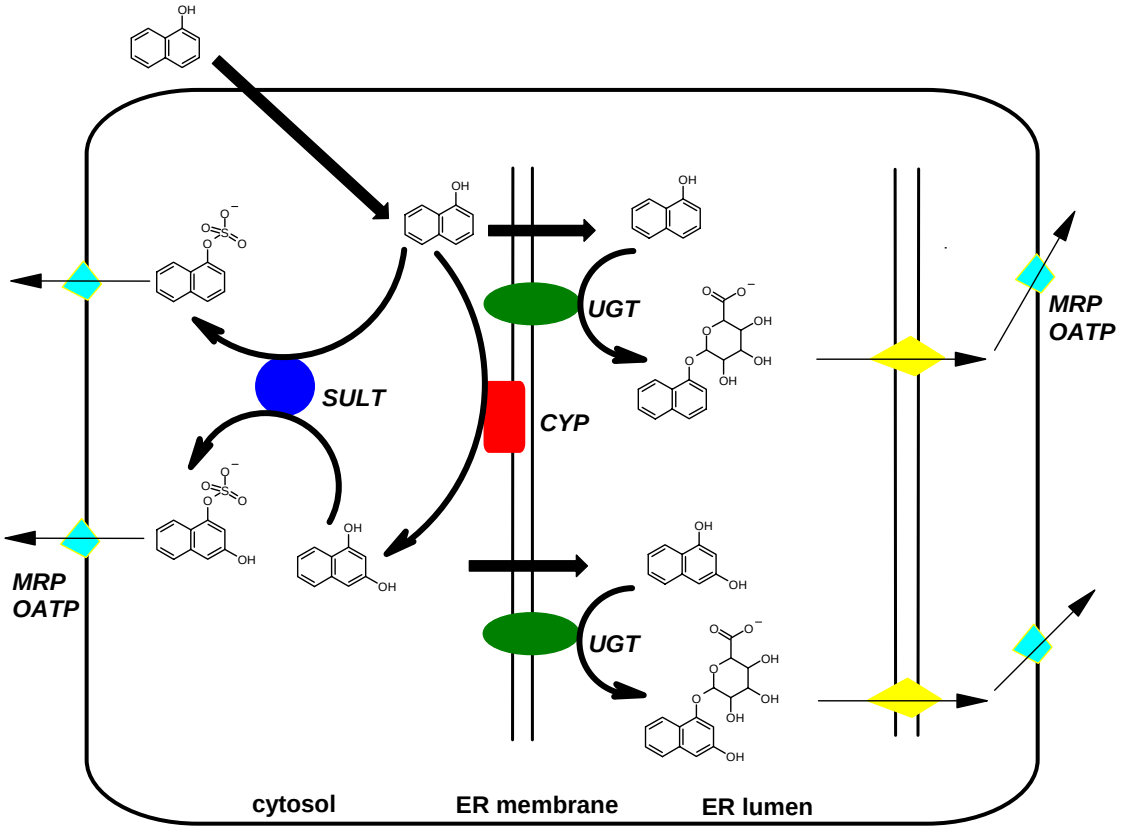

Figure 1-1. Schematic of select xenobiotic (represented by hydroxynaphthalene) biotransformation pathways in the mammalian cell. For abbreviations see text.

CHAPTER 2
PHASE II CONJUGATION: GLUCURONIDATION AND SULFONATION

Biotransformation has been conveniently categorized into two distinct phases. While the consecutive numbering of these processes implies a sequence, this is not always the case and the extent of involvement of both phases in the metabolism of a compound depends on both its chemical structure and physical properties. Phase I biotransformation usually consists of oxidations carried out largely by CYP enzymes and flavin monooxygenases and hydrolysis reactions executed by ester hydrolase, amidase and epoxide hydrolase (EH). A variety of chemical moieties can be conjugated to suitable acceptor groups on xenobiotics as part of Phase II biotransformation, including glucuronic acid (UGT), sulfonic acid (SULT), glutathione (GST), amino acids, and an acetyl group (N-acetyltransferase).

With the exception of acetylation, methylation and fatty acid conjugation, the strategy of Phase II biotransformation is to convert a xenobiotic to a more hydrophilic form via the attachment of a chemical moiety which is ionizable at physiological *p*H. The resulting anionic conjugate is then readily excreted in bile, feces, or urine, and is generally unable to undergo passive penetration of cell membranes. This metabolic transformation also results in reduced affinity of the compound for its cellular target. Enterohepatic recycling may result in the hydrolysis of biliary excreted conjugates and the regeneration of the parent compound, which is then subject again to biotransformation after being reabsorbed through the gut mucosa. In a few cases, the

conjugate is pharmacologically active, as in the case of morphine-6-glucuronide (Yoshimura et al., 1973) and minoxidil sulfate (Buhl et al., 1990).

The moieties attached to the xenobiotic in the case of sulfonation and glucuronidation are a sulfonate group (pK_a 2) or glucuronic acid (pK_a 4-5). The co-substrates which supply these highly polar species are, respectively, 3′-phosphoadenosyl-5′-phosphosulfate (PAPS) and uridine 5′-diphosphoglucuronic acid (UDPGA) (Figure 2-1). The mechanism of both reactions, which occurs as a ternary complex, is a S_N2 reaction, the deprotonated acceptor group of the substrate attacking the sulfur in the phosphosulfate bond of PAPS, or the C_1 of the pyranose ring to which UDP is attached in an α-glycosidic bond in the case of UDPGA. The resulting conjugates are then released. PAP and UDP also leave the enzyme's active site and are subsequently regenerated.

There may be competition for the same acceptor group, especially for phenols. Other acceptor groups that can be conjugated by both processes include alcohols, aromatic amines and thiols. Glucuronidation is also active on other functional groups, including carboxylic acids, hydroxylamines, aliphatic amines, sulfonamides and the C_2 of 1,3-dicarbonyl compounds. SULTs are generally high-affinity, low-capacity biotransformation enzymes that operate effectively at low substrate concentrations. Thus, typical K_ms for the sulfonation of xenobiotic substrates are usually significantly lower than K_ms for the same substrates undergoing biotransformation by the low-affinity, high-capacity UGTs. For example, kinetic parameters for the sulfonation and glucuronidation of the antimicrobial agent triclosan in human liver are K_m values of 8.5 and 107 μM and V_{max} of 96 and 739 pmol/min/mg protein respectively (Wang et al., 2004).

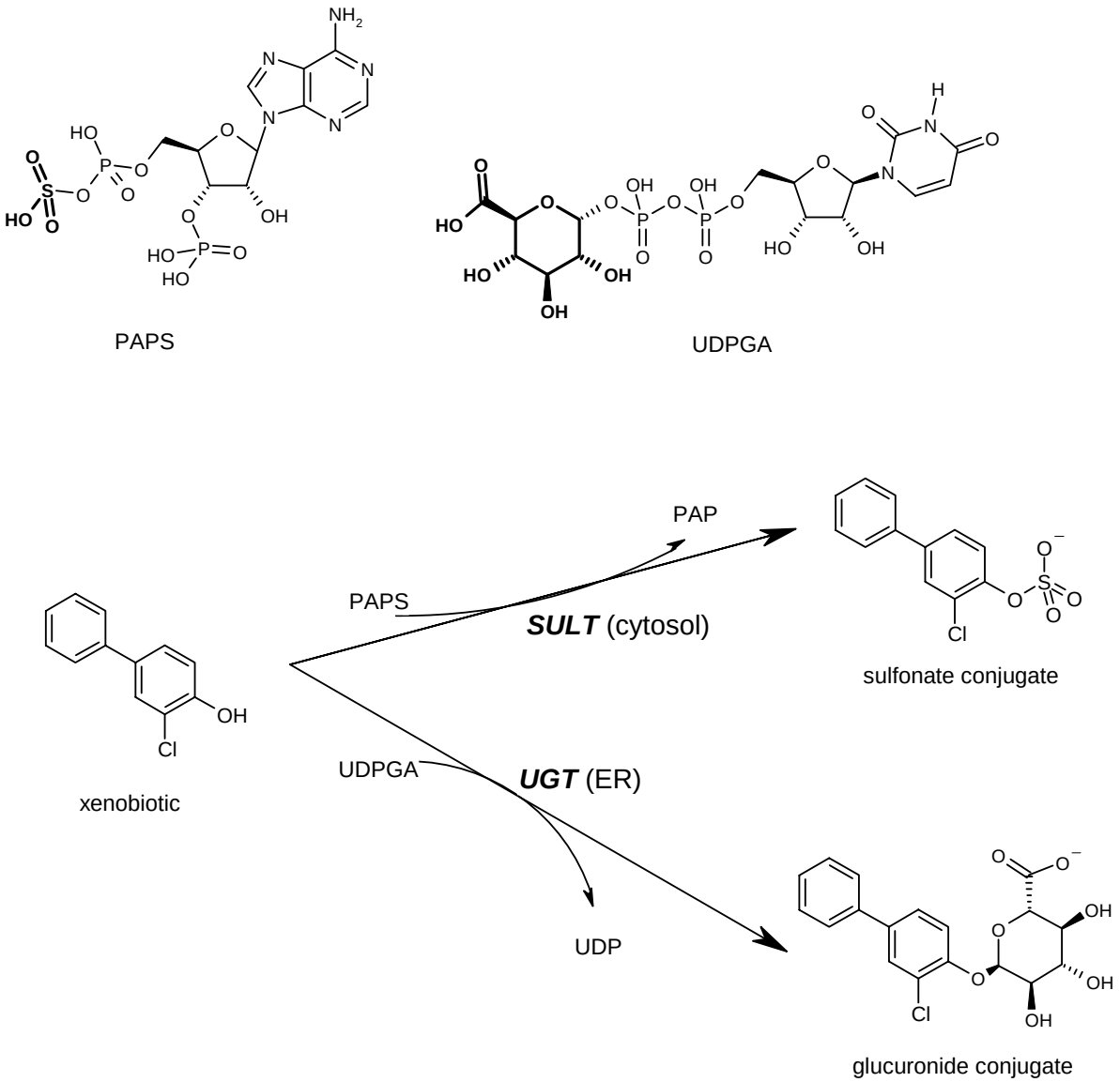

Figure 2-1. Structure of the co-substrates PAPS and UDPGA (transferred moieties shown in bold) and the formation of the polar sulfonate and glucuronide conjugates, shown here competing for the same substrate.

UDP-Glucuronosyltransferases (UGTs)

The primary sequence of human UGTs ranges from 529 to 534 amino acids in length (Tukey and Strassburg 2000). These 50-56 kDa proteins reside in the endoplasmic reticulum, whereby the amino terminus and around 95% of the subsequent residues are located in the lumen. A 17-amino acid-long transmembrane segment connects the lumenal part of the enzyme with the short (19-24 residues) carboxyl-terminus located in the cytosol (Figure 2-2). The active enzyme probably consists of dimers, linked together at the C-terminus (Meech and Mackenzie 1997). The existence of tetramers for the formation of the diglucuronide of B[a]P-3,6-diphenol has been suggested (Gschaidmeier and Bock 1994).

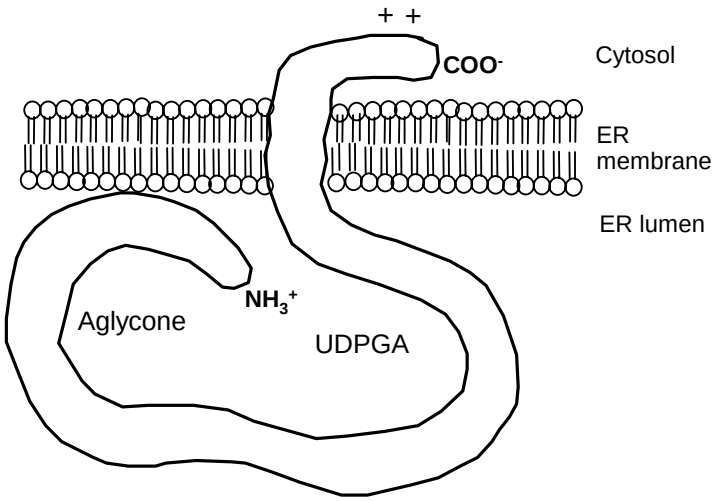

Figure 2-2. Proposed structure of UGT, based on amino acid sequence

Based on evolutionary divergence, mammalian UGTs have been classified into four distinct families (Mackenzie et al., 2005): family 1, which includes bilirubin, thyroxine and phenol UGTs; family 2, which includes steroid UGTs; family 3, which includes UGTs whose substrate specificity is, as yet, unknown (Mackenzie et al., 1997); family 8, represented by UGT8A1 which utilizes UDP-galactose as the sugar donor (Ichikawa et

al., 1996). Although the liver is the major site of glucuronidation in the living organism, several other tissues have been shown to express UGTs. The small intestine appears to be an equally important site of glucuronidation, particularly for ingested xenobiotics. In addition, expression of some UGT isoforms is tissue-specific (Table 2-1).

The nine family 1 UGT isoforms (UGT1) are all encoded by one gene that has multiple unique exons located upstream of four common exons on human chromosome 2q37 (Figure 2-3). The isoforms are generated by differential splicing of one unique first exon (which encodes two-thirds of the lumenal domain, starting from the N-terminus, 288 amino acids long) to the four common exons (exons 2-5, which encode the remainder of the lumenal domain, the transmembrane domain and the cytosolic tail, 246 amino acids long). Due to this unusual gene structure and splicing mechanism, the UGT1 isoforms have variable amino-terminal halves and identical carboxyl-terminal halves. While the first exon determines substrate specificity, the common exons specify the interaction with UDPGA (Ritter et al., 1992; Gong et al., 2001). Thus, the major bilirubin UGT (UGT1A1) of humans, rats and other species is encoded by exon 1 and the adjacent 4 common exons. The phenol UGT (UGT1A6) is encoded by exon 6 and the 4 common exons.

The human UGT2 gene family includes three members of the UGT2A subfamily and twelve members of the UGT2B subfamily (Mackenzie et al., 2005). The UGT2 proteins are encoded by separate genes consisting of six exons located on human chromosome 4q13. The region of the protein encoded by exons 1 and 2 is equivalent to that encoded by the unique exons 1 of the UGT1 isoforms, and the subsequent intron/exon boundaries are in corresponding positions in both gene families. Similar to

the UGT1A enzymes, the UGT2A1 and 2A2 proteins have identical C-termini and different N-termini that arise due to differential splicing of the first exon (Figure 2-4). By contrast, the UGT2A3 gene comprises six exons that are not shared with the other two.

Table 2-1. Expression of human UGT mRNA in various tissues[a]

UGT	Liver	Intestine	Esophagus & stomach	Kidney	Brain	Prostate	Other tissues
1A1	✓	✓	✓[b]				
1A3	✓	✓	✓[b]	✓		✓	
1A4	✓	✓					
1A6	✓	✓	✓[b]	✓	✓		testis, ovary
1A7[c]			✓				
1A8		✓	✓				
1A9	✓	✓		✓			
1A10[c]		✓	✓	✓			
2A1					✓		Olfactory epithelium, lung
2B4	✓	✓					
2B7	✓	✓	✓	✓	✓		Pancreas
2B10	✓		✓			✓	mammary gland,
2B11	✓			✓	✓	✓	mammary gland, adrenal, skin, adipose
2B15	✓		✓	✓		✓	mammary gland, adipose, skin, lung, testis, uterus, placenta
2B17						✓	

[a] Tukey and Strassburg 2000; King et al., 2000; Lin and Wong 2002; Wells et al., 2004
[b] only a third of the population expresses these isoforms in gastric epithelium (Strassburg et al., 1998)
[c] expressed in bile ducts

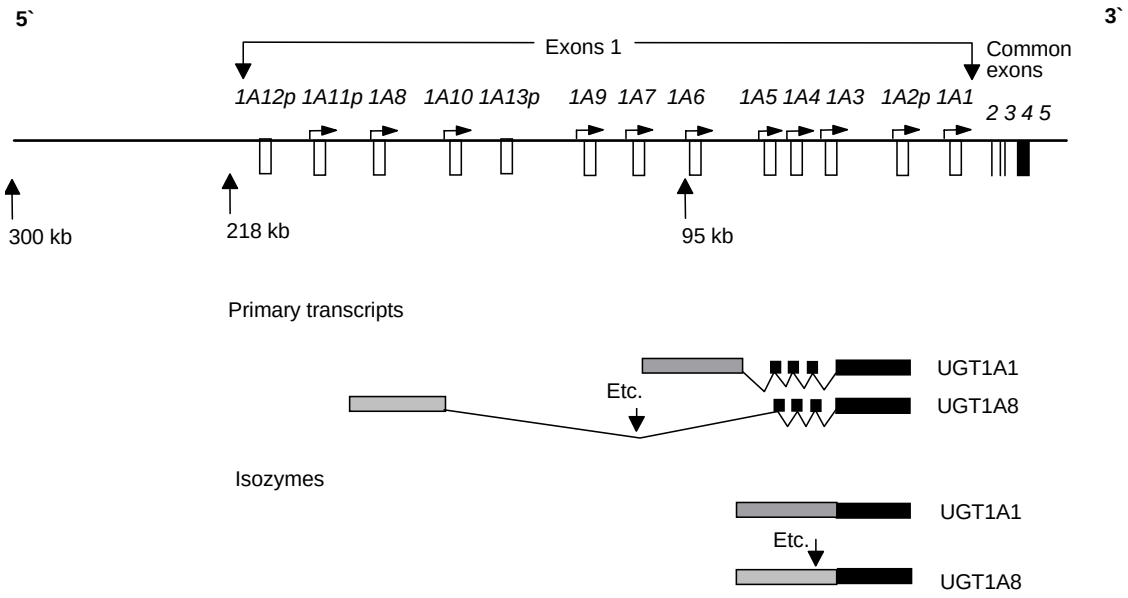

Figure 2-3. Complete human UGT1 complex locus represented as an array of 13 linearly arranged first exons.

Each first exon, except for the defective UGT1A12p and UGT1A13p pseudo ones, contains a 5´proximal TATA box element (bent arrow) that allows for the independent initiation of RNA polymerase activity that generates a series of overlapping RNA transcripts (Adapted from Gong et al., 2001).

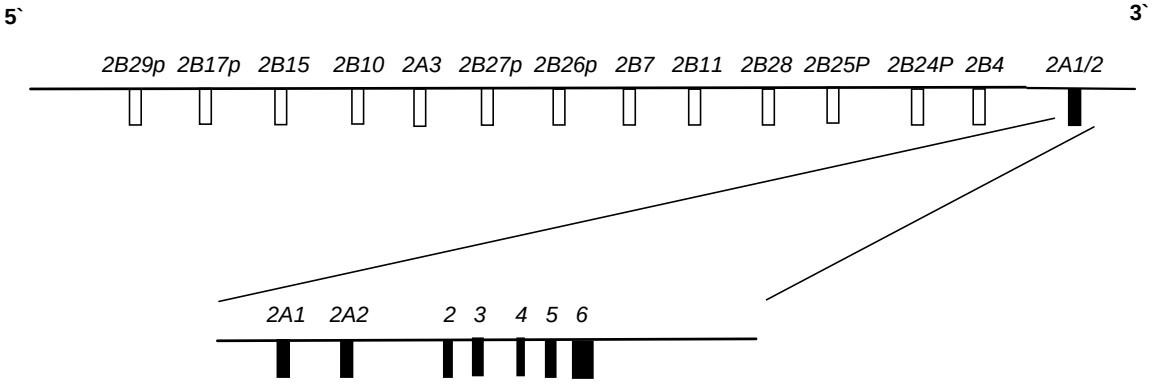

Figure 2-4. The human UGT2 family.

Each gene (not drawn to scale), consisting of six exons, is represented by a white rectangle, except for '2A1/2', which represents seven exons (1 unique first exon and shared exons 2-6). Adapted from Mackenzie et al. (2005).

Sulfotransferases (SULTs)

Sulfotransferases can be either membrane-bound in the Golgi or in the cytosol. While the membrane-bound SULTs sulfonate large molecules such as glucosaminylglycans, the cytosolic enzymes are involved in the inactivation of endogenous signal molecules (steroids, thyroid hormones, neurotransmitters) and the biotransformation of xenobiotics.

Each cytosolic SULT is a single α/β globular protein with a characteristic five-stranded parallel sheet, with α-helices flanking each sheet. The active enzyme is a homodimer, with each polypeptide chain having a MW of about 35,000. Kakuta et al. (1997) were the first group to solve the first X-ray structure for the SULT family. Mouse estrogen sulfotransferase (mEST) was shown complexed with PAP and the substrate estradiol (E2). The binding of estradiol to human SULT1A1 has also been demonstrated (Gamage et al., 2005). Both PAPS- and substrate-binding sites are located deep in the hydrophobic substrate pocket. The structures of four human cytosolic enzymes have also been elucidated: SULT 1A1 (Gamage et al., 2003), dopamine/catecholamine sulfotransferase (SULT1A3) (Bidwell et al., 1999; Dajani et al., 1999), hydroxysteroid sulfotransferase (SULT2A1; hHST) (Pedersen et al., 2000), and estrogen sulfotransferase (SULT1E1; hEST) (Pedersen et al., 2002).

Five SULT gene families have been identified in mammals (SULTs1-5). While SULT enzymes have different substrate specificities, the repertoire of suitable substrates is so broad that it is not uncommon that one substrate is biotransformed by more than one enzyme. SULTs are distributed in a wide variety of tissues (Table 2-2). In humans, liver cytosol has been shown to contain mostly SULTs1A1, 2A1, and 1E1, with lesser amounts

of SULTs 1A2, 1B1, 1E1 and 2A1. While SULT1A1 and SULT1E1 are responsible for most of the phenol and estrogen SULT hepatic activity respectively, SULT2A1 (hydroxysteroid SULT) shows greater affinity for alcohols and benzylic alcohols (Mulder and Jakoby, 1990; Glatt, 2002).

Table 2-2. Tissue distribution of SULTs (cDNA and mRNA) in humans[a]

SULT	Liver	Intestine	Esophagus & stomach	Kidney	Brain	Lung	Other tissues
1A1	✓	✓		✓	✓		Platelets
1A2	✓	✓		✓	✓	✓	
1A3		✓			✓		Platelets
1B1	✓	✓		✓	✓		Spleen, kidney, leukocytes
1C2				✓		✓[b]	Ovary, spinal cord, heart[a]
1C4	✓[b]		✓	✓	✓		Thyroid gland, ovary
1E1	✓	✓		✓[b]	✓	✓[b]	Endometrium, skin, mammary
2A1	✓	✓					Adrenal gland, ovary
2B1		✓	✓[c]		✓	✓	Placenta, prostate, platelets
4A1					✓		

[a] reviewed by Glatt 2002.
[b] mRNA of fetal tissues
[c] oral mucosa

Using 3-hydroxy-benzo(a)pyrene (3-OH-B[a]P) and 9-OH-B[a]P, the existence of multiple SULT isoforms in channel catfish liver and intestine, including a 3-methylcholanthrene-inducible form of phenol-SULT in liver, has been established (Gaworecki et al., 2004; James et al., 2001). The phenol-SULT in catfish liver and

intestine has been isolated as a 41,000 Da protein. A second protein with a molecular weight of 31,000 Da, isolated from liver, has not been identified to date. Interestingly enough, SULT activity with phenolic substrates is higher in intestine than liver (Tong and James 2000). Other hepatic SULTs isolated and characterized from fish include petromyzonol SULT from lamprey (*Petromyzon marinus*) larva (which displays 40% homology with mammalian SULT2B1a, or cholesterol SULT) and a bile steroid SULT from the shark *Heterodontus portusjacksoni* (Venkatachalam et al., 2004; Macrides et al., 1994).

CHAPTER 3
SULFONATION OF XENOBIOTICS BY POLAR BEAR LIVER

The lipophilicity and inherent chemical stability of persistent organic pollutants (POPs) renders them excellent candidates for absorption through biological membranes as well as accumulation in both organisms and their environment. Many POPs have been shown to biomagnify in food webs to potentially toxic levels in top predators such as the polar bear (*Ursus maritimus*), whose diet mainly consists of ringed seal (*Phoca hispida*) blubber (Kucklick et al., 2002).

Since the sulfonation of xenobiotics has never been studied in the polar bear, the objective of this study was to investigate the efficiency of this route of detoxification on a select group of known environmental pollutants: 4′-hydroxy-3,3′,4,5′-tetrachlorobiphenyl (4′OH-PCB79), 4′-hydroxy-2,3,3′,4,5,5′-hexachlorobiphenyl (4′-OH-PCB159), 4′-hydroxy-2,3,3′,5,5′,6-hexachlorobiphenyl (4′-OH-PCB165), pentachlorophenol (PCP), tris(4-chlorophenyl)-methanol (TCPM), 2-(4-methoxyphenyl)-2-(4-hydroxyphenyl)-1,1,1-trichloroethane (OHMXC), 3-hydroxybenzo(a)pyrene (3-OH-B[a]P), triclosan (2,4,4′-trichloro-2′-hydroxydiphenyl ether) (Figure 3-1). The OH-PCBs were named as PCB metabolites, according to the convention suggested by Maervoet et al. (2004).

Polychlorinated biphenylols (OH-PCBs), major biotransformation products of PCBs (James, 2001), have been shown to be present in relatively high concentrations in polar bears (Sandau and Norstrom 1998; Sandau et al., 2000). The abundance of these hydroxylated metabolites may be due to CYP induction (Letcher et al., 1996), inefficient

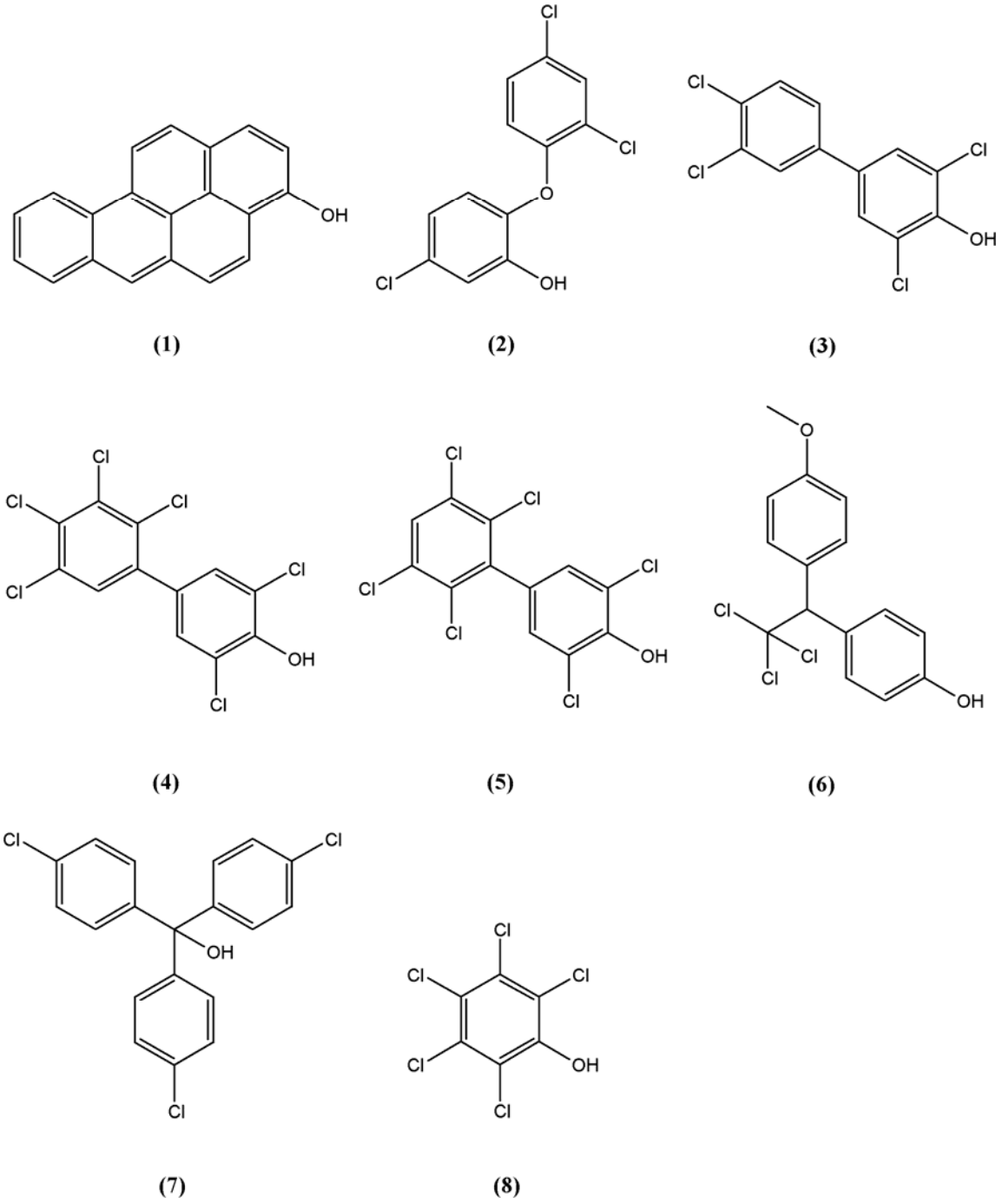

Figure 3-1. Structures of sulfonation substrates investigated in this study.

(1) 3-OH-B[a]P; (2) triclosan; (3) 4′-OH-PCB79; (4) 4′-OH-PCB159; (5) 4′-OH-PCB165; (6) OHMXC; (7) TCPM; (8) PCP. Full names of each compound are given in the text.

Phase II detoxication, and inhibition of their own biotransformation. The 4′-OH-PCB79 (an oxidation product of PCB congener 77) is a potent inhibitor of the sulfonation of several substrates, including 3-OH-B[a]P in channel catfish intestine and human liver (van den Hurk et al., 2002, Wang et al., 2005), 4-nitrophenol by human SULT1A1 (Wang et al., 2006), 3,5-diiodothyronine (T_2) in rat liver (Schuur et al., 1998), and estradiol by human SULT1E1 (Kester et al., 2000). Both 4′-OH-PCB159 and 4′-OH-PCB165 have been shown to inhibit the sulfonation of 3-OH-B[a]P and 4-nitrophenol by human SULT (Wang et al., 2005, 2006). Another compound detected in polar bears is PCP (Sandau and Norstrom 1998), a commonly used wood preservative that has been implicated in thyroid hormone disruption in Arctic Inuit populations (Sandau et al., 2002). TCPM is a globally distributed organochlorine compound of uncertain origin, which was reported in human adipose tissue (Minh et al., 2000). Polar bear liver contains 4000-6800 ng/g lipid weight TCPM, the highest levels recorded for this compound in all species studied (Jarman et al., 1992). TCPM is a potent androgen receptor antagonist *in vitro* (Schrader and Cooke 2002). OHMXC, formed by demethylation of the organochlorine pesticide methoxychlor, is an estrogen receptor (ER) α agonist, an ERβ antagonist and an androgen receptor antagonist (Gaido et al., 2000). The ubiquitous environmental pollutant benzo[a]pyrene is mainly metabolized to 3-OH-B[a]P, a procarcinogen that can be eliminated via sulfonation (Tong and James 2000). Together with its 7,8-dihydrodiol-9,10-oxide and 7,8-oxide metabolites, 3-OH-B[a]P can form adducts with macromolecules and initiate carcinogenesis (Ribeiro et al., 1986). Triclosan is an antimicrobial agent that has been detected in human plasma and breast milk (Adolfsson-Erici et al., 2002). *In vitro* studies

have shown that triclosan inhibits various biotransformation enzymes, including SULT and UDP-glucuronosyltransferases (UGT) (Wang et al., 2004).

The fact that 3-OH-B[a]P, triclosan, OHMXC, 4′-OH-PCB79, 4′-OH-PCB159 and 4′-OH-PCB165 have not been reported as environmental contaminants in polar bears to date may be due to non-significant levels in the Arctic environment or efficient metabolism via, for example, sulfonation. On the other hand, the presence of PCP and, particularly, high amounts of TCPM in these Arctic carnivores, may indicate poor sulfonation of these substrates. The polychlorobiphenylols 4′-OH-PCB159 and 4′-OH-PCB165 are of interest since though they have not been detected in polar bears, they are structurally similar to 4′-OH-PCB172, one of the major OH-PCBs found in polar bear plasma (Sandau et al., 2000). It is thus possible that these compounds are sulfonated with similar efficiencies. The other major Phase II biotransformation pathway for the above-mentioned compounds is glucuronidation. Polar bear liver efficiently glucuronidated 3-OH-B[a]P and several OH-PCBs (Sacco and James 2004).

Hypothesis

Sulfonation occurring in polar bear liver is an inefficient route of detoxification for a structurally diverse group of environmental contaminants.

Methodology

Unlabeled PAPS was purchased from the Dayton Research Institute (Dayton, OH). Uridine 5'-diphosphoglucuronic acid (UDPGA) was obtained from Sigma (St.Louis, MO). Radiolabeled [^{35}S]PAPS (1.82 or 3.56 Ci/mmol) was obtained from Perkin-Elmer Life Sciences, Inc. (Boston, MA). The benzo[a]pyrene metabolites 3-OH-B[a]P, B[a]P-3-O-sulfate and B[a]P-3-O-glucuronide were supplied by the Midwest Research Institute (Kansas City, MO), through contact with the Chemical Carcinogen Reference Standard

Repository of the National Cancer Institute. Dr. L.W.Robertson, U of Iowa, kindly donated the 4′-OH-PCB79, and 4′-OH-PCB159 and 4′-OH-PCB165 were purchased from AccuStandard, Inc. (New Haven, CT). PCP from Fluka Chemical (Milwaukee, WI) was used to prepare the water-soluble sodium salt (Meerman et al., 1983). Triclosan and sulfatase (Type VI from *Aerobacter*, S1629) were purchased from Sigma (St.Louis, MO), while methoxychlor and TCPM were purchased from ICN Biomedical (Aurora, OH) and Lancaster Synthesis, Inc. (Pelham, NH), respectively. The OHMXC was prepared by the demethylation of methoxychlor and purified by recrystallization (Hu and Kupfer 2002). Tetrabutyl ammonium hydrogen sulfate (PIC-A low UV reagent) was from Waters Corporation, Milford, MA. Other reagents were the highest grade available from Fisher Scientific (Atlanta, GA) and Sigma.

Animals. The samples used in this study were a kind donation from Dr. S. Bandiera (U British Columbia) and Dr. R. Letcher (Environment Canada). They were derived from the distal portion of the right lobe of livers of three adult male bears G, K and X. Bears G and K were collected as part of a legally-controlled hunt by Inuit in the Canadian Arctic in April 1993 near Resolute Bay, Northwest Territories, while bear X was collected in November 1993 near Churchill, Manitoba, just after the fasting period. Liver samples were removed within 10-15 minutes after death, cut into small pieces and frozen at -196ºC in liquid N_2. The samples were subsequently stored at -80ºC.

Cytosol and Microsomes Preparation. Prior to homogenization, the frozen polar bear liver samples (~2g) were gradually thawed in a few ml of homogenizing buffer. Homogenizing buffer consisted of 1.15% KCl, 0.05 M K_3PO_4 pH 7.4, and 0.2 mM phenylmethylsulfonyl fluoride, added from concentrated ethanol solution just before use.

Resuspension buffer consisted of 0.25 M sucrose, 0.01 M Hepes *p*H 7.4, 5% glycerol, 0.1 mM dithiothreitol, 0.1 mM ethylene diamine tetra-acetic acid and 0.1 mM phenylmethyl sulfonyl fluoride. The liver was placed in a volume of fresh ice-cold buffer equal to 4 times the weight of the liver sample. The cytosol and microsomal fractions were obtained using a procedure described previously (Wang et al., 2004). Microsomal and cytosolic protein contents were measured by the Lowry assay, using bovine serum albumin (BSA) as standard.

Sulfotransferase Assays

A. Fluorometric method. The activity was measured on the basis that at alkaline pH, the benzo[a]pyrene-3-O-sulfate has different wavelength optima for fluorescence excitation and emission (294/415 nm) from the benzo[a]pyrene-3-O-phenolate anion (390/545 nm) (James et al., 1997). Saturating concentrations of PAPS were determined by performing the assay at 1 μM 3-OH-B[a]P. The reaction mixture for detecting the sulfation of 3-OH-BaP by polar bear liver cytosol consisted of 0.1 M Tris-Cl buffer (*p*H 7.6), 0.4% BSA, PAPS (0.02 mM), 25 μg polar bear hepatic cytosolic protein, and 3-OH-B[a]P (0.05-25 μM) in a total reaction volume of 1.0 mL. SULT activity (pmol/min/mg) was calculated from a standard curve prepared with B[a]P-3-O-sulfate standards. Substrate consumption did not exceed 10%.

B. Radiochemical extraction method. This method, based on Wang and co-workers (2004), was employed in the study of the sulfonation of 4′-OH-PCB79, 4′-OH-PCB159, 4′-OH-PCB165, triclosan, PCP, TCPM and OHMXC. Cytosolic protein concentrations and incubation time were optimized for every test substrate to ensure that the reaction was linear during the incubation period. Substrate consumption did not exceed 5%. The

incubation mixture consisted of 0.1 M Tris-Cl buffer (*p*H 7.0), 0.4% BSA in water, 20 μM PAPS (10% labelled with ^{35}S), 0.1 mg polar bear hepatic cytosolic protein, or 0.005 mg in the case of 4′-OH-PCB79 and triclosan, and substrate in a total reaction volume of 0.1 mL, or 0.5 mL in the case of TCPM. The OH-PCBs, triclosan and OHMXC were added to tubes from methanol solutions, and the methanol was removed under N_2 prior to addition of other components. The TCPM was dissolved in DMSO, the solvent being present at a concentration not exceeding 1% in the final assay volume. Control determinations utilizing 1% DMSO had no inhibitory effect on sulfonation. Aqueous solutions of sodium pentachlorophenolate were utilized in the case of PCP. Tubes containing all components except the co-substrate were placed in a water bath at 37ºC and PAPS was added to initiate the reaction. Incubation times were 5 min (TCPM), 20 min (4′-OH-PCB79, triclosan), 30 min (PCP) and 40 min (OHMXC, 4′-OH-PCB159, 4′-OH-PCB165). The incubation was terminated by the addition of an equal volume of a 1:1 mixture of 2.5% acetic acid and PIC-A and water. The sulfated product was extracted with 3.0 mL ethyl acetate as described previously (Wang et al., 2004) and the phases were separated by centrifugation. Duplicate portions of the ethyl acetate phase were counted for quantitation of sulfate conjugates.

C. Radiochemical TLC method. Since the ethyl acetate phase contains sulfate conjugates formed from both the substrate of interest and substrates already present in polar bear liver, TLC was used to quantify substrate sulfation in cases where SULT activity was similar in samples and substrate blanks. After evaporating 2 ml of ethyl acetate extract from the SULT assay under N_2, the solutes were reconstituted in 40 μL methanol. For 4′-OH-PCB159, 4′-OH-PCB165, PCP and OHMXC, the substrate

conjugates were separated on RP-18F_{254s} reverse phase TLC plates with fluorescent indicator (Merck, Darmstadt, Germany) using methanol:water (80:20). For TCPM, Whatman $KC_{18}F$ reverse phase 200 μm TLC plates with fluorescent indicator in conjunction with a developing solvent system consisting of methanol:water:0.28 M PIC-A (40:60:1.9 by volume) were employed. Electronic autoradiography (Packard Instant Imager, Meriden, CT) was used to identify and quantify the radioactive bands separated on the TLC plate. The counts representing the substrate sulfate conjugate products were expressed as a fraction of the total radioactivity determined by scintillation counting, thus enabling the radioactivity due to the substrate conjugate to be accurately determined.

The identity of the conjugate of TCPM as a sulfate ester was verified by studying its sensitivity to sulfatase. Polar bear cytosol (0.5 mg) was incubated for 75 minutes with or without 200 μM TCPM. The incubation was terminated, and the product extracted into ethyl acetate as above. The ethyl acetate was evaporated to dryness and dissolved in 0.25 mL of Tris buffer, *p*H 7.5, containing 0 or 0.08 units of sulfatase. Following an overnight incubation at 35˚C, the reaction was stopped by the addition of methanol and the tubes were centrifuged. The supernatants were evaporated to dryness, reconstituted in methanol and analyzed by TLC as described above.

UDP-Glucuronosyltransferase Assay. The reaction mixture for detecting the glucuronidation of 3-OH-B[a]P by polar bear liver microsomes consisted of 0.1 M Tris-HCl buffer (*p*H 7.6), 5 mM $MgCl_2$, 0.5% Brij-58, UDPGA (4 mM), 5 μg polar bear hepatic microsomal protein, and 3-OH-B[a]P in a total reaction volume of 500 μL. The substrate, 3-OH-B[a]P in methanol, was blown dry under N_2 in the dark in a tube to which, after complete evaporation, a premixed solution of microsomal protein and Brij-

58 (in a 5:1 ratio) was added, vortexed, and left for 30 minutes on ice. Subsequently, the buffer and water were added in that order and vortex-mixed. Immediately preceding a 20-minute incubation at 37ºC, UDPGA was added to initiate the reaction. The reaction was terminated by the addition of 2 mL ice-cold methanol. Precipitated protein was pelleted by centrifugation at 2000 rpm for 10 minutes. The supernatant, 2 mL, was then mixed with 0.5 mL NaOH (1N) and the fluorescence of B[a]P-3-glucuronic acid measured at excitation/emission wavelengths of 300/421 nm (Singh & Wiebel, 1979). The activity of UGT (nmol/min/mg) was then determined.

Preliminary studies established the conditions for linearity of reaction with respect to time, protein and detergent concentrations, at the same time ensuring that substrate consumption did not exceed 10%. The apparent K_m for UDPGA was determined by performing experiments at a fixed concentration of 3-OH-B[a]P (10 μM). Saturating UDPGA concentrations were used in order to determine 3-OH-B[a]P glucuronidation kinetics.

Kinetic Analysis. Duplicate values for the rate of conjugate formation at each substrate concentration were used to calculate kinetic parameters using Prism v 4.0 (GraphPad Software, Inc., San Diego, CA). Equations used to fit the data were the Michaelis-Menten hyperbola for one-site binding (eq. 1), the Hill plot (eq. 2), substrate inhibition for one-site binding (eq. 3) (Houston and Kenworthy 2000), and partial substrate inhibition due to binding at an allosteric site (eq. 4) (Zhang et al., 1998).

$$v = V_{max}[S] / (K_m + [S]) \quad (1)$$

$$v = V_{max}[S]^h / (S_{50}{}^h + [S]^h) \quad (2)$$

$$v = V_{max}[S] / (K_m + [S] + ([S]^2/K_i)) \quad (3)$$

$$v = V_{max1}(1 + (V_{max2}[S]/V_{max1}K_i)) / (1 + K_m/[S] + [S]/K_i) \quad (4)$$

Values for K_m and V_{max} derived from equation 1 were used as initial values in the fitting of data to equations 3 and 4. Eadie-Hofstee plots were used in order to analyze the biphasic kinetics observed.

Results

Sulfonation and glucuronidation of 3-OH-B[a]P

Optimum conditions for sulfonation were 10 minutes incubation time and 25 μg cytosolic protein. A concentration of 0.02 mM PAPS provided saturating concentrations of the co-substrate and enabled kinetic parameters at 1.0 μM 3-OH-B[a]P to be calculated by the application of eq. 1 (Table 3-1a). The data for the sulfonation of 3-OH-B[a]P was fit to a two-substrate model (eq. 3), whereby the binding of a second substrate to the enzyme is responsible for the steep decline in enzyme activity at concentrations exceeding 1 μM (Figure 3-2a). Initial estimates of V_{max1} and K_m were provided by the initial data obtained at low [S] (non-inhibitory), while V_{max2} was constrained to 65 ± 20 pmol/min/mg, which is slightly below the plateau in Figure 3-2a.

The kinetic scheme (Figure 3-2b) illustrates the proposed partial substrate inhibition process, which assumes that substrate binding is at equilibrium, which is probable due to the low turnover rate of SULT. The best fit of the data was provided by a K_i of 1.0 ± 0.1 μM. Binding of the second substrate molecule results in a tenfold reduction in the rate of sulfonate formation.

Table 3-1. Estimated kinetic parameters (Mean ± SD) for (a) sulfonation and (b) glucuronidation of 3-OH-B[a]P by polar bear liver cytosol and microsomes. Values were calculated as described in the Methodology.

(a) sulfonation

Substrate	$V_{max1\ (app)}$ (pmol/min/mg)	$K_{m\ (app)}$ (μM)	V_{max1}/K_m (μL/min/mg)	$V_{max2\ (app)}$ [a] (pmol/min/mg)	$K_{i\ (app)}$ (μM)	V_{max2}/K_i (μL/min/mg)
3-OH-B[a]P	500 ± 8	0.41 ± 0.03	1220 ± 70	65.0 ± 20.0	1.01 ± 0.10	66.2 ± 26.8
PAPS	162 ± 35	0.22 ± 0.07	--	--	--	--

(b) glucuronidation

Substrate	$V_{max\ (app)}$ (nmol/min/mg)	$K_{m\ (app)}$ (μM)	V_{max} / K_m (μL/min/mg)
3-OH-B[a]P	3.00 ± 1.18	1.4 ± 0.2	1900 ± 544
UDPGA	1.53 ± 0.56[b], 1.47 ± 0.48[c]	42.9 ± 2.5[b], 200 ± 68[c]	--

[a] constrained variables to obtain best fit

[b] values for high-affinity component

[c] values for low-affinity component

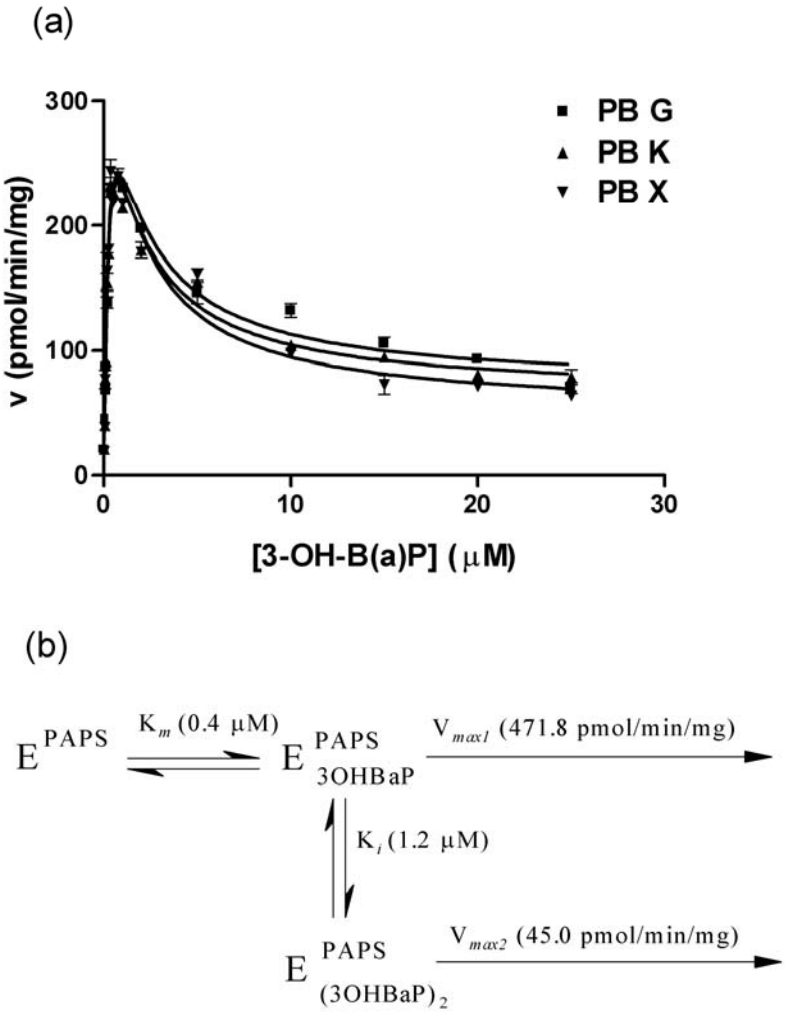

Figure 3-2. Sulfonation of 3-OH-B[a]P at PAPS = 0.02 mM.

A. Each data point represents the average of duplicate assays for each bear, while the error bars represent the standard deviation. The line represents the best fit to the data of equation (3). B) Kinetic model for partial substrate inhibition of SULT by 3-OH-B[a]P, after Zhang et al. (1998). E refers to SULT.

Optimum conditions for the glucuronidation of 3-OH-B[a]P by polar bear microsomes were found to be 5 µg microsomal protein and a 20-minute incubation. A concentration of 4 mM UDPGA was determined to be suitable for providing saturating concentrations of the co-substrate. The binding of UDPGA to UGT at 10 µM 3-OH-B[a]P was shown to be biphasic, with a fivefold reduction in affinity at higher UDPGA concentrations (Table 3-1b). The kinetic parameters for the co-substrate were calculated by deconvoluting the curvilinear data in the Eadie-Hofstee plot (Figure 3-3). In the presence of 4 mM UDPGA, the formation of B[a]P-3-O-glucuronide followed Michaelis-Menten kinetics (Table 3-1b).

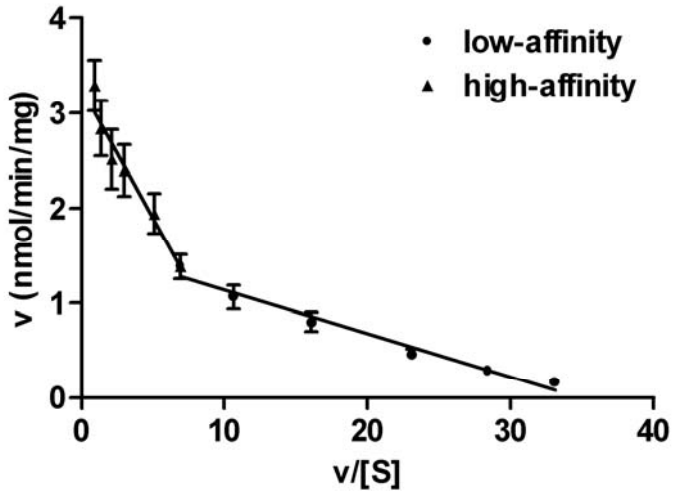

Figure 3-3. Eadie-Hofstee plot for the glucuronidation of 10 µM 3-OH-B[a]P, over a UDPGA concentration range of 5-3000 µM.

Each data point represents the average of duplicate assays for all bears, while the error bars represent the standard deviation.

Sulfonation of other substrates

Triclosan sulfate was formed rapidly, with the overall kinetics conforming to a hyperbolic curve (eq. 1) (Table 3-2). Substrate inhibition was observed for 4′-OH-PCB79 (Figure 3-4), with the data fitting equation (3). The value of K_i that gave the best fit was 217 ± 25 μM (Table 3-2). Sulfate conjugation of 4′-OH-PCB159 and 4′-OH-PCB165, which proceeded via Michaelis-Menten kinetics, was, respectively, 11 and 5 times less efficient than the sulfonation of 4′-OH-PCB79 (Table 3-2). At a concentration of 10 μM, 4′-OH-PCB165 was observed to inhibit sulfonation of substrates already present in polar bear liver cytosol by 60%.

Table 3-2. Kinetic parameters (Mean ± SD) for the sulfonation of various xenobiotics by polar bear liver cytosol, listed in order of decreasing enzymatic efficiency. All data fit equation (1), except for 4′-OH-PCB79 and PCP, which fit equations (3) and (2) respectively (see Methodology for equations).

Substrate	**V_{max} (pmol/min/mg)**	**K_m (μM)**	**V_{max} / K_m (μL/min/mg)**	**K_i (μM)**
triclosan	1008 ± 135	11 ± 2	90.8 ± 6.8	-
4′-OH-PCB79	372 ± 38	123 ± 20	3.1 ± 0.3	217 ± 25[a]
OHMXC	51.1 ± 7.8	67 ± 4	0.8 ± 0.1	-
4′-OH-PCB165	8.6 ± 2.0	17 ± 7	0.56 ± 0.17	-
TCPM	62.0 ± 11.2	144 ± 36	0.44 ± 0.06	-
4′-OH-PCB159	14.8 ± 2.3	60 ± 21	0.28 ± 0.12	-
PCP	13.8 ± 1.2	72 ± 14[b]	0.20 ± 0.05	-

[a] K_i for bears G, K and X were 240, 220 and 190 μM respectively. These values were constrained to obtain the best fit for the data

[b] S_{50}; h = 2.0 ± 0.4

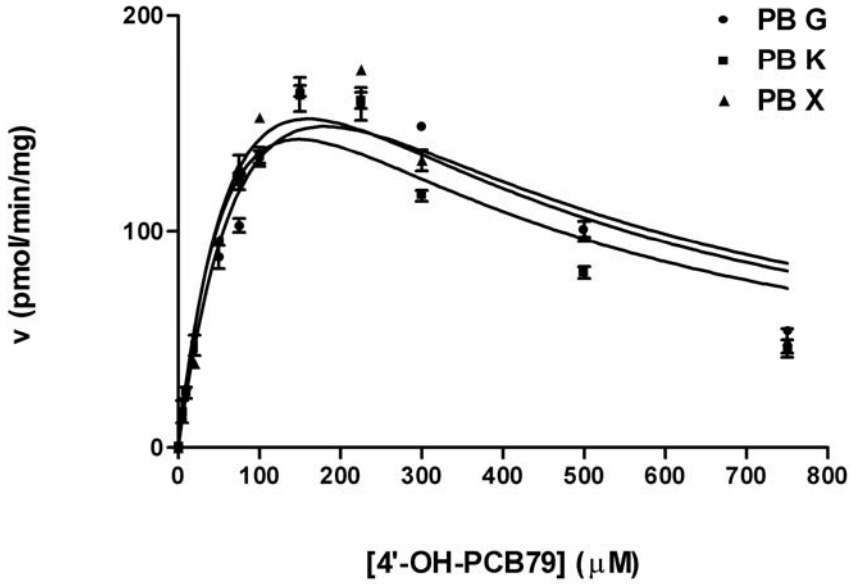

Figure 3-4. Sulfonation of 4′-OH-PCB79, PAPS = 0.02 mM.

Each data point represents the average of duplicate assays for each bear, while the error bars represent the standard deviation. The line represents the best fit to equation (4) for 4′-OH-PCB79.

Due to variable rates of sulfonation of these unknown substrates, autoradiographic counts corresponding to the OHMXC-*O*-sulfate band were used to correct the activities calculated from the scintillation counter data (Figure 3-5). This enabled the transformed data to be fit into a Michaelis-Menten model (Table 3-2). The autoradiograms obtained showed that increasing concentrations of OHMXC resulted in decreased counts for the unknown sulfate conjugates (Figure 3-5). Sulfonation of the unknown substrates in polar bear cytosol was reduced by half at OHMXC concentrations < 20 μM.

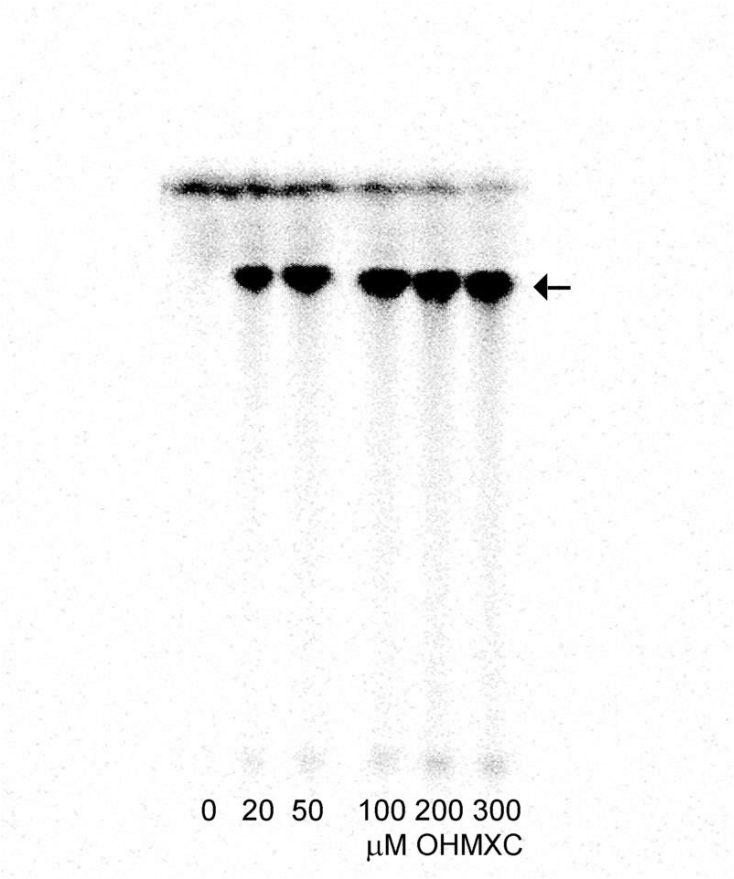

Figure 3-5. Autoradiogram showing the reverse-phase TLC separation of sulfonation products of OHMXC.

Incubations were carried out with the indicated concentrations of OHMXC. The arrow indicates the sulfate conjugate of the OHMXC, while other bands represent unidentified sulfate conjugates formed from endobiotics or other xenobiotics in polar bear liver cytosol.

The total TCPM sulfate conjugate production formed after 5 minutes under initial rate conditions did not exceed 30 pmol. TLC, followed by autoradiography, was thus used to distinguish the TCPM-sulfate band (R_f 0.54) from other sulfate conjugates (R_f 0.05 and 0.72) originating from compounds in the polar bear liver cytosol (Figure 3-6).

The data obtained followed hyperbolic kinetics (Table 3-2). Even though the TLC from the kinetic experiments showed a TCPM concentration-dependent increase of the band corresponding to the purported TCPM-sulfate, and this band was absent in the

substrate blank, the fact remained that we were apparently looking at the only instance ever reported of a successful sulfonation of an acyclic tertiary alcohol.

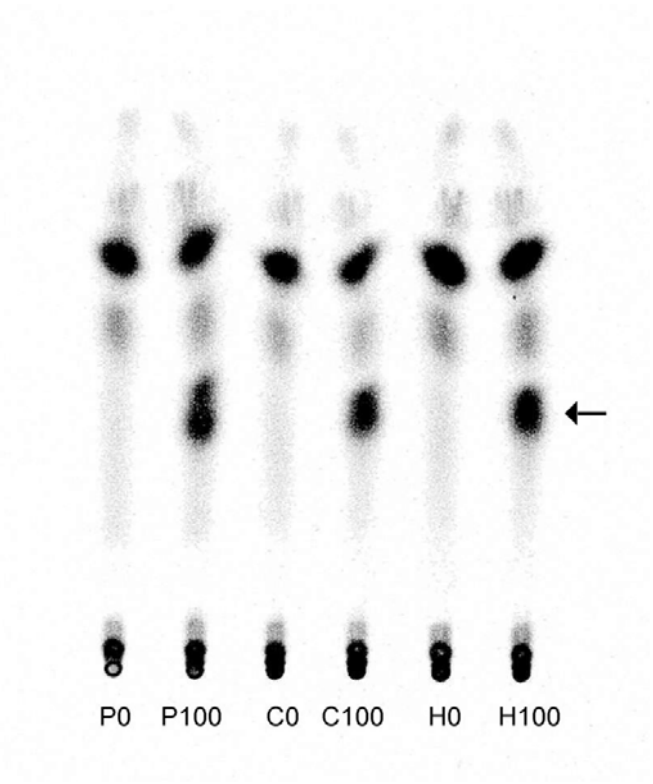

Figure 3-6. Autoradiogram showing the reverse-phase TLC separation of sulfonation products from incubations with TCPM using polar bear (P), channel catfish (C), and human (H) liver cytosol in the absence of (0), and presence of 100 μM TCPM (100).

The arrow indicates the sulfate conjugate of the substrate, while other bands represent unidentified sulfate conjugates formed from endobiotics or other xenobiotics in liver cytosol.

Thus, additional experiments were performed to verify the identity of this conjugate. The purity of the TCPM was tested in the event that the additional band was due to an impurity in the substrate. However, the substrate used was found to be free of contaminants by HPLC (C18 reverse phase column, with detection at 268 and 220 nm, using 90% methanol in water and a flow rate of 1 mL/min). A single peak was recorded

at 7.3 minutes. Another experiment involved a 60-minute incubation performed with 100 μM TCPM and 0.1 mg cytosolic protein from polar bear, channel catfish and human liver. For each of the three species, we detected a conjugate at $R_f = 0.54$. The substrate blanks showed no band at the same position (Figure 3-6). The TCPM sulfate conjugate from polar bear could be hydrolyzed by sulfatase (Figure 3-7), providing further evidence of the sulfonation of this alcohol.

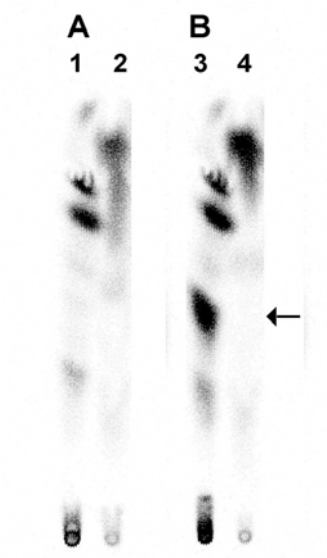

Figure 3-7. Autoradiogram showing the reverse-phase TLC separation of sulfonation products of TCPM and the effect of sulfatase treatment.

A, incubation in the absence of TCPM (lane 1), and following treatment with sulfatase (lane 2). B, incubation with 200 μM TCPM (lane 3), and following treatment with sulfatase (lane 4). The arrow indicates the sulfate conjugate of the TCPM, while other bands represent unidentified sulfate conjugates formed from endobiotics or other xenobiotics in polar bear liver cytosol.

Inhibition of sulfonation of substrates already present in the polar bear liver was noted upon adding 1 μM PCP (Figure 3-8). The data for PCP sulfonation fitted the nonlinear Hill plot (eq. 2) (Table 3-2).

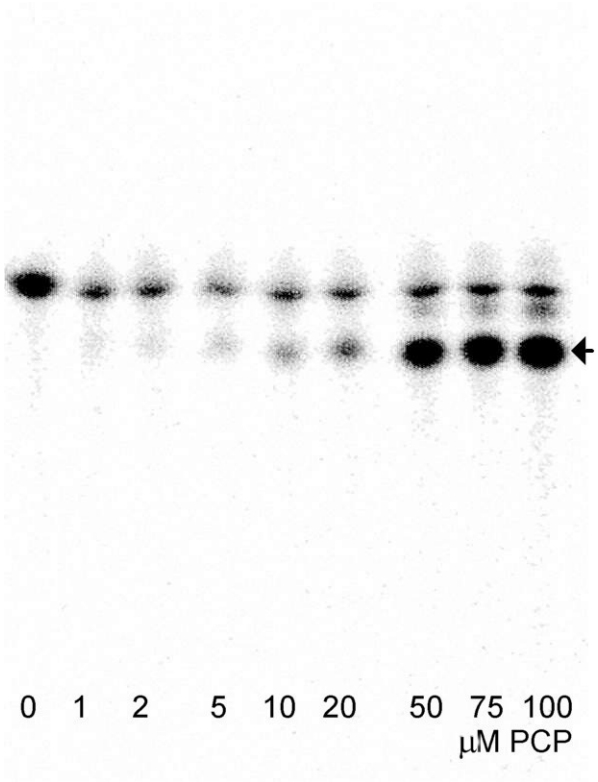

Figure 3-8. Autoradiogram showing reverse-phase TLC separation of sulfonation products from the study of PCP kinetics.

The arrow indicates the sulfate conjugate of PCP, while other bands represent unidentified sulfate conjugates formed from endobiotics or other xenobiotics in polar bear liver cytosol.

Discussion

The sulfonation of hydroxylated metabolites of benzo[a]pyrene has been reported in various species, including fish (James et al., 2001) and humans (Wang et al., 2004). Benzo[a]pyrene-3-glucuronide has been shown to be produced by fish (James et al., 1997), rats (Lilienblum et al., 1987) and humans (Wang et al., 2004). There are, however, few studies investigating the kinetics of these conjugation reactions. Glucuronidation of 3-OH-B[a]P was more efficient in polar bear liver than in human liver or catfish intestine. On the other hand, the efficiency of sulfonation was similar to that shown in human liver but around three times less than in catfish intestine (Wang et al.,

2004, James et al., 2001). From the limited comparative data available, it can be surmised that, in general, polar bear liver is an important site of 3-OH-B[a]P detoxication, particularly with respect to glucuronidation.

Substrate inhibition for the sulfonation of 3-OH-B[a]P has been observed at relatively low concentrations of the xenobiotic in other species such as catfish and human (Tong and James 2000, Wang et al., 2005). Data from the polar bear sulfonation assay fitted a two-substrate model developed for the sulfonation of 17β-estradiol by SULT1E1 (Zhang et al., 1998). This model was also used to explain the sulfonation profile observed for the biotransformation of 1-hydroxypyrene, a compound structurally similar to 3-OH-B[a]P, by SULTs 1A1 and 1A3 (Ma et al., 2003). In the original model, SULT1E1 was saturated with PAPS, and each of the estradiol substrate molecules bound independently to the enzyme. The estradiol binding sites were proposed to consist of a catalytic site, and an allosteric site that regulates turnover of the substrate (Zhang et al., 1998). The substrate inhibition observed with polar bear liver cytosol at higher 3-OH-B[a]P concentrations (>0.75 μM) can thus be explained by the binding of a second substrate molecule to an allosteric site, which leads to a two-fold decrease in affinity and an eightfold decrease in V_{max}.

SULTs are generally high-affinity, low-capacity biotransformation enzymes that operate effectively at low substrate concentrations. Thus, typical K_ms for the sulfonation of xenobiotic substrates are usually significantly lower than K_ms for the same substrates undergoing biotransformation by low-affinity, high-capacity glucuronosyltransferases (UGTs). In polar bear liver, both pathways showed similar apparent affinities for 3-OH-B[a]P, with K_ms of 0.4 and 1.4 μM for sulfonation and glucuronidation respectively,

suggesting these two pathways of Phase II metabolism compete at similar 3-OH-B[a]P concentrations. However, the apparent maximal rate of sulfonation was about 7.5 times lower than the rate of glucuronidation.

It was previously reported that the maximum rate of glucuronidation of 3-OH-B[a]P by polar bear liver was 1.26 nmol/min/mg, or around half the V_{max} value obtained in this study (Sacco and James 2004). However, the preceding study utilized 0.2 mM UDPGA, which, as seen from Table 3-2a, is equivalent to the K_m (for UDPGA) of the low-affinity enzyme, and thus does not represent saturating concentrations of the co-substrate. The affinity of the enzyme for 3-OH-B[a]P did not change significantly with a 20-fold increase in UDPGA concentrations, suggesting that substrate binding is independent of the binding of co-substrate. The binding of UDPGA was biphasic, indicating that multiple hepatic UGTs may be responsible for the biotransformation. Biphasic UDPGA kinetics have also been demonstrated in human liver and kidney for 1-naphthol, morphine, and 4-methylumbelliferone (Miners et al., 1988a,b; Tsoutsikos et al., 2004). While V_{max} was similar for both components, there was a fivefold decrease in enzyme affinity for UDPGA as the co-substrate concentration was increased. The involvement of at least two enzymes can be physiologically advantageous since it enables the maintenance of a high turnover rate even as UDPGA is consumed. Although physiological UDPGA concentrations in polar bear liver are unknown, mammalian hepatic UDPGA has been determined to be around 200-400 μM (Zhivkov et al., 1975, Cappiello et al., 1991), implying that the observed nonlinear kinetics in the polar bear may operate *in vivo*.

The rate of triclosan sulfonation was the highest of all the substrates studied; apparent V_{max} was twice as high as for 3-OH-B[a]P. However, the overall efficiency of sulfonation of the hydroxylated PAH was still 13 times higher than for triclosan sulfonation. The presence of three chlorine substituents (though none flanking the phenol group) does not hinder the sulfonation of triclosan when compared to the 'chlorine-free' 3-OH-B[a]P. Triclosan sulfonation in polar bear liver was similar to human liver with respect to enzyme affinity; however the maximum rate was tenfold higher in polar bears than in humans (Wang et al., 2004). This may be one reason why triclosan has not been detected in polar bear plasma or liver to date.

Our data fitted a model that indicates the substrate inhibition observed for 4′-OH-PCB79 may be due to a second substrate molecule interacting with the enzyme-substrate complex at the active site rather than an allosteric site, resulting in a dead-end complex. Unlike 3-OH-B[a]P, sulfonation can only proceed via the single substrate-SULT complex. Models of SULT1A1 and 1A3, with two molecules of *p*-nitrophenol or dopamine at the active site respectively, have been proposed as a mechanism of substrate inhibition (Gamage et al., 2003, Barnett et al., 2004), while the crystal structure of human EST containing bound 4,4′-OH-3,3′,5,5′-tetrachlorobiphenyl at the active site has not provided any evidence of an allosteric site (Shevtsov et al., 2003). The slower sulfonation of 4′-OH-PCB79 compared with 3-OH-B[a]P may result from the inductive effect of the chlorines flanking the phenolic group rather than steric hindrance (Duffel and Jakoby, 1981). However, polar bear liver sulfonated 4′-OH-PCB79 more rapidly than the other OH-PCB substrates studied.

The inclusion of two additional chlorine substituents on the non-phenol ring (with respect to 4′-OH-PCB79) resulted in both 4′-OH-PCB159 and 4′-OH-PCB165 being very poor substrates. Inefficient sulfonation may be one reason why the related compound 4′-OH-PCB172 accumulates in polar bears. Some degree of substrate inhibition may also be expected to contribute to this accumulation, as was observed with 4′-OH-PCB165.

Sulfonation was not an efficient pathway of OHMXC detoxification. The rate of OHMXC-sulfonate formation was around 7 times lower than for 4′-OH-PCB79. Since resonance delocalization of negative charge on the phenolic oxygen by the flanking chlorines in chlorophenols may decrease V_{max} by increasing the energy of the transition state of the reaction (Duffel and Jakoby, 1981), it is possible that in the case of OHMXC (with no chlorines flanking the phenolic group), product release, rather than sulfonate transfer, may have been the rate-limiting step.

TCPM was a poor substrate for sulfonation, and this may be one reason why it has been measured in such high amounts in polar bear liver. To our knowledge, sulfonation of acyclic tertiary alcohols has not been reported in the literature. Despite the considerable steric hindrance of three phenyl groups, the alcohol group could be sulfonated. Although the alcohol in TCPM is not of the benzylic type, the presence of three proximal phenyl groups may give this group some benzylic character, rendering sulfonation of the alcohol possible. Both SULT 1E1 and SULT 2A1 have been shown to sulfonate benzylic alcohol groups attached to large molecules (Glatt, 2000). Sulfation of the benzylic hydroxyl group leads to an unstable sulfate conjugate that readily degrades to the reactive carbocation or spontaneously hydrolyzes back to the alcohol. Attempts to

recover TCPM-O-sulfonate from TLC plates resulted in recovery of TCPM from the conjugate band, perhaps because of the conjugate's instability.

A study of the sulfonation of PCP was complicated by the fact that it is a known SULT inhibitor, often with K_is in the submicromolar range. In our experiments, this was seen as a 74% decrease in formation of the unidentified sulfonate conjugates (band shown at the solvent front in Figure 3-8) upon addition of 1 μM PCP. Although PCP was a strong inhibitor of SULT1E1 (Kester et al., 2000), and has been postulated to be a dead-end inhibitor for phenol sulfotransferases (Duffel and Jakoby, 1981), it was possible that polar bear SULT 1A isoforms were not completely inhibited by PCP, or that other SULT isoform(s) were responsible for the limited sulfonation activity observed. Thus, we have shown that, *in vitro* at least, one mammalian species is capable of limited PCP sulfonation. Even though the tertiary alcohol of TCPM was a poor candidate for sulfonation, it was metabolized at twice the efficiency of PCP, which has a phenolic group that is usually more susceptible to sulfonation. This demonstrates the extent of the decreased nucleophilicity on the phenolic oxygen due to the resonance delocalization afforded by the five chlorine substituents.

Conclusions

In summary, this study demonstrated that, in polar bear liver, 3-OH-B[a]P was a good substrate for sulfonation and glucuronidation. Other, chlorinated, substrates were biotransformed with less efficiency, implying that reduced rates of sulfonation may contribute to the persistence of compounds such as hexachlorinated OH-PCBs, TCPM and PCP in polar bear tissues.

CHAPTER 4
GLUCURONIDATION OF POLYCHLORINATED BIPHENYLOLS BY CHANNEL CATFISH LIVER AND INTESTINE

Polychlorinated biphenyls (PCBs) were extensively used as dielectrics in the mid-twentieth century. Despite a ban on their use in the US, Europe and Japan since the mid 1970s, the chemical stability of PCBs has resulted in their persistence at all trophic levels around the globe. Enzyme-mediated biotransformation is an important influence on PCB persistence, and its significance in PCB toxicokinetics is dependent on congener structure and the metabolic capacity of the organism.

Polychlorinated biphenylols (OH-PCBs) are products of CYP-dependent oxidation of PCBs (James 2001). While OH-PCBs are more polar than their parent molecules, they are still lipophilic enough to be orally absorbed, and distribute to several tissues (Sinjari et al., 1998). Thus, not only have these compounds been detected in the plasma (which represents recent dietary exposure, biotransformation, and remobilization into the circulation) of a variety of animal species, such as polar bear (Sandau et al., 2004), bowhead whale (Hoekstra et al., 2003), catfish (Li et al., 2003), and humans (Fängström et al., 2002; Hovander et al., 2002), but also significantly, from a developmental toxicology aspect, in fetuses and breast milk (Sandau et al., 2002; Guvenius et al., 2003).

OH-PCBs may contribute significantly to the recognized toxic effects of PCBs such as endocrine disruption (Safe 2001; Shiraishi et al., 2003), tumor promotion (Vondráček et al., 2005) and neurological dysfunction (Sharma and Kodavanti 2002; Meerts et al., 2004).

Elimination of these toxic metabolites via Phase II conjugation reactions, such as glucuronidation and sulfonation, are thus important routes of detoxification. In view of the persistence of certain OH-PCBs, it is surprising that only a few studies have attempted to investigate the biotransformation of these compounds in animals or humans, particularly by glucuronidation (Tampal et al., 2002; Sacco and James 2004; Daidoji et al., 2005), which is normally a higher-capacity pathway than sulfonation.

Glucuronidation is catalyzed by a family of endoplasmic reticular membrane-bound enzymes, the UDP-glucuronosyltransferases (UGTs), which transfer a D-glucuronic acid moiety from the co-substrate UDP-glucuronic acid (UDPGA) to a xenobiotic containing a suitable nucleophilic atom such as oxygen, nitrogen and sulfur. UGTs are mainly found in the liver, but also in extrahepatic tissues, such as the small intestine and kidney (Wells et al., 2004).

The various chlorine and hydroxyl substitution patterns possible on the biphenyl structure may lead to significant differences in glucuronidation kinetics. One explanation for the retention of certain OH-PCBs may thus be that they are poor substrates for glucuronidation. Tampal and co-workers (2002) studied the glucuronidation of a series of OH-PCBs by rat liver microsomes. Efficiency of glucuronidation varied widely, and substitution of chlorine atoms at the *m*- and *p*-positions on the nonphenolic ring greatly lowered V_{max}. Weak relationships were observed between the dihedral angle, pK_a, log D and enzyme activity. The experimentally determined kinetic parameters determined in the Tampal et al study were subsequently related to the physicochemical properties and structural features of the OH-PCBs by means of a quantitative structure-activity

relationship (QSAR) study. Hydrophobic and electronic aspects of OH-PCBs were shown to be important in their glucuronidation (Wang, 2005).

Most of the persistent OH-PCBs found in human plasma are hydroxylated at the *p*-position, in addition to being *meta*-chlorinated on either side of the phenolic group. The remaining substitution pattern on both rings is highly variable (Bergman et al., 1994; Sjödin et al., 2000). An OH group in the *para* position, with two flanking chlorine atoms was associated with estrogen and thyroid hormone sulfotransferase inhibitory activity (Kester et al., 2000; Schuur et al., 1998), and exhibited the highest affinity for transthyretin (TTR) (Lans et al., 1993), the major transport protein in non-mammalian species (Cheek et al., 1999). Such OH-PCBs were potent inhibitors of the sulfonation of 3-hydroxybenzo[a]pyrene (Wang et al., 2005). In contrast, the OH-PCBs having an unhindered hydroxyl group substituted at the *para* position (relative to the biphenyl bond) have exhibited the strongest binding to the rodent estrogen receptor (ER), although the competitive ER binding affinities were ≤100-fold lower than that observed for estradiol (Korach et al., 1988; Arulmozhiraja et al., 2005).

In the channel catfish, individual OH-PCBs have been shown to inhibit the *in vitro* intestinal glucuronidation of several hydroxylated metabolites of benzo[a]pyrene (BaP) (van der Hurk et al., 2002; James and Rowland-Faux 2003). The *in situ* hepatic glucuronidation of a procarcinogenic BaP metabolite, the (-)benzo[a]pyrene-7,8-dihydro-diol, was also inhibited by a mixture of OH-PCBs, consequently increasing the formation of DNA adducts (James et al., 2004). It is possible that these compounds inhibit their own glucuronidation. The OH-PCB metabolites of 3,3,4,4-tetrachlorobiphenyl (CB-77), one of the most toxic PCBs known, were poor substrates for catfish intestinal glucuronidation

(James and Rowland-Faux, 2003). This may help to explain the persistence of these compounds.

Hypothesis

The glucuronidation kinetics of a series of potentially toxic *p*-OH-PCBs by channel catfish liver and proximal intestine is influenced by the structural arrangement of the chlorine substituents around the biphenyl ring.

Methodology

Chemicals. A total of 14 substrates were used in this study (Figure 4-1). The nomenclature of the OH-PCBs is based on the recommendations of Maervoet and co-workers (2004).

The following substrates (Catalog no. in parentheses) were purchased from Accustandard (New Haven, CT): 4-OHCB2 (1003N), 4-OHCB14 (2004N), 4'-OHCB69 (4008N), 4'-OHCB72 (4009N), 4'-OHCB106 (5005N), 4'-OHCB112 (5006N), 4'-OHCB121 (5007N), 4'-OHCB159 (6001N), and 4'-OHCB165 (6002N). The compounds 4'-OHCB35, 4-OHCB39, 4'OHCB68, 4'-OHCB79 were synthesized by Suzuki-coupling (Lehmler and Robertson, 2001; Bauer et al., 1995). The 4-hydroxy biphenyl (4-OHBP) was purchased from Sigma (St.Louis, MO). ^{14}C-UDPGA (196 μCi/μmol) was obtained from PerkinElmer Life and Analytical Sciences (Boston, MA). The ^{14}C-UDPGA was diluted with unlabelled UDPGA to a specific activity of 1.5-5 μCi/μmol for use in enzyme assays. PIC-A (tetrabutylammonium hydrogen sulfate) was obtained from Waters Corp. (Milford, MA). Other reagents were the highest grade available from Fisher Scientific (Atlanta, GA) and Sigma.

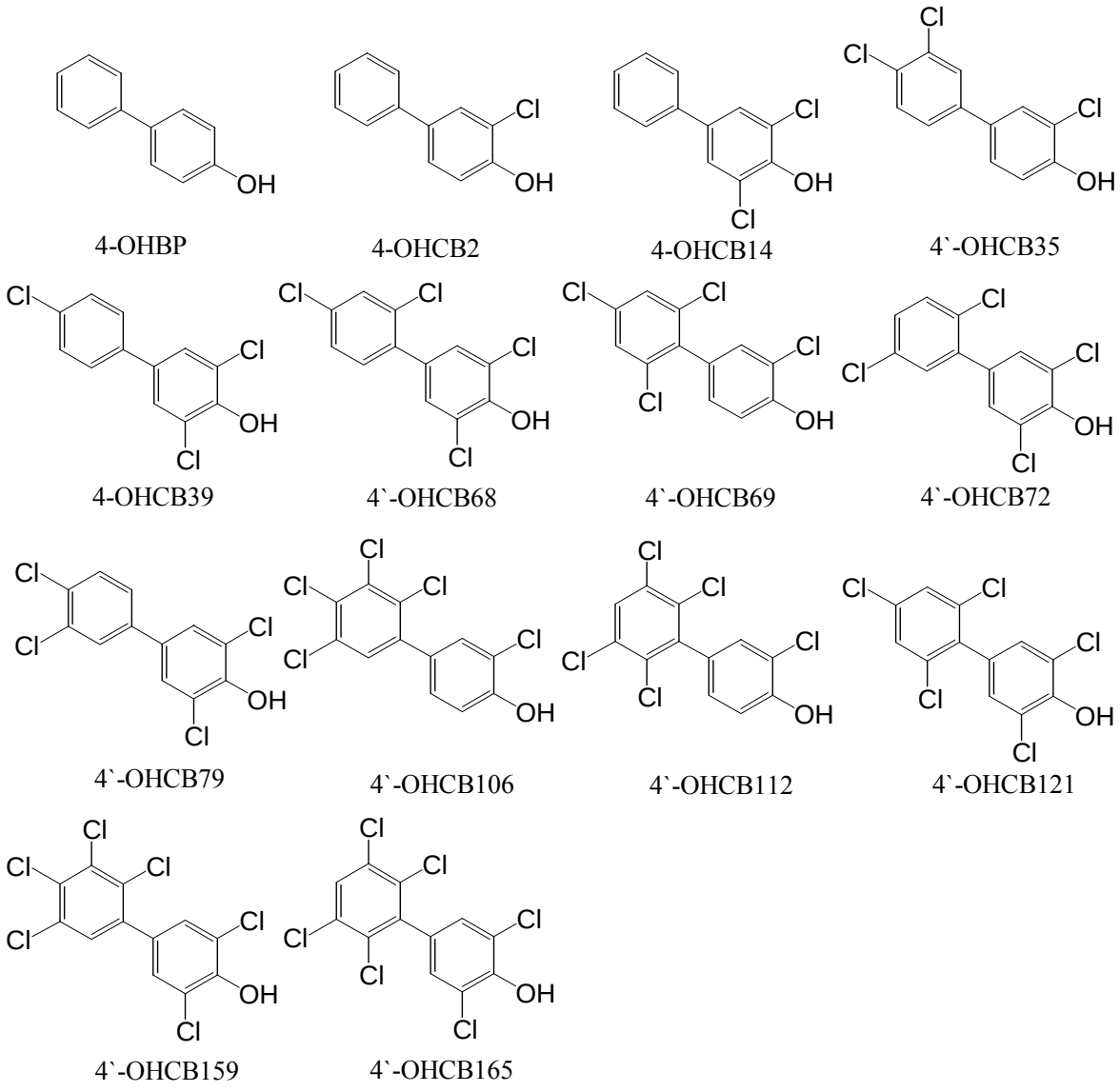

Figure 4-1. Structure of substrates used in channel catfish glucuronidation study.

Animals. Channel catfish (*Ictalurus punctatus*), with weights ranging from 2.1 – 3.7 kg, were used for this study. All fish were kept in flowing well water and fed a fish chow diet (Silvercup, Murray, UT). Care and treatment of the animals was conducted as per the guidelines of the University of Florida Institutional Animal Care and Use Committee. The microsomal fractions were obtained from liver and intestinal mucosa

using a procedure described previously (James et al., 1997). Only the proximal portion of the intestine was used in the study. Protein determination was carried out by the method of Lowry and co-workers (1951) using bovine serum albumin as protein standard.

Glucuronidation assay. A radiochemical ion-pair extraction method was employed to investigate the glucuronidation of the 4-OHPCBs and 4-OHBP. Substrate consumption did not exceed 10%. Initial experiments determined the saturating concentrations of UDPGA to be employed. The incubation mixture consisted of 0.1 M Tris-Cl buffer (*p*H 7.6), 5 mM $MgCl_2$, 0.5% Brij-58, 200 μM or 1500 μM [^{14}C]UDPGA (intestine and liver, respectively), 100 μg catfish intestinal or hepatic microsomal protein, and substrate in a total reaction volume of 0.1 mL. Initially, the OH-PCBs were added to tubes from methanol solutions and evaporated under nitrogen. In all cases, the protein and Brij-58 were added to the dried substrate, thoroughly vortexed and left on ice for 30 minutes. Subsequently, the buffer, $MgCl_2$, and water were added in that order and vortex-mixed. After a pre-incubation of 3 minutes at 35ºC, UDPGA was added to initiate the reaction, which was terminated after 30 minutes incubation by the addition of a 1:1 mixture of 2.5% acetic acid and PIC-A in water, such that the final volume was 0.5 mL. The glucuronide product was extracted by two successive 1.5 mL portions of ethyl acetate. The phases were separated by centrifugation, and duplicate portions of the ethyl acetate phase were counted for quantitation of glucuronide conjugate.

Physicochemical parameters. The structural characteristics of the OH-PCBs were calculated using ChemDraw 3D (CambridgeSoft Corp., Cambridge, MA). Parameters used were: the Connolly Accessible Surface Area (CAA, the locus of the center of a probe sphere, representing the solvent, as it is rolled over the molecular shape), the

Connolly Molecular Surface Area (CMA, the contact surface created when a probe sphere (radius = 1.4 Å, the size of H_2O), representing the solvent, is rolled over the molecular shape), the Connolly Solvent-Excluded Volume (CSV, the volume contained within the contact molecular surface, or that volume of space that the probe is excluded from by collisions with the atoms of the molecule), the ovality (the ratio of the Molecular Surface Area to the Minimum Surface Area, which is the surface area of a sphere having a volume equal to CSV of the molecule), and dihedral angle (the angle formed between the planes of the two rings, which is related to the extent of coplanarity of the molecule). ACD/ILab software (Advanced Chemistry Development, Ontario, Canada) was used to predict log P, log D (at *p*H 7.0), and the pK_a (of the phenolic group).

Kinetic analysis. Duplicate values were employed for the rate of conjugate formation at each substrate concentration to calculate kinetic parameters using Prism v4.0 (GraphPad Software, Inc., San Diego, CA). Equations used to fit the data were the Michaelis-Menten hyperbola for one-site binding and the Hill plot for positive cooperativity.

Results

The kinetics for UDPGA were analyzed for the glucuronidation of three representative OH-PCBs (Table 4-1). Saturating concentrations of UDPGA were higher in liver than in intestine (Figure 4-2). The glucuronidation of most of the OH-PCBs tested followed Michaelis-Menten kinetics (Figure 4-3A). In the case of the glucuronidation of 4`OHCB35 by liver and 4`OHCB112 by proximal intestine, the data fitted the Hill plot (Figure 4-3B).

Table 4-1. Estimated kinetic parameters (mean ± S.D.) for the co-substrate UDPGA in the glucuronidation of three different OH-PCBs.

Substrate	**Substrate Concentration (μM)**	**V_{max} (app) (nmol/min/mg)**	**K_m (app) (μM)**
Liver			
4′-OHCB-35	500	0.87 ± 0.20	697 ± 246
4′-OHCB-72	250	0.32 ± 0.14	247 ± 162
Intestine			
4′-OHCB-69	200	0.20 ± 0.11	27 ± 14

The estimated apparent maximal rate of glucuronidation of polychlorinated biphenylols by channel catfish ranged from 124-784 pmol/min/mg for proximal intestine and 404-2838 pmol/min/mg for the liver (Table 4-2). The K_ms for individual OH-PCBs tended to be different in the two organs, with a few exceptions (4OHCB2, 4`OHCB165). V_{max} was significantly higher in liver than in intestine. Conversely, the affinity of intestinal catfish UGTs (K_m range: 42-572 μM) for the OH-PCBs tested was higher than for liver UGTs (K_m range: 111-1643 μM). These contrasting differences are reflected in the lack of any difference in the efficiency of glucuronidation in both organs when all the OH-PCB substrates were considered (Table 4-3). V_{max} for OH-PCB glucuronidation in both organs were strongly correlated with each other (R^2=0.74). This relationship did not exist for K_m (R^2=0.003).

A

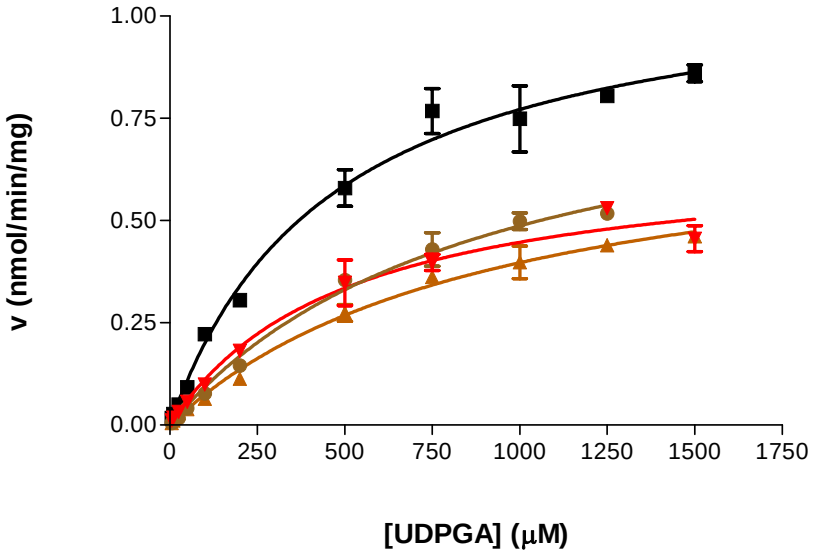

B

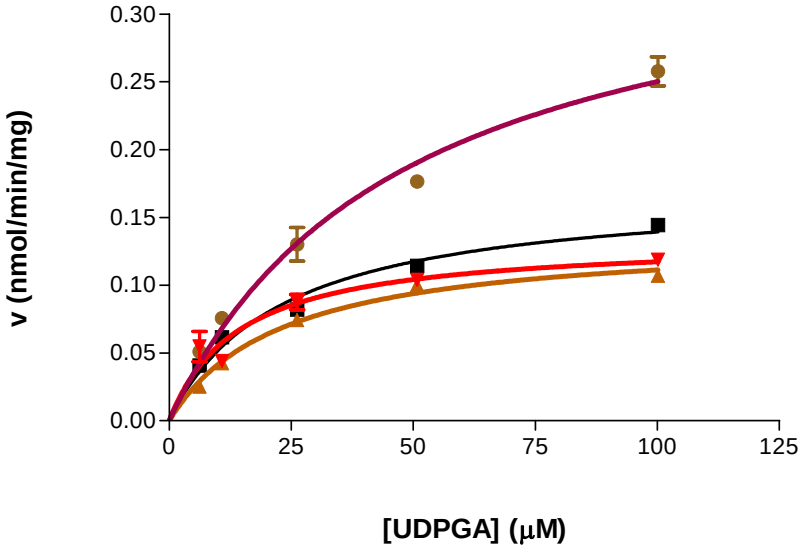

Figure 4-2. UDPGA glucuronidation kinetics in 4 catfish.

A) in liver, using 500 µM 4′-OH-CB35. B) in proximal intestine, using 200 µM 4′-OH CB69

A

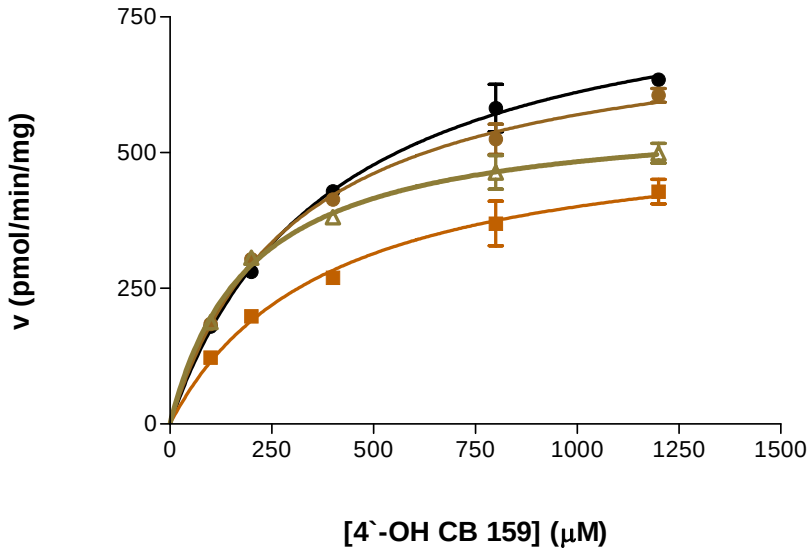

B

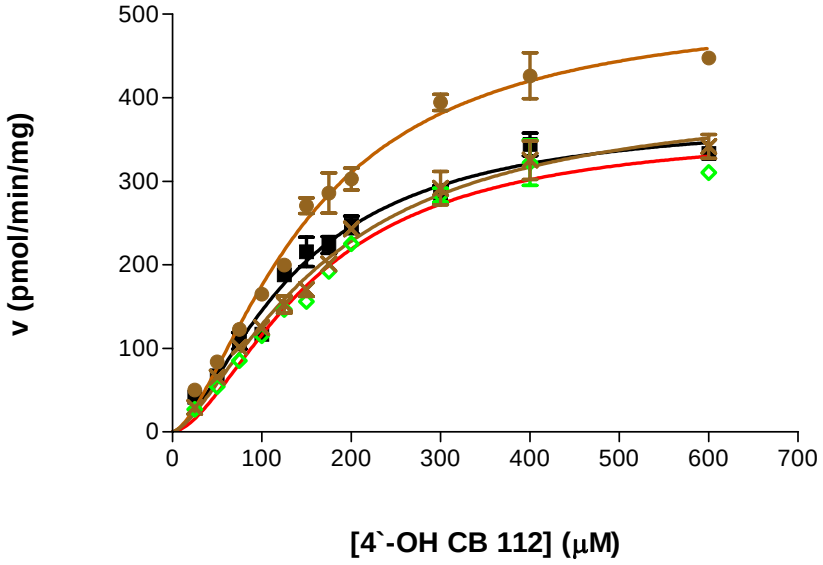

Figure 4-3. Representative kinetics of the glucuronidation of OH-PCBs in 4 catfish.

A) Michaelis-Menten plot for 4′-OHCB-159 by liver. B) Hill plot for 4′-OHCB-112 by proximal intestine

Table 4-2. Kinetic parameters (Mean ± S.D.) for the glucuronidation of 4-OHBP and OH-PCBs.

	Intestine		Liver	
Substrate	**V_{max} (app)**	**K_m (app)**	**V_{max} (app)**	**K_m (app)**
4-OHBP	43 ± 10	599 ± 110	182 ± 78	502 ± 235
4-OHCB2	417 ± 57	572 ± 47	2277 ± 849	583 ± 95
4-OHCB14	255 ± 59	387 ± 65	2022 ± 936	614 ± 202
4′-OHCB35	784 ± 348	265 ± 85	2838 ± 1456	**455 ± 89**
4-OHCB39	220 ± 90	134 ± 36	1716 ± 536	242 ± 76
4′-OHCB68	213 ± 91	119 ± 75	ND	ND
4′-OHCB69	751 ± 253	42 ± 21	2774 ± 1153	1071 ± 410
4′-OHCB72	401 ± 236	183 ± 126	ND	ND
4′-OHCB79	124 ± 36	87 ± 21	869 ± 318	476 ± 201
4′-OHCB106	431 ± 60	183 ± 58	1579 ± 645	798 ± 122
4′-OHCB112	401 ± 67	**163 ± 24**	2144 ± 1007	1643 ± 545
4′-OHCB121	220 ± 39	130 ± 21	1046 ± 408	207 ± 97
4′-OHCB159	188 ± 66	213 ± 136	681 ± 141	318 ± 91
4′-OHCB165	163 ± 26	137 ± 44	404 ± 116	111 ± 28

Units for K_m and V_{max} are μM and pmol/min/mg protein, respectively. Bold indicates S_{50} in place of K_m. ND, not done.

Table 4-3. Comparison of the estimated kinetic parameters for OH-PCB glucuronidation in catfish liver and proximal intestine

Parameter	**Liver**	**Intestine**	***p*-value**
V_{max} (app)	1370 ± 275	364 ± 70	0.002
K_m (app)	567 ± 128	210 ± 46	0.016
V_{max}/K_m	3.7 ± 0.6	3.4 ± 1.8	0.857

(Mean ± SEM for all OH-PCB substrates)

The V_{max} for glucuronidation in both proximal intestine and liver was significantly decreased upon addition of a second chlorine substituent flanking the phenolic moiety, while keeping the chlorine substitution pattern in the rest of the molecule constant (Table 4-4, Figure 4-4). The affinity of hepatic UGTs for the OH-PCBs appeared to increase with the addition of a second flanking chlorine atom; however, this relationship did not achieve statistical significance.

Table 4-4. Comparison of kinetic parameters (Mean ± SEM) for the glucuronidation of OH- PCBs grouped according to the number of chlorine atoms flanking the phenolic group

Parameter	**Flanking chlorines**		***p*-value**
	1	**2**	
Liver			
V_{max} (app), pmol/min/mg	2247 ± 204	1002 ± 274	0.007
K_m (app), μM	856 ± 209	342 ± 88	0.053
Intestine			
V_{max} (app), pmol/min/mg	560 ± 85	190 ± 23	0.003
K_m (app), μM	274 ± 97	191 ± 53	0.473

The effect of chlorine substituents on the nonphenolic ring on glucuronidation of OH-PCBs was also investigated. No significant differences on K_m and V_{max} could be observed between the absence or presence of specific chlorine substituents on the nonphenolic ring. The only exception was that the presence of an *ortho*-chlorine significantly (p=0.03) decreased the K_m in the proximal intestine.

A

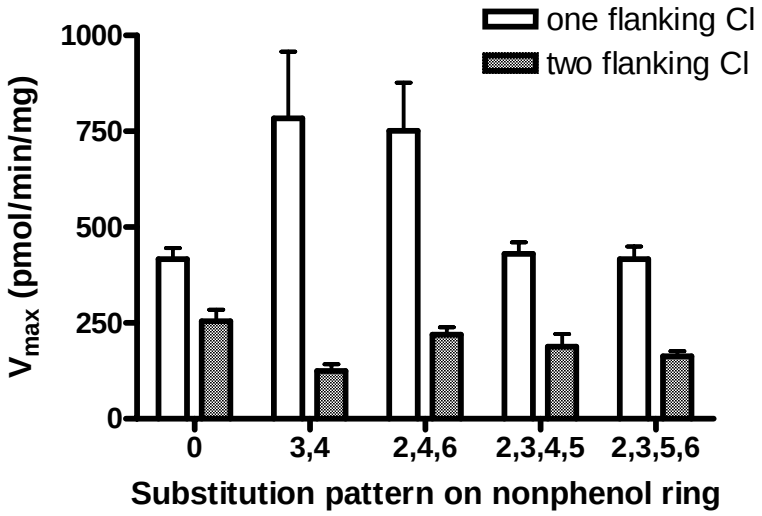

B

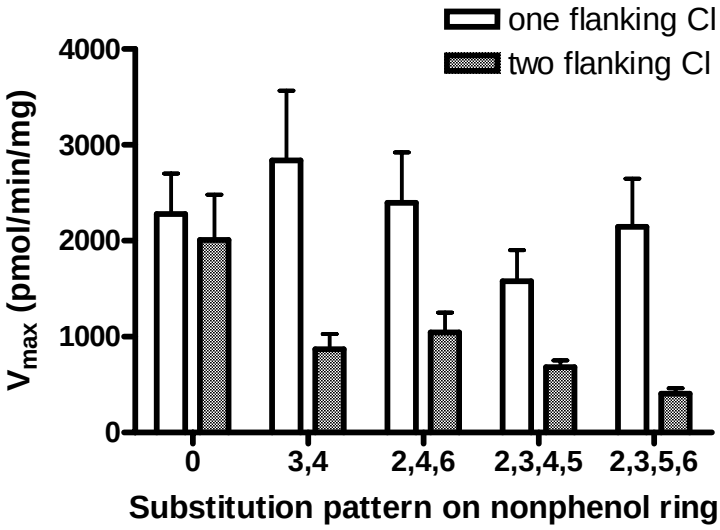

Figure 4-4. Decrease in V_{max} with addition of second chlorine atom flanking the phenolic group, while keeping the chlorine substitution pattern on the nonphenolic ring constant.

A) proximal intestine. B) liver.

Regression analysis was performed between the kinetic parameters for the glucuronidation of OH-PCBs and several physical parameters for these substrates (Table 4-5). The data for 4OHBP was not used since this compound is not a OH-PCB. The affinity of intestinal UGTs was negatively correlated with the Connolly solvent-accessible surface area, the molecular surface area, solvent-excluded volume, ovality, dihedral angle, log P, and positively correlated with pK_a. The maximum rate of hepatic glucuronidation was negatively correlated with the Connolly solvent-accessible surface area, the molecular surface area, solvent-excluded volume, ovality, and log P, and positively correlated with pK_a (which showed a similar relationship with intestinal V_{max}). Ovality was also significantly negatively correlated with the maximum rate of intestinal glucuronidation of the OH-PCBs studied (Figure 4-5).

A paired t-test performed in order to investigate the physicochemical parameters involved in the significant decrease in V_{max} observed for the glucuronidation of OH-PCBs with two chlorine atoms flanking the phenolic group revealed that, for OH-PCBs with this structural arrangement, pK_a was decreased (p=0.02), while log P, and parameters indicating molecular size (CAA, CMA, CSEV, ovality) were all increased (all p <0.0001).

Table 4-5. Results of regression analysis performed in order to investigate the relationship between the glucuronidation of OH-PCBs by catfish proximal intestine and liver and various estimated physical parameters.

Physical		**Intestine**		**Liver**	
Parameter	**Statistic**	**V_{max} (app)**	**K_m (app)**	**V_{max} (app)**	**K_m (app)**
CAA	R^2	0.060	0.439 (-)	0.253 (-)	0.004
	p-value	0.079	**<0.0001**	**0.0005**	0.685
CMA	R^2	0.056	0.423 (-)	0.249 (-)	0.002
	p-value	0.087	**<0.0001**	**0.0006**	0.780
CSEV	R^2	0.047	0.396 (-)	0.236 (-)	<0.001
	p-value	0.118	**<0.0001**	**0.0008**	0.962
Ovality	R^2	0.114 (-)	0.431 (-)	0.286 (-)	0.068
	p-value	**0.014**	**<0.0001**	**0.0002**	0.088
Dihedral	R^2	0.002	0.248 (-)	0.077	0.026
angle	*p*-value	0.755	**0.0002**	0.068	0.296
log P	R^2	0.058	0.111 (-)	0.250 (-)	0.061
	p-value	0.086	**0.044**	**0.003**	0.137
log D	R^2	0.011	0.035	0.015	<0.001
(*p*H 7.0)	*p*-value	0.467	0.271	0.490	0.963
pK_a	R^2	0.143 (+)	0.108 (+)	0.306 (+)	0.093
	p-value	**0.006**	**0.047**	**0.0007**	0.063

Sign in parentheses indicates type of correlation where it achieved significance.

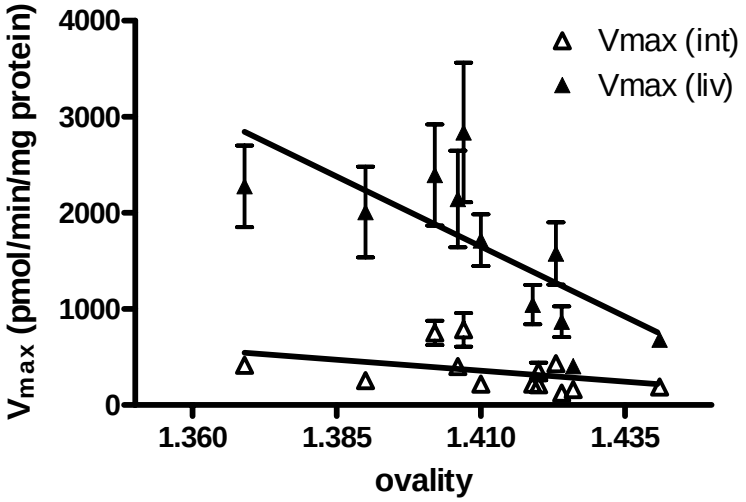

Figure 4-5. Relationship between V_{max} for OH-PCB glucuronidation in intestine and liver and ovality

Discussion

In comparison to catfish intestine, catfish liver displayed higher rates of glucuronidation of OH-PCBs, however both organs collectively biotransform the OH-PCBs studied with similar efficiency. This occurred because while the glucuronidation V_{max} in the intestine was lower than in the liver, the affinity of intestinal UGTs for the OH-PCBs was higher than liver UGTs. However, the efficiency of glucuronidation of 4′-OHCB69 was seven times higher in the proximal intestine; when the data for this substrate was excluded, the efficiency of glucuronidation was significantly higher (p=0.01) in liver.

The total UGT capacity in the liver is much greater than in intestine when the total content of microsomal protein in these two organs is taken into consideration. In fact, the levels of microsomal protein from liver were always higher than in the intestine of each individual fish studied, possibly because of the decreased amount of endoplasmic

reticulum in enterocytes relative to hepatocytes (DePierre et al., 1987). Thus, the intestine appears to compensate for the lower glucuronidation capacity by expressing UGTs with a higher affinity.

No relationship was established between K_ms for the glucuronidation of OH-PCBs in liver and intestine. When individual OH-PCBs were considered, there were significant differences in efficiency. These results suggest that these two organs have different UGT isoform profiles, with the intestine possessing one or more isoforms that display greater specificity for OH-PCBs. Possible UGT isoforms responsible may be catfish enzymes analogous to rat UGT1A1, UGT1A6 and UGT2B1 (Daidoji et al., 2005), and to plaice hepatic UGT1B1, which has been shown to conjugate planar phenols (Clarke et al., 1992).

The substrates 4′-OHCB69 and 4-OHCB39 were glucuronidated with the highest efficiency in the intestine and liver respectively. 4′-OHCB35 showed the highest rates of glucuronidation in both liver and intestine. The poorest substrates were 4-OHCB14 in the intestine and 4′-OHCB112 in the liver. In contrast, rat liver glucuronidates 4-OHCB14 with the highest efficiency, relative to other OH-PCBs studied (Tampal et al., 2002). Overall, the efficiency of glucuronidation of the OH-PCBs by rat liver is higher than in catfish liver. While these dissimilarities may be ascribed to differences in UGT isoform type and expression due to the different species and tissues in the two studies, it may also indicate an increased susceptibility of catfish to the toxic effects of OH-PCBs due to an increased bioavailability.

Compared to the OH-PCBs, 4-OHBP was the poorest substrate for glucuronidation. This compound had the lowest V_{max} in both liver and proximal intestine. The affinity for

4-OHBP in the intestine was also the lowest. In the liver however, the K_m was comparable to other OH-PCBs. These results are surprising in view of the fact that 4-OHBP has been shown to be a good substrate for glucuronidation using rat, guinea pig, beagle dog and rhesus monkey liver microsomes (Yoshimura et al., 1992), and human expressed UGTs (King et al., 2000; Ethell et al., 2002). In isolated rat hepatocytes, 4-OHBP is a cytotoxic major metabolite of biphenyl, impairing oxidative phosphorylation (Nakagawa et al., 1993). These results suggest that this compound may be potentially more toxic to catfish than to mammals, unless cleared by another pathway such as sulfonation.

While the decreased glucuronidation of 4-OHBP may be due to the lack of a specific phenol UGT isoform in catfish, the known broad substrate specificity of phenol UGTs, together with the observed higher rates of glucuronidation for the OH-PCBs, leads us to hypothesize that this compound may be such a poor substrate due to its lower lipophilicity, as has been observed for other substituted phenols (Kim 1991). In fact, addition of a single chlorine atom flanking the phenolic group (as represented by 4OHCB2) resulted in at least a tenfold increase in V_{max} in both liver and intestine, with no significant change in K_m (with respect to 4-OHBP). This increased lipophilicity (represented by an estimated log P increase from 3.2 to 3.8) appeared to impact the formation of the glucuronide and not the initial binding of substrate to UGT. Good UGT substrates tend to be lipophilic compounds which are thought to diffuse through the endoplasmic reticular bilayer and reach the substrate-binding site in the lumenal *N*-terminal part of the enzyme, which contains a region of strong interaction with the membrane (Radominska-Pandya et al., 2005). For all the OH-PCBs studied, we only

observed weak inverse correlations (R^2<0.3) between log P and intestinal K_m and liver V_{max}. No significant relationship could be observed between parameters of lipophilicity and intestinal V_{max}. The absence and weakness of such relationships may reflect the need for OH-PCBs with additional structural variation to be included in studies of this type. Another explanation may be the perturbation of the lipid bilayer of the microsomes, resulting in rate-limiting partitioning, which would not be present *in vivo* (Tampal et al., 2002).

As the estimated pK_a of the OH-PCBs increased, so did hepatic and intestinal V_{max} for glucuronidation. These results are in agreement with a previous OH-PCB glucuronidation study in rats (Tampal et al., 2002). Thus, a greater proportion of ionized OH-PCB molecules appear to have an adverse effect on glucuronidation. Such charged molecules present at the active site of UGT may interfere with the charge-relay system that relies on a basic negatively charged residue to deprotonate the phenolic group, prior to transfer of glucuronic acid (Yin et al., 1994).

Since the use of microsomal systems to elucidate structure-activity relationships involves incubations of substrate with a heterogeneous population of UGTs exhibiting different levels of expression and activity, it was not the intention of this study to attempt to predict the effect of molecular structure and physicochemical parameters on the glucuronidation of OH-PCBs, which is better achieved using individual isoforms. However, if any such effects can be observed at a microsomal level, then it is likely that such processes are occurring in the organism, whose detoxification route depends on various UGTs metabolizing substrate simultaneously and not in isolation. This may help to further delineate the different toxicokinetics of OH-PCBs.

The *p*-OH-PCBs used in this study all had one or two chlorine atoms flanking the phenolic group. This structural motif is of interest since it imparts several toxic properties to these compounds. OH-PCBs with two flanking chlorines were found to be poorer substrates than compounds with one flanking chlorine atom, in both liver and intestine. Thus, for example, while 4′-OHCB35 was a very good substrate for glucuronidation, addition of a second flanking chlorine (as in 4′-OHCB79) resulted in a greater decrease in V_{max} than the addition of two adjacent chlorine substituents on the aphenolic ring (as in 4′-OHCB106). A comparison of the physicochemical parameters of the two different structural arrangements suggests that lipophilicity, pK_a, and molecular size may all be contributing to this effect on V_{max}.

The addition of a second chlorine atom imparts additional lipophilicity to the molecule and may increase positive charge on the phenolic carbon atom, which results in stronger binding to the active site (Wang 2005). This study did show a non-significant decrease in K_m with the addition of the second chlorine atom for both organs. On the other hand, the 3,5-chlorine substitution pattern may interfere with the mechanism of glucuronidation because of steric hindrance, although this has been disputed (Mulder and Van Doorn 1975; Tampal et al., 2002).

The estimated pK_as for OH-PCBs with two flanking chlorine substituents were significantly lower than similar molecules with one flanking chlorine atom. This is supported by limited experimental data showing that OH-PCBs with two flanking chlorine atoms have pK_a values as low as 6.4 (for 4´-OHCB39, Miller 1978). The population of OH-PCB molecules which are ionized at physiological *p*H is significantly more than OH-PCBs with one flanking chlorine atom, resulting in the adverse effect on

the enzymatically-catalyzed charged relay system described above. In studies conducted with rat liver microsomes, a decreased maximal rate of glucuronidation was also observed amongst OH-PCBs differing only in the number of chlorines flanking the phenolic group (1 pair of OH-PCBs in Tampal et al., 2002; 2 pairs of OH-PCBs in Daidoji et al., 2005). According to Daidoji and co-workers (2005), UGT2B1 is the primary rat hepatic UGT isoform responsible for metabolizing OH-PCBs with one flanking chlorine atom. UGT1A1 appears to metabolize both, though with a preference for structures with two flanking chlorines

These results are significant from a toxicological standpoint since almost all the major OH-PCBs found in human plasma incorporate a 4`-hydroxy-3`,5`-dichloro structure (Sandau et al., 2002; Fangstrom et al., 2002; Hovander et al., 2002). It is possible that one reason for the persistence of these OH-PCBs may be a reduced rate of glucuronidation due to this structural arrangement.

Two or more chlorine substituents that are *ortho* to the biphenyl bond cause the molecule to twist and assume a non-coplanar conformation. In the parent PCBs this leads to toxicological differences, such as loss of AhR agonist activity. The estimated dihedral angles for the compounds investigated in this study ranged from 36°-76°. The affinity of intestinal, but not hepatic, UGTs appeared to increase with the degree of twisting, suggesting that the predominant isoform(s) in catfish intestine binds more strongly to the more twisted OH-PCBs. While this may be additional evidence of differences with respect to isoform profiles between liver and intestine, the weakness of the relationship (R^2~0.3) precludes using this result to solidly support this hypothesis.

Similar to what has been reported for the glucuronidation of OH-PCBs in rats (Tampal et al., 2002) and simple phenols by human UGT1A6 (Ethell et al., 2002), the maximal rate of hepatic glucuronidation decreased with increased steric bulk. In the case of intestinal glucuronidation this relationship was weaker. The enzyme affinity of intestinal UGTs increased with increasing molecular size, perhaps because the bulkier molecules tended to be more lipophilic. However, in contrast, the affinity of the liver UGTs was not affected as much by the molecular size, at least within the restricted size range offered by the OH-PCBs studied. At this point, no explanation for this discrepancy between these two tissues is forthcoming.

Conclusions and Recommendations

OH-PCBs are glucuronidated with similar efficiency by channel catfish liver and proximal intestine. There appear to be differences in the UGT isozyme profile in both organs. The V_{max} for both hepatic and intestinal glucuronidation was decreased with the addition of a second chlorine atom flanking the phenolic group, which is an arrangement typical of OH-PCBs that persist in organisms. Future research may be directed towards cloning, sequencing and characterizing these catfish UGTs, in order to have a better understanding of the specificity of individual UGT isoforms for particular chlorine substitution patterns in OH-PCBs.

CHAPTER 5
CLONING OF UDP-GLUCURONOSYLTRANSFERASES FROM CHANNEL CATFISH LIVER AND INTESTINE

Piscine UGT Gene Structure and Isoforms

Fish are the most ancient vertebrate phylum, and account for over 40% of all living vertebrate species (Clarke et al. 1992a). Clarke and co-workers (1992b) compared the hepatic glucuronidation of several xenobiotics and endobiotics in plaice (*Pleuronectes platessa*) and rat (*Rattus norvegicus*), species that are separated by more than 350 million years of evolutionary divergence. Despite the fact that the plaice showed reduced glucuronidation activity towards substrates such as morphine, bilirubin and steroids, weak immunological cross-reactivity was obtained when anti-rat UGT antibodies were used, indicating the presence of conserved common structural motifs between the two vertebrates.

Characterization of plaice UGT1B1 (Accession number (AN): X74116), an isoform which conjugates planar phenols and is inducible by polyaromatic hydrocarbons (PAH), confirmed the strong degree of conservation in gross exon structure and amino acid character (signal peptide, membrane insertion, and stop sequences) between fish and mammals. The greatest degree of similarity in amino acid sequence was found with UGT1 rather than UGT2 (Clarke et al., 1992b, George et al., 1998). Allelic variations in this UGT1B1 gene are presumed to be functionally silent (George and Leaver 2002). While there is strong evidence for other distinct isoforms conjugating bilirubin, estrogen and androgens, to date these have not been characterized. At least six distinct UGTs

exhibited tissue-specific expression in plaice (Clarke et al., 1992c). UGT1B2 mRNA has recently been sequenced from marbled sole (*Pleuronectes yokohamae*) liver (AN: AB120133), and a partial sequence of an unidentified UGT isoform has been obtained from the orange-spotted grouper (*Epinephelus coioides*) (AN: AY735003). The existence of a number of partial length sequences of UGT homologues from zebrafish (*Dario rerio*) EST projects in GenBank provide evidence for the cDNA of 10 distinct UGTs. The absence of cDNAs with the same 3′sequence and dissimilar 5′exon 1 coding sequence suggests the absence of alternative splicing of UGT1A genes as seen in mammals. Thus, George and Taylor (2002) have suggested the existence of three family 1-related UGTs and another two related to the UGT 2 family in the zebrafish. In general, however, it appears that fish possess multiple UGTs with similar functional and structural properties to mammalian UGT.

Toxicologically, it is important to know whether xenobiotic pollutants such as PAHs compete with steroids or bilirubin for the same active site on UGT, resulting in physiological perturbations in reproductive and/or liver function. For example, Atlantic salmon (*Salmo salar*) suffering from a multiple pollutant-induced jaundice were shown to have decreased bilirubin UGT activity (George et al. 1992). Channel catfish are also exposed to pollutants (such as PAHs and PCBs) which accumulate in sediments. Thus, this organism may be a useful indicator of the bioavailability of these pollutants in such sedimentary environments. In addition, the use of this fish in aquaculture makes it essential to understand every aspect of its detoxification mechanisms, since these will ultimately impact human health.

While no UGTs have yet been cloned and characterized from channel catfish, this species shows glucuronidation activity towards a variety of toxic xenobiotics, including mono- and di-hydroxy metabolites of benzo[a]pyrene and OH-PCBs (James et al., 2001; van den Hurk and James 2001; Gaworecki et al., 2004). As with other aquatic species, pollutants which are direct substrates for glucuronidation, such as pentachlorophenol, several OH-PCBs, 4-OH-heptachlorostyrene, and which have been shown to be estrogenic and thyroidogenic, have been detected in channel catfish (Li et al., 2003). Kinetic differences have been observed between hepatic and intestinal UGT activities, suggesting expression of different isozymes in these two organs. Thus, knowing more about the identity and substrate specificity of catfish UGTs will assist our understanding of the effect of glucuronidation on the contributions of such metabolites to toxicity. Since the absence of cDNAs with the same 3′sequence and dissimilar 5′exon 1 coding sequence in fish suggests the absence of alternative splicing of UGT1A genes as seen in mammals (Gong et al., 2001), additional information on piscine UGT gene structure is also important from a phylogenetic perspective.

Hypothesis

Multiple UGT isoforms are present in channel catfish liver and intestine

Methodology (part 1)

For convenience, a flowchart summarizing the various steps involved in the cloning process is shown in Figure 5-1. Because the study utilizing the gene specific primers was dependent on an initial study which utilized degenerate primers and led to the cloning of partial sequences of UGT, the methodology and results sections are split correspondingly in two parts.

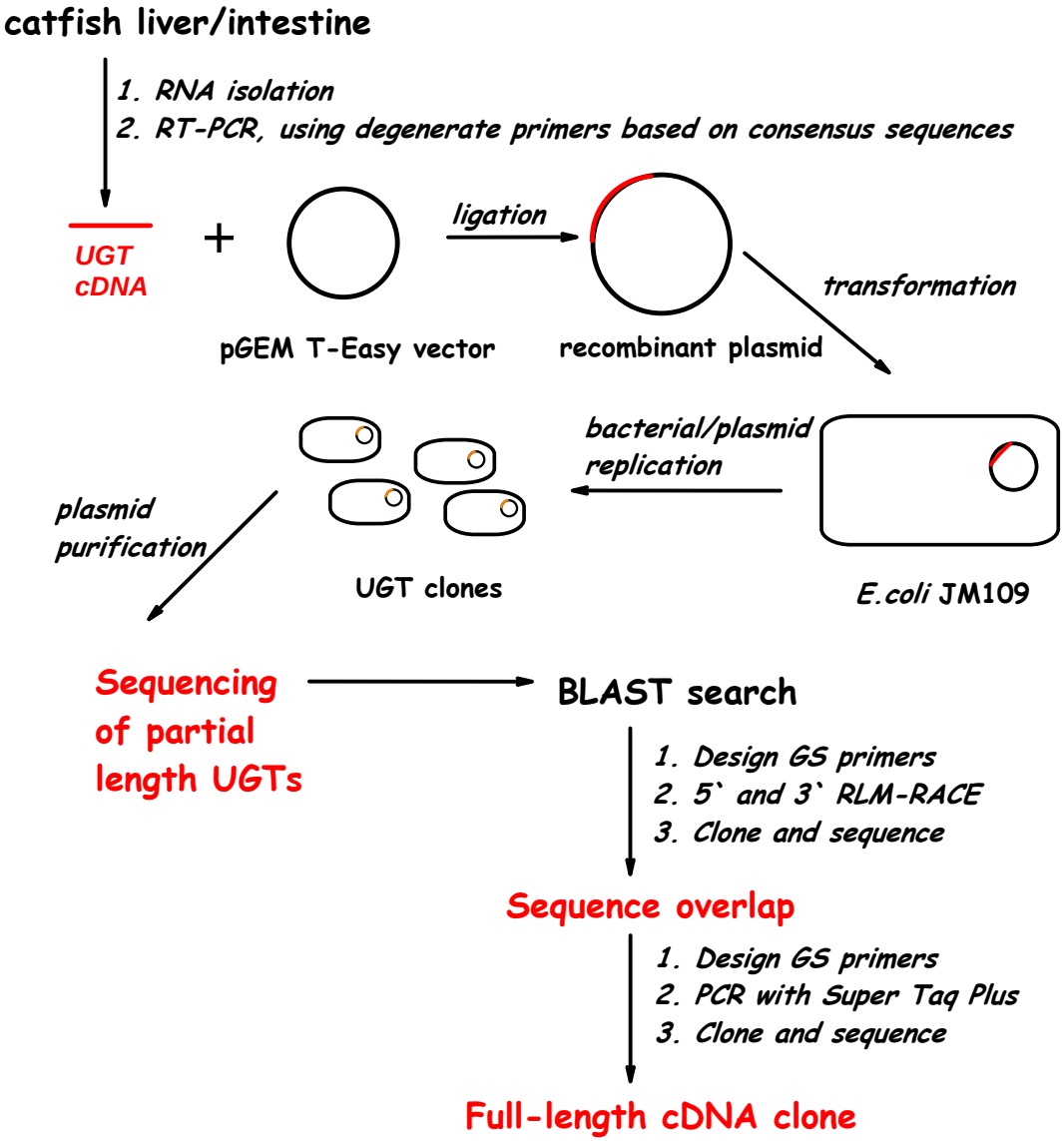

Figure 5-1. Summary of methods used to clone channel catfish UGT

Animals. A single female adult catfish was sacrificed. Total weights of liver and intestinal mucosa were recorded. Tissues were immediately processed for RNA isolation.

RNA isolation. Approximately 0.1g of tissue from the liver and proximal intestinal mucosa were homogenized in separate tubes with 1 mL Trizol® reagent and placed on ice. The homogenates were incubated for 5 min at room temperature (15-30°C) to enable complete dissociation of nucleoprotein complexes. Chloroform, 0.2 mL, was added and

the tubes were shaken vigorously by hand for 15 seconds and then incubated at room temperature for 2-3 min. The samples were then centrifuged at 12,000g for 15 min at 2-8°C. This separated the solution into an aqueous phase containing the RNA and an organic phase containing DNA. The colorless upper aqueous phase was transferred to an RNase-free tube. The RNA was precipitated by the addition of 0.5 mL propan-2-ol. The samples were then incubated at room temperature for 10 min, followed by centrifugation at 12,000g for 10 min at 2-8°C. The RNA precipitate was now visible as a gel-like pellet on the side and bottom of the tube. The supernatant was removed and the RNA pellet was washed once with 1 mL 75% ethanol. The sample was vortex-mixed and centrifuged at 7,500g for 5 minutes at 2-8°C. The RNA pellet was left to air-dry for a few minutes following decantation of the ethanol. The RNA was dissolved in 100 μL RNase-free water for intestine, and 200 μL RNase-free water for liver (since the solution in this case appeared to be more concentrated), by passing the solution a few times through a pipette tip. The solution was then incubated for 10 minutes at 55-60°C. The samples were stored at -80°C. The purity of the RNA was checked by running the sample on 1% agarose gel (with 9.5% formaldehyde) and 10x MOPS buffer. Bands corresponding to the 28S and 18S ribosomal subunits were observed. The purity of the RNA was also checked by diluting the sample in 10mM Tris HCl, *p*H 7.5 and measuring the A_{260}/A_{280} absorbance ratio (ideally should be between 1.8 and 2.1).

DNase treatment of RNA samples. This procedure was done in order to remove contaminating DNA from RNA preparations, and to subsequently remove the DNase and divalent cations from the sample. Portions of the RNA solutions were diluted to 100 μg/mL with RNase-free water. The Ambion ® (Austin, TX) DNA-removal kit was used.

The reaction mix, consisting of 25 μL RNA, 2.5 μL 10xDNaseI buffer, and 3 μL DNase I was incubated at 37°C for 1 hour. DNase inactivation reagent, 5 μL, was added by means of a wide pipette tip (due to the thick consistency of this reagent). The tubes were then incubated for 2 min at room temperature, with gentle flicking. The tubes were then centrifuged at 10,000g for ~1 min to pellet the DNase inactivation reagent. The supernatant containing the RNA was transferred to a new RNase-free tube and stored at -80°C.

Generation of cDNA library. The Retroscript® reagent kit manufactured by Eppendorf (Westbury, NY) was employed in order to heat-denature the RNA. To each of the two tubes were added 10 μL liver or intestinal RNA (equivalent to 1 μg) and 2 μL random decamers. The tubes were mixed, centrifuged briefly and heated for 3 min at 70-85°C in the thermocycler. Tubes were removed and left on ice for 1 minute. They were centrifuged and put on ice again. The following components were added to each tube: 2 μL 10xRT buffer, 1 μL dNTP mix (10mM), 0.5 μL RNase inhibitor, 1 μL reverse transcriptase, and RNase-free water to 20 μL. The tubes were gently mixed and centrifuged briefly. They were placed in the thermocycler for 1 hr at 42-44°C, followed by 92°C for 10 min. The resulting cDNA was either stored at -20°C or subjected to a second round of PCR (liver, see below; for the intestine this procedure was performed a few days after cDNA generation).

Degenerate primer design. A characteristic 'signature sequence', 44-amino acids long, probably corresponding to the UDPGA binding site, has been shown to be highly conserved amongst mammals and other vertebrates (Mackenzie et al., 1997). The relevant amino acid and nucleotide sequences were compared in 4 species of fish using ClustalW.

The species investigated were *Pleuronectes platessa* UGT1B1, *P.platessa* UGT, *Pleuronectes yokohamae* UGT1B2, *Epinephelus coiodes* UGT and *Danio rerio* UGT. Five primers were designed which could hypothetically bind to this sequence. The application of exclusion criteria (degeneracy <100-fold, poor or no matches with fish sequences resulting from BLASTn searches, %GC content <40%, potential to self-dimerize < -20 kcal/mol) resulted in the selection of two primers, designated as UGT_R3 and UGT_R4, and chosen to be reverse primers (Table 5-1). An additional reverse primer (UGT_R5) was chosen due to its low degeneracy (4-fold) and its complementarity to the highly conserved N-terminal domain downstream of the signature sequence. Five additional primers (UGT_F3-7) were also chosen based on these same criteria. Since these primers were complementary to sequences upstream of the signature sequence, they were selected to be forward primers (Table 5-1).

Table 5-1. 5'→3' Sequences of degenerate primers chosen.

ID	Sequence	Direction
UGT_F3	GTGGTSCTGGTSCCYGAAASYAGY	Forward
UGT_F4	CTTACWGAYCCMTTCYTKCCSTGYGGC	Forward
UGT_F5	AACATGGTYYWWATYGGRGGYATCAACTGT	Forward
UGT_F6	ATYGGRGGYATCAACTGTGCA	Forward
UGT_F7	GAGTTTGTSVAHGGCTCWGGA	Forward
UGT_R3	AAACAGHGGRAACATCAVCAT	Reverse
UGT_R4	YCCYTGSTCKSCAAACAGHGG	Reverse
UGT_R5	GTGRTACTGRATCCAGTTCAG	Reverse

The primer pairs were selected in such a way that their melting temperatures did not vary by more than 6°C and their potential to heterodimerize was more than –20 kcal/mol (Table 5-2)

Table 5-2. Primer pairs chosen, showing annealing temperature and estimated amplicon length

Pair	Forward	Reverse	Amplicon length (bp)[1]	T (°C)
3	UGT_F6	UGT_R5	618	52.6
4	UGT_F7	UGT_R3	288	53.8
5	UGT_F6	UGT_R3	339	53.8
6	UGT_F7	UGT_R5	567	52.6
7	UGT_F5	UGT_R4	363	61.1
8	UGT_F3	UGT_R4	1003	61.1
9	UGT_F4	UGT_R4	729	61.1

[1] Based on *Danio rerio* UGT sequence (Accession number NP_998587.1)

PCR amplification of UGT cDNA. A 10 μM solution of each primer in nuclease-free water was made up. Each PCR tube consisted of 2 μL DNA template (from catfish), 2 μL forward primer, 2 μL reverse primer, 0.5μL Taq DNA polymerase (5U/μL, in Mg 10x buffer), 1 μL dNTP mix (10mM), 5 μL 10xPCR buffer, and nuclease-free water up to 50 μL. Prior to the initiation of the PCR reaction, with the tubes in place, the thermocycler lid was heated for two minutes at 110°C to prevent sample evaporation. Thermocycler parameters (utilizing a gradient PCR program to adjust for the different optimal annealing temperatures required by the various primer pairs) were as follows:

Stage	Temp /°C	Duration/min
Initial Denaturation	94	2
Denaturation	94	0.5
Annealing	57±5 (L); 55±5 (I)[1]	0.5
Extension	72	1.0
Final extension	72	7.0

[1] annealing temperatures used for: L, liver; I, intestinal cDNA
The program consisted of 35 cycles of denaturation, annealing and extension.

The PCR products were subjected to electrophoresis on 1% agarose gel at 100V (in 1x TAE buffer (40 mM Tris base, 5 mM sodium acetate, 1 mM EDTA, *p*H 8.0)) using 30 μL of PCR product; a 100bp DNA ladder was used for size estimates. The DNA bands were visualized by placing on a UV transilluminator and recorded by photography.

Recovery of PCR product from gel and purification. The desired DNA band was excised from the gel using a clean scalpel and transferred to a pre-weighed 1.5mL microcentrifuge tube. The Wizard ® SV Gel Clean Up system (Promega, Madison, WI) was used to purify the PCR product by centrifugation. Membrane binding solution (4.5 M guanidine isothiocyanate, 0.5 M potassium acetate, *p*H 5.0), 10 μL per 10 mg gel, was added to the gel slice. The mixture was vortexed and incubated at 51°C for 10 min in order to dissolve the gel slice. The tube was then briefly centrifuged at room temperature. For every solution (derived from the cut gel slices), the following procedure was adopted. One SV Minicolumn was placed in a collection tube. The dissolved gel mixture was transferred to the SV Minicolumn assembly and incubated for 1 min at room temperature. The assembly was centrifuged in a microcentrifuge at 16,000*g* for 1 minute and the liquid

in the collection tube was discarded. The column was washed by 700 μL of Membrane Wash Solution (10 mM potassium acetate, *p*H 5.0, 16.7 μM EDTA, *p*H 8.0, 80% ethanol). The assembly was centrifuged for 1 min at 16,000g, and the collection tube was emptied. Another 500 μL Membrane Wash Solution was added to the assembly, followed by centrifugation for 5 minutes at 16,000g. The collection tube was emptied, and the collection tube was recentrifuged for 1 minute to dry the column. The SV Minicolumn was transferred to a clean 1.5 mL microcentrifuge tube and 50 μL nuclease-free water was applied to the column and incubated for 1 minute at room temperature. The Minicolumn/micro-centrifuge tube was centrifuged for 1 minute at 16,000g. The Minicolumn was discarded and the tube containing the eluted DNA was stored at -20°C. A portion of this DNA was diluted with 10 mM Tris-HCl, 1 mM EDTA, *p*H 8.0, and used to calculate the DNA concentration by its absorbance at 260nm.

Ligation and transformation of *E.coli*. LB plates with ampicillin were first prepared. LB Agar, 8.75 g, was weighed and dissolved in 250 mL, and the *p*H was adjusted to 7.2 with NaOH. The solution was autoclaved for 30 min at 120°C. After the medium cooled to around 50°C, ampicillin was added to a final concentration of 100 μg/mL. Some of the medium, 30-35 mL, was poured into 85-mm Petri dishes and the agar left to harden. The plates were left overnight at room temperature and subsequently stored in an inverted position at 4°C

The ligation was performed using the p-GEM T-Easy Vector System® supplied by Promega. The volume of PCR product to be used in the ligation reaction could not exceed 3 μL. The amount required was calculated from the following equation, which assumes that the optimal insert:vector molar ratio is 3:1:

$$\frac{50 \text{ ng vector} \times a \text{ kb insert}}{3.0\text{kb vector}} \times \frac{3}{1} = \text{ng insert required}$$

where *a* is the approximate size of amplified insert

Because of this limit in sample volume, the amount of insert actually used was less than that recommended since the concentration of purified DNA was relatively low. The ligation reactions were setup as follows (all volumes in μL) in 0.5 mL tubes:

Component	Standard Reaction	Positive Control	Background Control
2x Rapid Ligation Buffer, T4DNA ligase	5	5	5
pGEM T-Easy Vector (50 ng)	1	1	1
PCR-product (9 ng)	3	---	---
Control insert DNA	---	2	---
T4 DNA ligase (3 Weiss units/μL)	1	1	1
DNase-free water	0	1	3

The ligation buffer was mixed vigorously before use. The reactions were mixed by pipetting and incubated for 1 hour at room temperature, followed by storing overnight at 4°C.

JM109 high-efficiency competent cells (≥1x10^8 cfu/μg DNA; Promega) were used for transformation. The following procedure was performed using aseptic technique (sterile tips and tubes, use of Bunsen flame to create upward convection in work area). The tubes containing the ligation reactions were centrifuged for 1 minute at 10,000 rpm and placed on ice. Another tube (transformation control, TC) was set up on ice; this contained 0.1 ng uncut plasmid (0.1 μL of 0.1 mg/μL solution used) in order to determine the transformation efficiency of the competent cells. Tubes containing frozen aliquots of JM109 cells were removed from -80°C storage and placed on ice until thawed (~5 min).

The cells were mixed by gentle flicking of the tubes. Each ligation reaction, 2μL, was added to a 1.5 mL microcentrifuge tube on ice, followed by 50 μL of cells (100 μL were added to the TC). The tubes were mixed by gentle flicking and left on ice for 20 minutes. The cells were heat-shocked by placing in a 42°C water bath for 45-50 sec. The tubes were then returned to ice for 2 minutes. S.O.C medium (Invitrogen Corp., Carslbad, CA), 950 μL, was added to each tube (900 μL was added to the TC). The tubes were then incubated for 1.5 h at 37°C with shaking (~150 rpm). The ampicillin/LB plates were removed from 4°C storage, 100 μL of 100 mM isopropylthiogalactoside (IPTG, a β-galactosidase inducer) and 20 μL of 50 mg/mL 5-bromo-4-chloro-3-indolyl-β-*D*-galactoside (X-Gal, hydrolyzed by β-galactosidase to yield a blue product) were added, and the mixture spread on each plate. The agar was allowed to absorb these compounds for 30 min at 37°C. Samples, 100 μL, of each transformation culture were transferred to, and streaked on, duplicate LB/ampicillin/IPTG/ X-Gal plates; for the TC, 20μL of tube culture was diluted with 180 μL of S.O.C. medium, and 100 μL of this dilution was applied to the agar plates. The plates were incubated overnight (~16h) at 37°C. Plates were then stored at 4°C for 30 minutes to facilitate color development. The white colonies should contain plasmids with the insert, while the blue colonies do not contain the insert since the protein-encoding sequence of the *lac Z* gene in the vector is not interrupted by the insert and hence can lead to β-galactosidase synthesis and catalysis of the X-Gal reaction.

Colony PCR and culturing E.coli with insert of interest. Two white and one blue colony from each plate were picked by a sterile wooden toothpick, which was inserted in a PCR tube containing 5 μL 10x PCR buffer, 5 μL 10mM dNTP mix, 1 μL

PUC/M13 forward primer, 1 μL PUC/M13 reverse primer, 0.5 μL Taq DNA polymerase, and DNase-free water to 50 μL. The pGEM T-Easy Vector contains binding sites for the PUC/M13 primers. Thermocycler parameters were as shown previously, but with an annealing temperature of 55°C (no temperature gradient). PCR products were run on 1% agarose gel at 100V, using 15 μL of the PCR product.

Samples from colonies which showed the presence of insert on the gel were extracted by an ethanol-flame sterilized metal hoop and dispensed into 14 mL sterile, round-bottomed Falcon tubes containing 4 mL of LB medium with ampicillin by swirling. The tubes were incubated with shaking for 16-20 h at 37°C.

Purification of plasmid DNA. A sample, 850 μL, of each culture medium was diluted up to 1000 μL with sterile glycerol and stored at -80°C. The rest of the culture medium was dispensed in 1.5 mL microcentrifuge tubes, which were centrifuged for 2 min at 10,000g. The supernatant was poured off and the tubes were blotted upside-down on a paper towel to remove excess media. For plasmid purification, the Promega Wizard Plus Minipreps ® DNA Purification System was used. The cell pellets were resuspended in 200 μL of cell resuspension solution (50 mM Tris-HCl (*p*H 7.5), 10 mM EDTA, 100 μg/mL RNase A). Cell lysis (0.2 M NaOH, 1% SDS) solution, 200 μL, was added and the tubes inverted 4 times to clarify the solution. Neutralization solution (1.32 M potassium acetate, *p*H 4.8), 200 μL, was added and mixed by inverting the tubes for 4 times, resulting in a white precipitate. The lysate was centrifuged at 10,000g for 5-20 minutes, depending on whether a cell pellet was clearly visible.

One Wizard® Minicolumn was prepared for every Miniprep. A plunger was removed from a 3 mL disposable syringe and set aside. The syringe barrel was attached

to the Luer-Lok® extension of the Minicolumn. DNA purification resin (7 M guanidine HCl), 1 mL, was pipetted in the barrel, followed by the cell lysate. The syringe plunger was inserted in the barrel and used to push the slurry through the Minicolumn. The syringe was detached from the Minicolumn and the plunger removed from the syringe barrel. The barrel was then reattached to the Minicolumn. Column wash solution (80 mM potassium acetate, 8.3 mM Tris-HCl (*p*H 7.5), 40 μM EDTA, 55% ethanol), 2 mL, were pipetted into the barrel of the Minicolumn/syringe assembly, and the solution was pushed through the Minicolumn by the plunger. The syringe was removed, and the Minicolumn was transferred to a 1.5 mL microcentrifuge tube, which was centrifuged at 10,000g for 2 min to dry the resin. The Minicolumn was transferred to a new 1.5 mL microcentrifuge tube and 50 μL nuclease-free water was added to the column and left for 1 minute. The DNA was eluted by centrifuging at 10,000g for 20 sec. The Minicolumn was removed and discarded, and the DNA solution stored at -20°C. Products were visualized by 1% agarose gel electrophoresis run at 100V, using 3 μL of purified DNA and 10 μL quantitative 1kb plus DNA ladder (0.5 μg).

Digestion with ecoRI. To ensure that the two DNA bands seen in the purified plasmid DNA run on agarose gel were due to supercoiling of the DNA and not contamination, the plasmid DNA was digested with the restriction enzyme ecoRI (pGEM T-Easy Vector has restriction sites on either side of the insert). Plasmid DNA, 3 μL, was added to a tube containing 0.2 μL acetylated BSA, 2 μL 10x buffer, and 14.3 μL DNase-free water, and mixed by pipetting. ecoRI restriction enzyme (12 U/μL), 0.5 μL, was added and the solution mixed by pipetting. The tubes were briefly centrifuged and

incubated for 2h at 37°C. The products were run in 1% agarose at 100V, using all the incubation mixture.

DNA sequencing and data processing. The concentration of the purified plasmid DNA was determined prior to submission for sequencing. The DNA sequencing core requires 1.5 μg DNA for adequate processing. Cloned DNA sequences obtained were then compared with nucleotide sequences in GenBank using the BLASTn tool provided online (http://www.ncbi.nlm.nih.gov/BLAST). Multiple sequence comparisons were done with SeqWeb, while two-sequence comparisons were done with the BLASTn 2.2.12 program.

Results and discussion (part 1)

Primer pairs 4 and 6 successfully amplified cDNA from catfish liver; while primer pair 4 amplified cDNA from proximal intestine. The size of the amplicons were approximately 300bp (pair 4) and 600bp (pair 6) in size, with the gel-clean up system effectively removing primer dimers and other contamination (Figure 5-2). The controls indicated that ligation and transformation of the plasmid into *E.coli* were successful. Purified plasmid DNA was obtained from several colonies (Figure 5-3), which were denoted as L1-L8 for the liver and I1-I4 for the proximal intestine. The two bands seen in these gels, did not represent contamination, as verified by the restriction digest of the plasmid, which resulted in a band corresponding to the vector and one corresponding to the smaller insert (Figure 5-4).

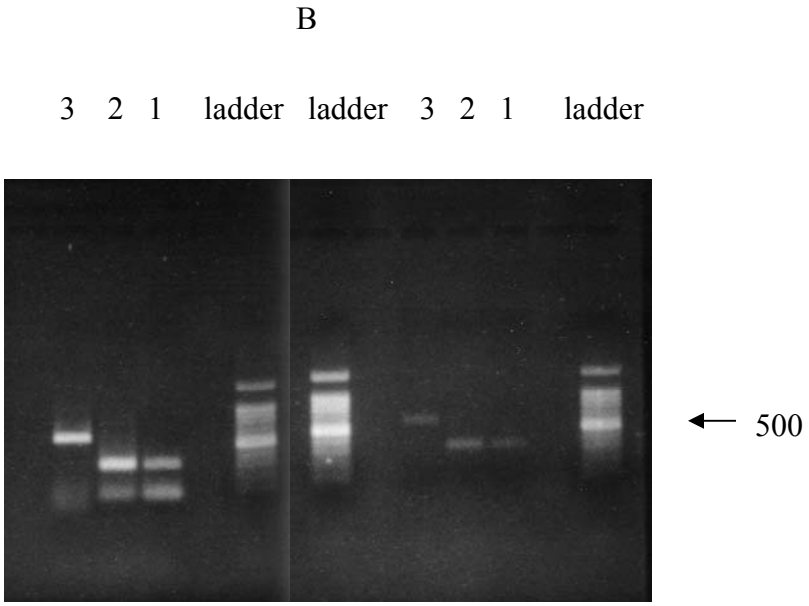

Figure 5-2. Products of PCR reaction. 1(from intestine), 2 and 3 (from liver)

A. pre-cleanup; B. post-cleanup with the gel clean-up system. 100kb ladder shown for size estimation.

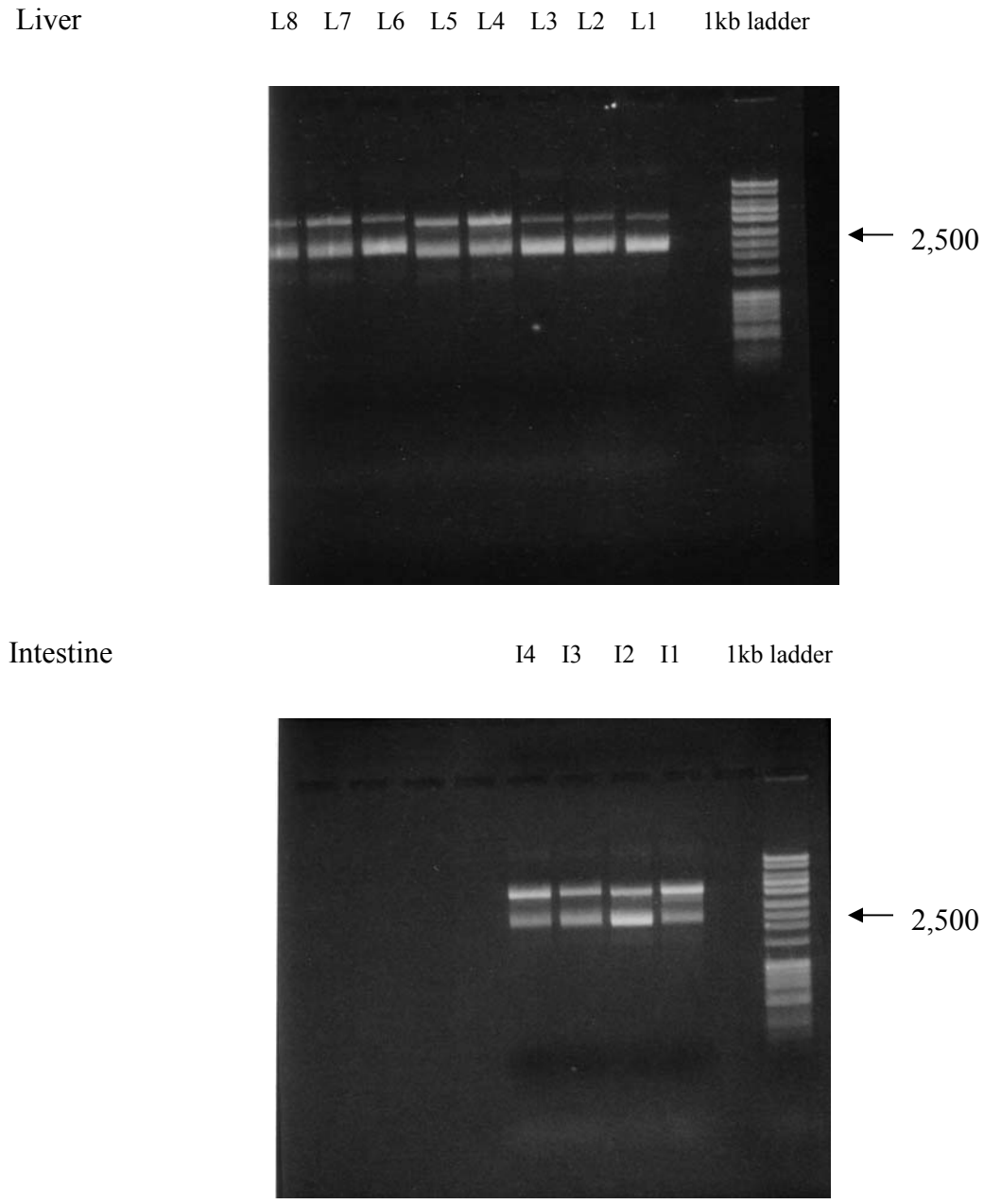

Figure 5-3. Plasmid DNA obtained from cultures transformed with vector containing inserts from liver and intestine.

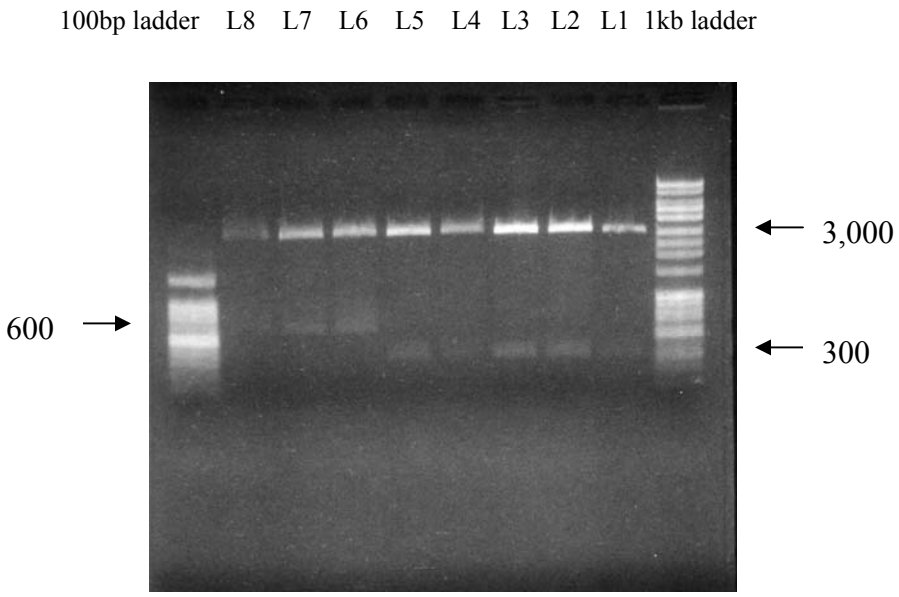

Figure 5-4. Product of ecoRI digest of purified plasmids containing liver inserts L1-L8

The DNA sequences obtained are detailed in Appendix A. The results of the BLASTn search (best five sequences for each insert) are summarized below (Table 5-3). Very good matches were obtained with the *Tetraodon nigroviridis* cDNA, as well as *Pleuronectes yokohamae* UGT1B2, several *Danio rerio* sequences and *Strongylocentrotus purpuratus* (sea-urchin) UGT2B sequences. There was also a good similarity between the longer insert and the mammalian UGT1A sequences.

Better matches were obtained with the longer cDNA insert obtained from the liver (95 sequences with score >50) than with the shorter insert from liver or intestine (9 sequences with score >50).

Table 5-3. Results of BLASTn search of cloned putative partial UGT sequences

Accession no.	Short description	Insert	Score (bits)	E-value
CNS0EY06	*Tetraodon nigroviridis*, full length cDNA	L1	123	3E-25
		L4	115	8E-23
		L7	113	6E-22
		I1	107	2E-20
CNSOEVYF	*Tetraodon nigroviridis*, full length cDNA	L1	123	3E-25
		L4	115	8E-23
		L7	113	6E-22
		I1	107	2E-20
AB120133.1	*Pleuronectes yokohamae* UGT1B2 mRNA	L7	85.7	1E-13
		L1	67.9	2E-08
		L4	67.9	2E-08
		I1	60.0	4E-06
AF104339	*Macaca fascicularis* UGT1A01, mRNA	L7	63.9	5E-07
BC109404.1	*Danio rerio* cDNA clone	L7	61.9	2E-06
BC100055.1	*Danio rerio* cDNA clone	L1	60.0	4E-06
		I1	52.0	1E-03
BX005348.9	*Danio rerio* DNA sequence from clone	L1	60.0	4E-06
		I1	52.0	1E-03
XM 792456.1	*Strongylocentrotus purpuratus*, UGT2B34	L4	54.0	3E-04
XM792428.1	*Strongylocentrotus purpuratus*, UGT2B17	L4	54.0	3E-04

SeqWeb analysis of the sequences showed that the short inserts were almost identical with almost all the differences being located in the primer regions and thus may be attributed to the degenerate nature of the primers. Sequence L1 was found to be 98% similar to both sequences L7 and I1. While this implied that all these sequences are derived from the same isozyme, this could not be ascertained since most of the sequence differences between UGT isoforms arise from the N-terminal (substrate-binding) domain and only that part of the gene which codes for the highly conserved C-terminal domain was cloned.

Methodology (part 2)

The next step in the cloning study was thus to design GSPs in order to extend the partial UGT sequences obtained so far to the full-length gene.

Overview of RLM-RACE

RNA-ligase mediated rapid amplification of cDNA ends, or RLM-RACE is a procedure used to extend a known DNA sequence towards its 5′- and its 3′- ends (Maruyama and Sugamo, 1994; Shaefer 1995).

In 5′-RACE, total RNA is treated with calf intestinal phosphatase (CIP) to remove free 5'-phosphates from molecules such as ribosomal RNA, fragmented mRNA, tRNA, and contaminating genomic DNA. The cap structure found on intact 5'-ends of mRNA is not affected by CIP. The RNA is then treated with tobacco acid pyrophosphatase (TAP) to remove the cap structure from full-length mRNA, leaving a 5'-monophosphate. A 45 base RNA Adapter oligonucleotide is ligated to the RNA population using T4 RNA ligase. The adapter cannot ligate to dephosphorylated RNA because these molecules lack the 5'-phosphate necessary for ligation. During the ligation reaction, the majority of the full-length decapped mRNA acquires the adapter sequence as its 5'-end. A random-primed reverse transcription reaction and nested PCR then amplifies the 5'-end of a specific transcript (Figure 5-5). The Ambion kit used in this study provided two nested primers corresponding to the 5'-RACE Adapter sequence, while two nested antisense primers were designed to be specific to the target gene.

In 3′-RACE, first-strand cDNA is synthesized from total RNA using the supplied 3'-RACE Adapter. The cDNA is then subjected to PCR using one of the 3'-RACE primers which are complimentary to the anchored adapter, and a user-supplied primer for the gene under study (Figure 5-5). Although 3'-RACE may not require a nested PCR

reaction, this may also be performed if no significant amplicons are detected after the outer PCR.

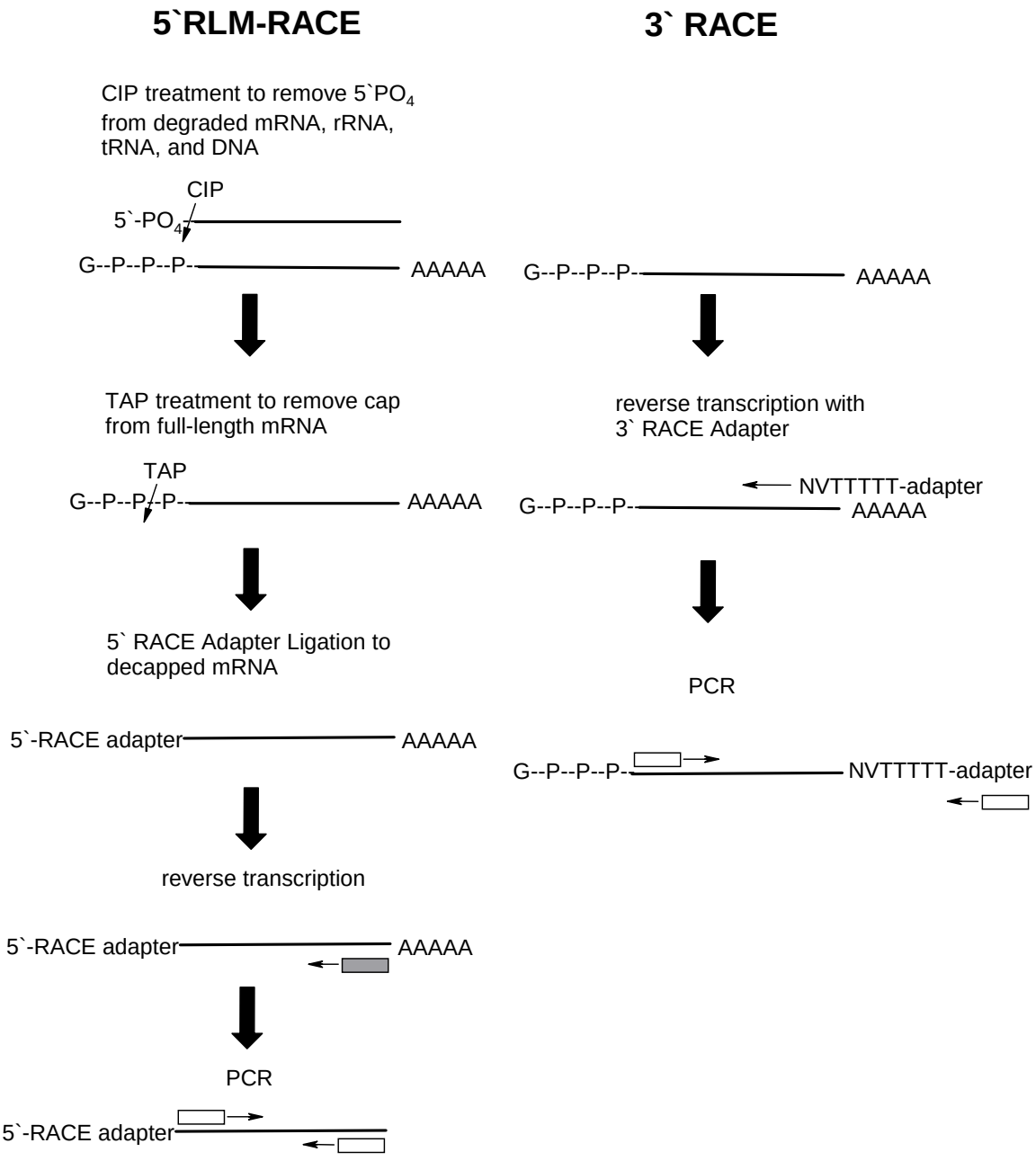

Figure 5-5. 5′- RLM-RACE and 3′- RACE

Design of gene-specific primers (GSPs) for initial 5′-RACE study. The initial primers used for RACE were designed to be 20-24 bases in length, with 50% G:C content, and with no secondary structure. Primers contained less than 3G or C residues in the 3`-most 5 bases, and did not have a terminal G at the 3`-end. An online oligonucleotide analyzer (www.idtdna.com) was used to determine whether potential primers self-hybridized or hybridized to the primers supplied with the RLM-RACE Kit. Figure 5-6 shows where the gene-specific primers and the primers supplied with the kit should be positioned with respect to the DNA template.

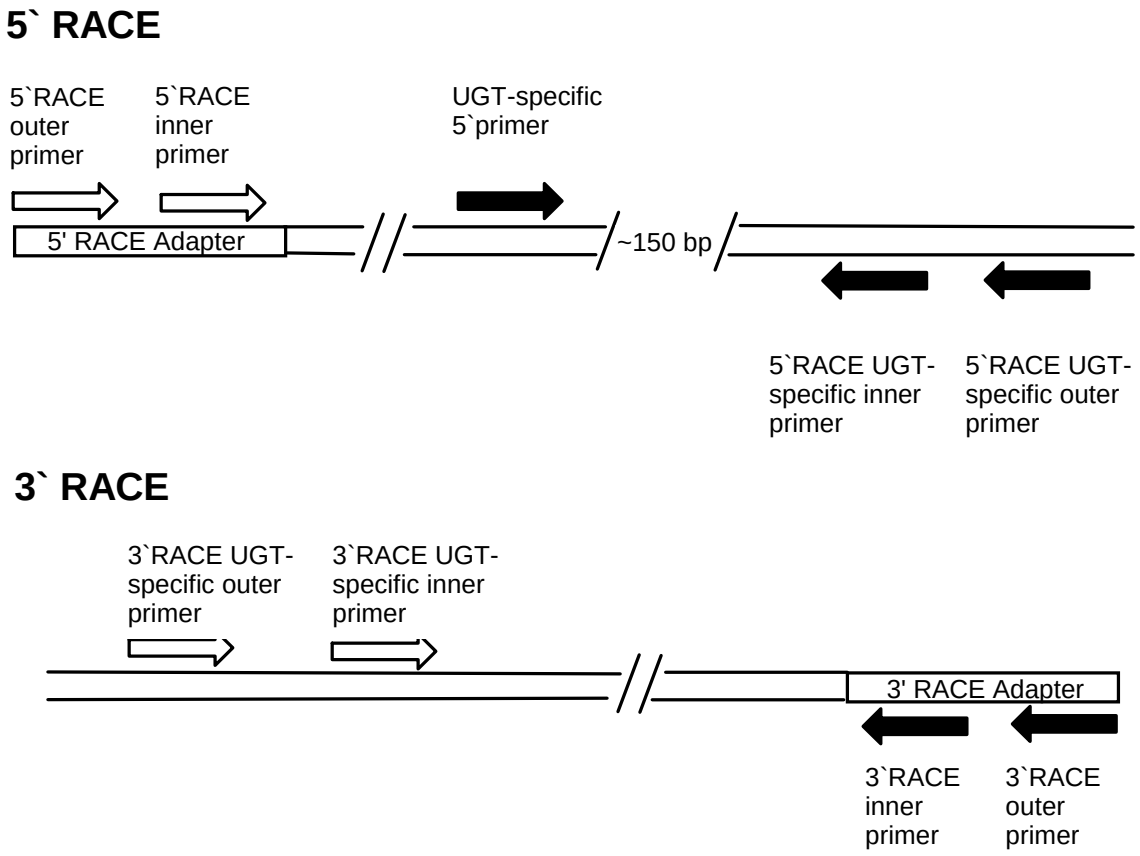

Figure 5-6. Primer positions for 5′- and 3′-RACE.

The DNA templates selected were those identified from the previous study, that is, the sequence isolated from liver (L6) and intestine (I4). The primers used in this initial study are shown in Table 5-4.

Table 5-4. Gene-specific primers used in initial 5`RLM-RACE study.

GSP ID	Sequence (5′→3′)	Start position[1]	PCR step
GSP_OUT	TGCTCTGAGGTCAGGTCGAA	397	Outer
GSP_INN	ACAGATACCCTCGTAGATGCCA	280	Inner

[1] From 5′ end of sense strand of partial sequence L6

Based on homology with the complete sequences of *Pleuronectes platessa* UGT1 (PPL249081) and *Macaca fascicularis* UGT1A1 (AF104339) it was estimated that, for the UGT sequence isolated from catfish liver, this sequence needed to be extend by ~920 bp to the 5`-end, and ~183 bp to the 3`-end. Unfortunately, the use of these primers led to sequences which still lacked the 5′-end (L15R, L25R, L35R, I15R, I25R, I35R; see Appendix A). In addition, a high degree of non-specific binding was noted.

Design of GSPs for succeeding 5′- and 3′-RACE study. A new batch of GSPs was designed (Table 5-5) using different criteria than the ones mentioned above in an attempt to improve sensitivity. Primer 3.0 Software (http://frodo.wi.mit.edu/cgibin/primer3/primer3_www.cgi) was used to design primers, based on the following criteria:

a. For 5′-RACE, GSPs with a GC-clamp at the 3′-end in order to reduce non-specific binding were used,

b. The outer and inner primer melting temperatures for the GSPs were within a degree of the RACE kit supplied primers,

c. For 5′-RACE, the inner primer was long (~27 bp) in order to reduce nonspecific binding, and

d. The primers were designed to anneal close (50-75 bp) to the existing 5′-end to avoid large overlaps.

Different sets of primers were designed based on the cDNAs obtained by the study involving the degenerate primers (I4) and the initial 5′-RACE study (I35R and L25R).

Table 5-5. Gene-specific primers used in succeeding RLM-RACE study

GSP ID	Sequence (5′→3′)	RACE	Start[1]	PCR step
(a) Liver L25R				
UGT_5OUT1	ATTGGGCATTACAGGTCTCG	5`	119	Outer
UGT_5INN1	CGAGGACGTCTCTGAACGTAACATCC	5`	51	Inner
UGT_3OUT1	GATTCCTCAGAGGGTTCTGT	3`	320	Outer
UGT_3INN1	GGGGTCATTCCCAAAGACAT	3`	351	Inner
(b) Intestine I4				
UGT_5OUT2	GCCGTTACAGATACCCTCGT	5`	282	Outer
UGT_5OUT2A	GTATCGCCACAGAACCCTCT	5`	138	Outer
UGT_5INN2	ACACGAAGGAGCTCAAAGTGAACACG	5`	61	Inner
UGT_5INN2A	GCCACTTCATCACTTTGACATTTTCAGG	5`	190	Inner
UGT_3OUT2	AATGTCAAAGTGATGAAGTGG	3`	169	Outer
UGT_3OUT2A	GACATTCCTGAAAATGTCAAA	3`	157	Outer
UGT_3INN2	CCCAAGGCTAAGGTGTTCATC	3`	217	Inner
UGT_3INN2A	GACCTCTTAGCACACCCCAAG	3`	202	Inner
(b) Intestine I35R				
UGT_5OUT3	TGTTAATGACCTTCGGTGTGA	5`	236	Outer
UGT_5OUT3A	ATGACCTTCGGTGTGAGTTTT	5`	231	Outer
UGT_5INN3	AAACCTAAGAGGTCATTCTGCGGAAGC	5`	70	Inner
UGT_5INN3A	ATGGGGACCGGGTGTCTATTTATTACG	5`	115	Inner
UGT_3OUT3	TTTCCAGCTAACACTACTTGG	3`	178	Outer
UGT_3OUT3A	TTACACGTCCTCTAACCGTAA	3`	73	Outer
UGT_3INN3	CCCAAGGCTAAGGTGTTCATC	3`	355	Inner
UGT_3INN2A	CCATGGCATCTACGAGGGTAT	3`	390	Inner

[1] Start position from partial DNA sequences obtained so far

5` RLM-RACE procedure

Calf intestinal phosphatase (CIP) treatment. Total RNA (not DNase treated) (2 μL for liver; 1 μL for intestine), 10 μg, as well as 10 μg of control RNA (mouse thymus) were gently mixed with CIP buffer, CIP, and nuclease-free water in a total volume of 10 μL. The mixture was incubated at 37°C for 1 hour, and terminated by the addition of 15 μL ammonium acetate solution. A 115 μL volume of nuclease-free water was added, followed by 150 μL acid phenol-chloroform. The mixture was then vortexed thoroughly and centrifuged for 5 minutes at room temperature and at ≥ 10,000g. The aqueous phase was transferred to a new tube, 150 μL chloroform were added, and the mixture was thoroughly vortexed and centrifuged for 5 minutes at ≥ 10,000g. The top aqueous layer was transferred to a new tube, 150 μL isopropanol were added, followed by thorough vortexing and chilling on ice for 10 minutes. The mixture was then centrifuged at maximum speed (16,000g) for 20 minutes. The pellet was rinsed with 0.5 mL cold 70% ethanol and centrifuged for 5 minutes at 16,000g. The ethanol was carefully removed and discarded, and the pellet was allowed to air dry (but not completely). The pellet was resuspended in 11 μL nuclease-free water and placed on ice. At this point 1 μL of the CIP-treated RNA was reserved for the "minus-TAP" control reaction. This RNA was carried through adapter ligation, reverse transcription and PCR in order to demonstrate that the products generated by RLM-RACE were specific to the 5`-ends of decapped RNA.

Tobacco Acid Pyrophosphatase (TAP) treatment. CIP'd RNA, 5 μL, was gently mixed with TAP, 10XTAP buffer and nuclease-free water in a total volume of 10 μL. The mixture was incubated at 37°C for 1 hour.

**5`RACE Adapter Ligation.** CIP/TAP-treated RNA, 2 μL, and 2 μL of CIP-treated RNA (minus-TAP control) was gently mixed with 1 μL 5`RACE adapter (5`-GCUGAUGGCGAUGAAUGAACACUGCGUUUGCUGGCUUUGAUGAAA - 3`), 1 μL 10XRNA Ligase buffer (before use, the buffer was quickly warmed by rolling it between gloved hands to resuspend any precipitate), T4 DNA Ligase (2.5 U/μL), and nuclease-free water in a total volume of 10 μL. The mixture was incubated at 37°C for 1 hour, after which it was stored at -20°C.

Reverse transcription (RT). Ligated RNA, 2μL, or minus-TAP control were gently mixed with 4 μL dNTP mix, 2 μL random decamers, 2 μL 10XRT buffer, 1 μL RNase inhibitor, 1 μL M-MLV reverse transcriptase, and nuclease-free water in a total volume of 20 μL. The mixture was incubated at 42°C (or 50°C, see results) for 1 hour. The reactions were stored at -20°C.

Outer PCR. Each tube contained: 1 μL RT reaction, 5 μL 10XPCR buffer, 4 μL dNTPmix (4 mM), 2 μL gene-specific or outer control (reverse) primer (10 μM), 2 μL outer (forward) primer (10 μM) (5`-GCTGATGGCGATGAATGAACACTG-3`), 0.25 μL Taq DNA polymerase (5 U/μL), and nuclease-free water in a total volume of 50 μL. A minus-template control was also included to ensure that one or more of the PCR reagents was not contaminated with DNA.

Thermocycler parameters were as follows (Lid heating at 110°C):

Step	Stage	Temp/°C	Duration/min
1	Initial denaturation	94	3
2	Denaturation	94	0.5
3	Annealing	59 ± 2[1]	0.5
4	Extension	72[2]	1[3]
5	Final extension	72	7

35 cycles of steps 2 – 4 were performed
[1,2,3] These parameters were frequently changed to optimize the PCR. The values given above are representative of parameters used with the GSP_OUT and control primers.

Inner nested PCR. A mixture was prepared, identical to the one for outer PCR, except that the DNA template was now 1 μL of the outer PCR, and 2 μL each of both inner primers. The sequence for the inner 5`RACE primer supplied with the kit was 5`-CGCGGATCCGAACACTGCGTTTGCTGGCTTTGATG - 3`. The thermocycler parameters were similar except for the annealing temperature, which was typically higher than the one used for the outer PCR.

3` RACE procedure

Reverse transcription. The following components were assembled in a nuclease-free microfuge tube: 1 μg total RNA (DNase-treated) from intestine or liver or control (mouse thymus RNA), 4 μL dNTP mix, 2 μL 3`RACE Adapter (5` - GCGAGCACAGAATTAATACGACTCACTATAGG T12VN - 3`), 2 μL 10XRT buffer, 1 μL RNase inhibitor, 1 μL M-MLV reverse transcriptase, and nuclease-free water to 20 μL. The reaction was mixed gently and incubated at 42°C or 50°C for 1 hour.

PCR. The procedure for the outer and inner PCR was similar to the one performed for 5`-RACE, the only difference being the GSP and the kit-supplied primers used. The

sequences for the latters were as follows: Outer 5`-GCGAGCACAGAATTAATACGACT-3`, Inner 5`-CGCGGATCCGAATTAATACGACTCACTATAGG-3`

PCR amplification of entire UGT gene

Elucidation of the complete gene sequence for liver UGT from catfish by RLM-RACE (via partial sequence overlap) enabled the design of gene specific primers which are complementary to the gene itself as well as the untranslated region. The primers used are shown in Table 5-6. All primers complementary to the untranslated region (UTR) were designed with the help of Primer3 software, except for the pair of primers that were complementary to the exact start and end of the gene (LIVUGT_F1 and LIVUGT_R1 respectively).

Table 5-6. Primers used for amplifying liver and intestinal UGT gene

GSP ID	Sequence (5'→3')	Start position
UTR_F1	CTGCTTCCTCTAGACGTAATTAGAAAC	- 40
UTR_F2	CTCACATTCCTCCTCCTTCTTTTT	- 76
UTR_R1	GAACGTGGTGATGAGAACACTATAACT	+ 121
UTR_R2	TAGTGACATCATAACAACCGTAACTGC	+ 190
LIVUGT_F1	ATGCCTCGTCTTCTTGCAGCTCTCTGT	1
LIVUGT_R1	TCACTCCTTTTTGCTCTTCTGAGCCCT	1568

Due to the length of the amplicon (~1.6kb), Super Taq Plus polymerase (Ambion Inc) was employed. This enzyme results in higher yields with amplicons >1kb. In addition, this enzyme mixture has a proof-reading ability, which will be important for future expression of the gene, as well as providing greater fidelity and processivity than ordinary thermos Taq DNA polymerase. An extension temperature of 68°C and an extension time of 1.75 min were used for this PCR. Different combinations of UTR

primer pairs were tested in order to ensure optimal conditions for amplification of the full-length gene.

This experiment was repeated for intestinal cDNA in order to investigate whether a similar isoform to that identified from liver is present in the catfish intestine.

PCR product purification, ligation and cloning. The procedure followed was identical to the one used for the initial study utilizing degenerate primers.

Samples were submitted to the UF DNA Sequencing Core Facility for DNA sequence analysis. DNA sequencing was carried out on both UGT clones as well as products purified from PCR. At least three clones containing the same insert or two separate RACE PCR reactions for PCR amplification products (comprising 4 sequencing reactions) were sequenced and compared with each other for sequence similarity and verification.

Bioinformatic analysis of DNA sequences. The DNA sequences obtained were subjected to BLAST search (Altschul et al., 1997) for studying their similarity with other sequences in GenBank. Protein sequences were predicted by ExpAsy (available online, http://ca.expasy.org/tools/dna.html). Multiple sequence alignments for both nucleotide and predicted amino acid sequences utilized online tools such as ClustalW (available online, http://www.ebi.ac.uk/clustalw/), Basic Local Alignment Search Tool (BLAST, available online http://www.ncbi.nlm.nih.gov/blast/), as well as BioEdit (downloadable program available from http://www.mbio.ncsu.edu/BioEdit/bioedit.html). Nucleotide sequence data was analyzed using the BDGP Neural Network Promoter Predictor (http://www.fruitfly.org/seq_tools/promoter.html). Protein sequence data was analyzed by the NCBI Conserved Domain Database Search tool (http://www.ncbi.nlm.nih.gov/

Structure/cdd/cdd.shtml; Marchler-Bauer and Bryant 2004), Emboss software (http://www.bioweb.pasteur.fr) and CLC Protein Workbench v.1.5.2 (http://www.clcbio.com).

Results (part 2)

The RACE studies enabled the successful amplification and cloning of several partial DNA sequences with good similarity to known UGTs and unknown fish sequences. In the case of the liver, partial overlapping sequences obtained via cloning and amplification of PCR products resulted in the recovery of the whole gene (livUGTn, Figure 5-7), including untranslated regions at both ends. For the intestine, only partial sequences, corresponding to two distinct isoforms were obtained (I4_3R and I35R_PCR) by RACE. However, the use of GSPs UTR_F1 and UTR_R2 resulted in the amplification and cloning of an identical gene from intestine (intUGTn), which was identical to the I4-3R partial sequence. The I35R_PCR sequence was only 39% homologous with the full length UGTs obtained from liver and intestine. A comparison of the relative sizes of these sequences with respect to the full-length liver and intestinal UGT genes is shown in Figure 5-8. For both liver and intestine truncated forms of UGT were identified (L25R_5A, I4_6A, I35R_PCR). These lacked the coding sequence for the trans-membrane segment at the 3`-end of the gene.

The sequences for the amplified, partial-sequence cDNAs that were sequenced directly or when cloned are given in Appendix A.

Nucleotide sequence analysis

a. Full-length UGT from liver/intestine. The UGTn sequence was subjected to a BLASTn search (Table 5-7), showing that the sequence exhibited a high degree of similarity to known UGT sequences. However, DNA sequences are inherently noisy (due

to the 25% probability of a match at any specific position). Cleaner results were obtained by using the predicted protein sequence (Refer to following section). A further advantage of searching at the protein level is that related proteins are generally more conserved than are the genes encoding for them. The GC content was found to be around 50% and a 50 bp long sequence at the 5'-end was predicted to be a possible promoter binding site (Table 5-8), although this may be the promoter of another gene due to its overlap with the translated part of the sequence.

```
1    GGAATGCTAA GAGCTCGAGT ACCGGGCCTG TTCTTCTCAC ATTCCTCCTC CTTCTTTTTT
61   TCCTCCAAAA TCTGCTTCCT CTAGACGTAA TTAGAAACTT TTAAGCTAAA AATGCCTCGT
121  CTTCTTGCAG CTCTCTGTCT CCAGATTTAT CTTTGCAGCT TTTTAGGACC AGTGGAAGGA
181  GGGAAGGTCC TGGTGATGCC CGTGGACGGC AGCCACTGGC TCAGTATGAA GATCTTGGTG
241  GAGGAATTGT CTCGGAGAGG ACATGAAATG GTGGTCCTGG TTCCCGAGAC AAGCGTGTTG
301  ATCCATGGCT CTGACGCGTA CGCCGCTCGG AGCTTTAAGG TTCCGTACAC CAAGGCTGAA
361  CTGGATGAAA GCATGAATAA GTTGAAGGAG GGCATTACGA AAGCACCGCG GATCTCTGAC
421  TTATTGGAGA ACATCATCGG GCTCCTCAGC TTCACGAACA TGCAGGTGAA AGGATGCGAG
481  GCGCTGCTGT ATAACGAGCC TCTGATGCAG AACCTGCGCG AGGAACACTT CGATCTCATG
541  CTCACCGATC CCTTCCTGCC TTGTGGCCCC ATCATCGCCG AGGCTTTCTC CCTCCCCGCC
601  GTTTATTTCC TGCGTGGGCT TCCCTGCGGA TTGGATCTGG AAGCCGCTCA GTGCCCATCG
661  CCTCCGTCCT ACGTCCCGCG CTTTTTCACA GGCAACACCG ACGTCATGAC GTTTTCTCAG
721  AGGGTCAAGA ACGTGCTCAT GACGGGATTC GAGAGCATCC TTTGCAAAAT ATTTTTCTCC
781  AGCTTTGATG AGCTCACCAG CAGATATCTC AAGAAGGATG TTACGTTCAG AGACGTCCTC
841  GGACATGCCG CGATTTGGCT TTATAGATAT GACTTCACCT TTGAGTACCC GAGACCTGTA
901  ATGCCCAATG CGGTCAGAAT TGGTGGCATC AACTGTGCCA AGAAGAATCC TCTGCCTGCC
961  GATCTGGAGG AGTTCGTGGA CGGTTCTGGA GATCACGGCT TCATCGTGTT CACTTTGGGC
1021 TCCTTCGTGT CCGAGCTGCC GGAGTTCAAA GCCCGGGAGT TTTTCGAGGC TTTTCGGCAG
1081 ATTCCTCAGA GGGTTCTGTG GCGATACACC GGGGTCATTC CCAAAGACAT TCCTGAAAAT
1141 GTCAAAGTGA TGAAGTGGCT TCCGCAGAAC GACCTCTTAG CACACCCCAA GGCTAAGGTG
1201 TTCATCACGC ACGGAGGAGC CCATGGCATC TACGAGGGTA TCTGTAACGG CGTGCCGATG
1261 GTGATGATCC CGCTGTTCGG AGATCAGGTA GACAACGTTC TACGCATGGT GCTGCGTGGA
1321 GTCGCAGAGA GCCTGACCAT GTTCGACCTG ACCTCAGAGC AACTGCTGGG GGCACTCAGG
1381 AAAGTCCTCA ACAACAAGCG CTACAAAGAG AAGATAACAC AGCTGTCTTT GATCCATAAA
1441 GACCGTCCGA TCGAGCCGCT GGACTTGGCC GTGTTCTGGA CCGAGTTTGT GATGAGACAC
1501 GGAAGTGCCG AGCACCTGAG ACCGGCCGCT CACCACCTCA ACTGGGTTCA GTACCACAGT
1561 CTCGATGTCA TCGCCTTCCT CCTGCTCGTT CTATCCACCG TCGTTTTTAT CGCCGTCAAA
1621 ACCTGCGCGC TCTGTTTCAG GAAGTGTTTC CGGAGGGCTC AGAAGAGCAA AAAGGAGTGA
1681 AACGGCCAGT GAATGATCAG GAATGGATTT GGTGCCGTCT TTAATTAACG CCGATGGTTT
1741 ATCGGCGTGA TGTCATACTG TGAAAACCTG AAATAGTTAT AGTGTTCTCA TCACCACGTT
1801 CAATTTAATA TTCAGGGGTG CCAGCAATTA TGGTTTAGCC ATTGCAGTTA CGGTTGTTAT
1861 GATGTCACTA AAAAAAAAAA A
```

Figure 5-7. Full nucleotide sequence obtained for hepatic catfish UGT (livUGTn), derived from 4 sequencing runs each.

Highlighted areas indicate start and stop codons (identified after analysis of predicted amino acid sequence).

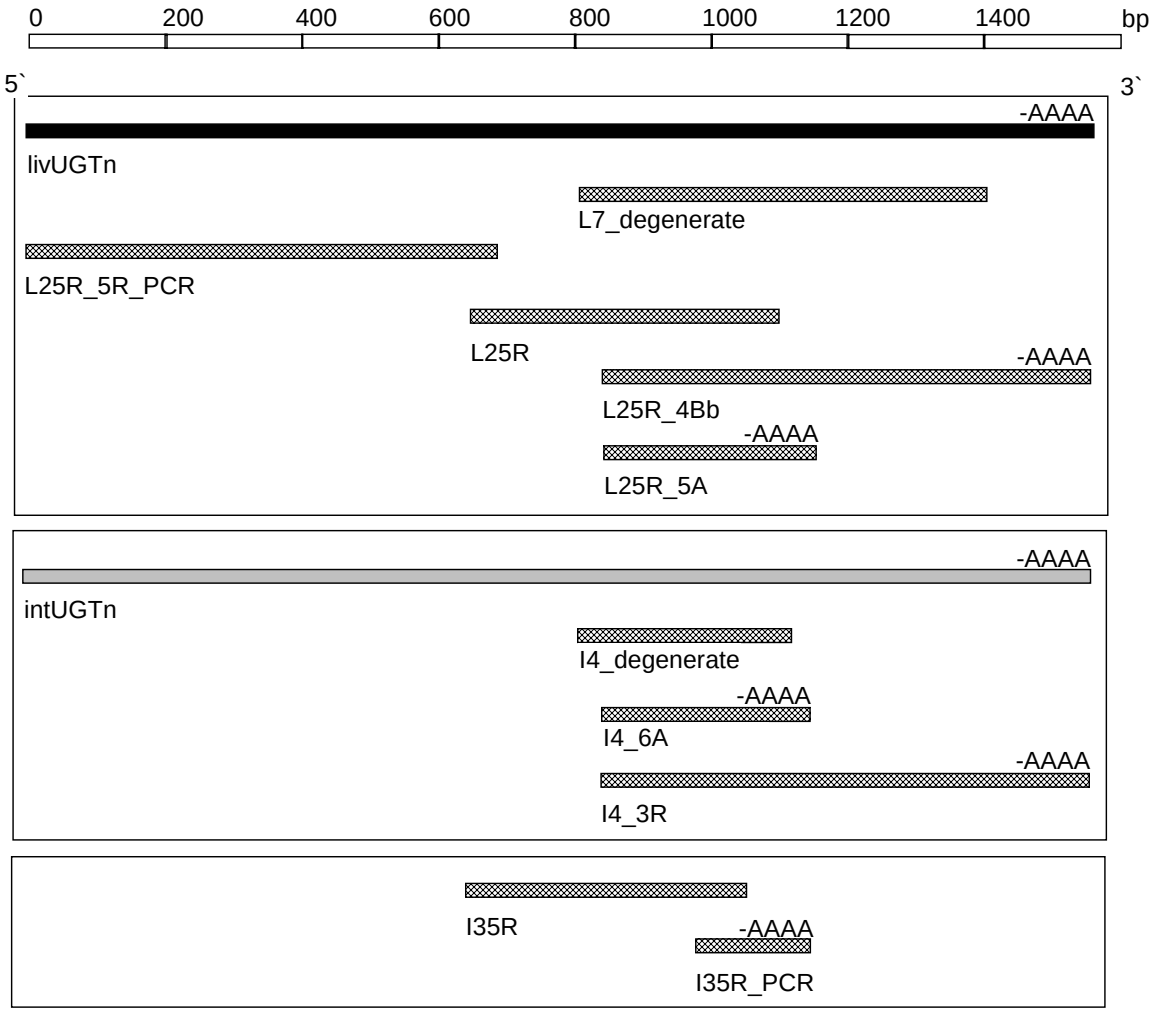

Figure 5-8. Sizes and positions of partial UGT sequences (cross-hatched rectangles) from intestine and liver, corresponding to two distinct isoforms, relative to complete sequences for liver and intestinal UGT (solid rectangles).

The -AAAA indicates 3′-polyA tail while the suffix _PCR indicates amplicons that were not cloned but sequenced directly.

Table 5-7. Results of blastn search for livUGTn (and intUGTn)

Sequences producing significant alignments:	Score (Bits)	E Value
gi|56324617|emb|CR646752.3|CNS0EY06 *Tetraodon nigroviridis* full-length cDNA	97.6	1e-16
gi|56242288|emb|CR644097.2|CNS0EVYF *Tetraodon nigroviridis* full-length cDNA	97.6	1e-16
gi|34850459|dbj|AB120133.1| *Pleuronectes yokohamae* UGT1B2 mRNA, complete cds	75.8	5e-10
gi|71679708|gb|BC100055.1| *Danio rerio* cDNA clone IMAGE:7284571, partial cds	71.9	7e-09
gi|68369305|ref|XM_682293.1| PREDICTED: *Danio rerio* similar to UGT 1, mRNA	71.9	7e-09
gi|68369293|ref|XM_681739.1| PREDICTED: *Danio rerio* similar to UGT1, mRNA	71.9	7e-09
gi|46518141|emb|BX005348.9| Zebrafish DNA sequence from clone, complete sequence	71.9	7e-09
gi|46016516|emb|BX323548.11| Zebrafish DNA sequence from clone, complete sequence	71.9	7e-09
gi|6537143|gb|AF104339.1|AF104339 *Macaca fascicularis* UGT1A01 mRNA comp. cds	63.9	2e-06
gi|47087384|ref|NM_213422.1| *Danio rerio* zgc:66393 (zgc:66393), mRNA, complete cds	60.0	3e-05
gi|33416924|gb|BC055635.1| *Danio rerio* zgc:66393, mRNA (cDNA) complete cds	60.0	3e-05
gi|50370246|gb|BC075892.1| *Danio rerio* zgc:66393, mRNA (cDNA) complete cds	60.0	3e-05
gi|62531208|gb|BC093347.1| Danio rerio zgc:66393, mRNA (cDNA) complete cds	60.0	3e-05
gi|32251578|emb|AL954329.7| Zebrafish DNA sequence from clone, complete sequence	60.0	3e-05
gi|81097721|gb|BC109404.1| *Danio rerio* zgc:123097, mRNA (cDNA) complete cds	60.0	3e-05
gi|82658295|ref|NM_001037428.1| *Danio rerio* zgc:123097 (zgc:1230), mRNA	60.0	3e-05
gi|50750130|ref|XM_421883.1| PREDICTED: *Gallus gallus* similar to UGT, mRNA	58.0	1e-04
gi|89572711|gb|AC161471.3| *Gallus gallus* BAC clone CH261-21B3, complete sequence	58.0	1e-04
gi|46425671|emb|BX931804.2| *Gallus gallus* finished cDNA, clone ChEST795f19	58.0	1e-04

Table 5-8. Promoter prediction. Predicted transcription start is shown in larger font.

Start	End	Score	Promoter Sequence
97	**147**	**0.99**	**AA TTAGAAACTT TTAAGCTAAA AATGCCTCGT CTTC<u>T</u>TGCAGCTCT**
480	530	0.98	GAAAGGATGCGAGGCGCTGCTGTATAACGAGCCTCTGATG<u>C</u>AGAACCTGC
1425	1475	0.93	GATAACACAGCTGTCTTTGATCCATAAAGACCGTCCGATC<u>G</u>AGCCGCTGG
1710	1760	0.95	CAGGAATGGATTTGGTGCCGTCTTTAATTAACGCCGATGG<u>T</u>TTATCGGCG

Bold sequence indicates most likely promoter

The open reading frame (ORF) was identified by translating the sequence data of all possible frames (Figure 5-9) and choosing the one that showed the least stop codons (Frame +1). The translated sequence (Figure 5-10) was then subjected to a blastp search with other protein sequences in GenBank (Table 5-9), followed by alignment of these sequences. In this way, the untranslated regions (UTRs) were also identified (Figure 5-11). The catfish liver sequence was found to have the best similarity with *Danio rerio*

UGTs and other unidentified proteins of the same species (Figure 5-12). The livUGTp sequence was also aligned with mammalian UGTs (Figures 5-13 and 5-14).

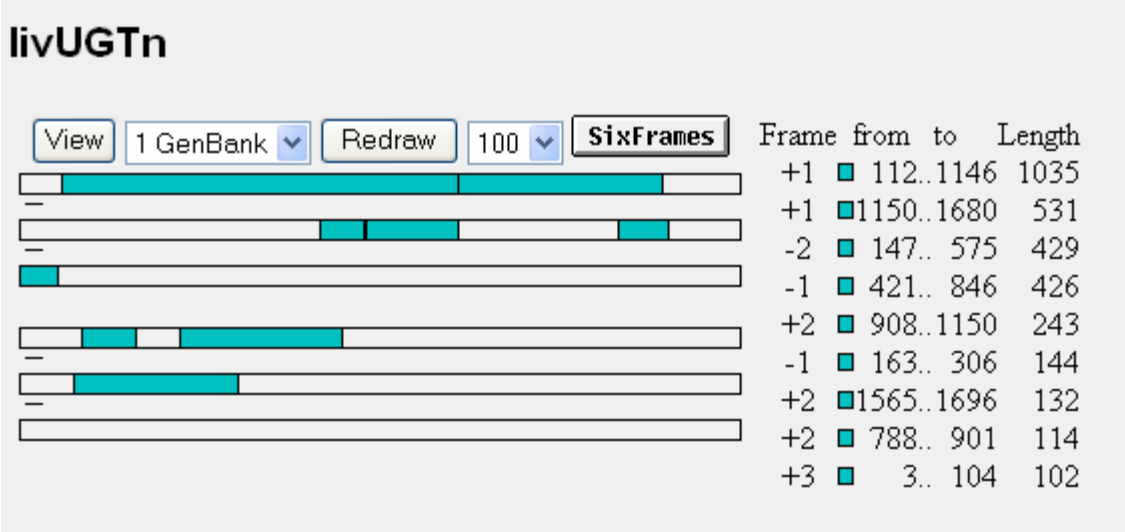

Figure 5-9. Identification of open reading frame using ORF Finder

```
1   GMLRARVPGL FFSHSSSFFF SSKICFL*T* LETFKLKMPR LLAALCLQIY
51  LCSFLGPVEG GKVLVMPVDG SHWLSMKILV EELSRRGHEM VVLVPETSVL
101 IHGSDAYVAR SFKVPYTKAE LDESMNKLKE GITKAPRISD LLENIIGLLS
151 FTNMQVKGCE ALLYNEPLMQ NLREEHFDLM LTDPFLPCGP IIAEAFSLPA
201 VYFLRGLPCG LDLEAAQCPS PPSYVPRFFT GNTDVMTFSQ RVKNVLMTGF
251 ESILCKIFFS SFDELTSRYL KKDVTFRDVL GHAAIWLYRY DFTFEYPRPV
301 MPNAVRIGGI NCAKKNPLPA DLEEFVDGSG DHGFIVFTLG SFVSELPEFK
351 AREFFEAFRQ IPQRVLWRYT GVIPKDIPEN VKVMKWLPQN DLLAHPKAKV
401 FITHGGAHGI YEGICNGVPM VMIPLFGDQV DNVLRMVLRG VAESLTMFDL
451 TSEQLLGALR KVLNNKRYKE KITQLSLIHK DRPIEPLDLA VFWTEFVMRH
501 GSAEHLRPAA HHLNWVQYHS LDVIAFLLLV LSTVVFIAVK TCALCFRKCF
551 RRAQKSKKE* NGQ*MIRNGF GAVFN*RRWF IGVMSYCENL K*L*CSHHHV
601 QFNIQGCQQL WFSHCSYGCY DVTKKKK
```

Figure 5-10. Predicted protein sequence liv/intUGTp from liv/intUGTn

* indicate stop codons; highlighted residues indicate start and stop residues, determined after comparison with known UGT sequences, see Figure 5-11 below)

Table 5-9. Results of blastp search for liv/intUGTp

Sequences producing significant alignments:	Score (Bits)	E Value
gi|47087385|ref|NP_998587.1| hypothetical protein LOC406731 [*Danio rerio*]	725	0.0
gi|81097722|gb|AAI09405.1| Hypothetical protein LOC641488 [*Danio rerio*]	692	0.0
gi|50370247|gb|AAH75892.1| Zgc:66393 protein [*Danio rerio*]	691	0.0
gi|71679709|gb|AAI00056.1| Unknown (protein for IMAGE:7284571) [*Danio rerio*]	671	0.0
gi|47205148|emb|CAG04937.1| unnamed protein product [*Tetraodon nigroviridis*]	620	6e-176
gi|34850460|dbj|BAC87829.1| UDP-glucuronosyltransferase [*Pleuronectes yokohamae*]	602	2e-170
gi|5579028|emb|CAB51368.1| UDP-glucuronosyltransferase [*Pleuronectes platessa*]	601	3e-170
gi|6272259|emb|CAB51369.2| UDP-glucuronosyltransferase [*Pleuronectes platessa*]	598	2e-169
gi|62531209|gb|AAH93347.1| Zgc:66393 protein [*Danio rerio*]	580	8e-164
gi|47210873|emb|CAF91810.1| unnamed protein product [*Tetraodon nigroviridis*]	573	8e-162
gi|68369306|ref|XP_687385.1| PREDICTED: similar to UGT1 family [*Danio rerio*]	570	5e-161
gi|68369294|ref|XP_686831.1| PREDICTED: similar to UGT1 family [*Danio rerio*]	568	3e-160
gi|2842546|dbj|BAA24692.1| UDP-glucuronosyltransferase [*Felis catus*]	555	2e-156
gi|57163903|ref|NP_001009359.1| UDP glycosyltransferase 1A1 [*Felis catus*]	554	4e-156
gi|56785765|gb|AAW29020.1| UDP-glucuronosyltransferase [*Epinephelus coioides*]	547	6e-154
gi|975702|emb|CAA52214.1| UDP-glucoronosyl transferase [*Pleuronectes platessa*]	544	4e-153
gi|40849838|gb|AAR95631.1| UGT1A2 [*Rattus norvegicus*]	542	2e-152
gi|40849834|gb|AAR95629.1| UGT1A1 [*Rattus norvegicus*]	541	3e-152
gi|207579|gb|AAA42312.1| bilirubin UDP-glucuronosyltransferase [*Rattus norvegicus*]	541	3e-152
gi|2507507|sp|P20720|UD12_RAT UGT 1-2 precursor [*Rattus norvegicus*]	541	3e-152
gi|46518737|gb|AAS99732.1| UGT1A1 [*Homo sapiens*]	536	1e-150
gi|40849842|gb|AAR95633.1| UGT1A6 [*Rattus norvegicus*]	535	3e-150
gi|62533164|gb|AAH93516.1| UGT1A1 [*Mus musculus*]	535	3e-150
gi|89519335|gb|ABD75811.1| UDP glycosyl transferase 1A1 [*Papio anubis*]	535	3e-150
gi|8170744|gb|AAB26033.2| UDP-glucuronosyltransferase [*Mus sp.*]	534	4e-150
gi|6537144|gb|AAF15549.1| UGT1A01 [*Macaca fascicularis*]	534	5e-150
gi|74136303|ref|NP_001028041.1| UGT1A01 [*Macaca mulatta*]	533	7e-150
gi|2501477|sp|Q64638|UD15_RAT UGT1A5 precursor [*Rattus norvegicus*]	533	7e-150

Scores

SeqA	Name	Len(aa)	SeqB	Name	Len(aa)	Score
1	livUGTp	627	2	D.rerioPR	526	67
1	livUGTp	627	3	P.platessaUGT	530	54
1	livUGTp	627	4	T.nigroviridisPR	501	59
1	livUGTp	627	5	P.yokohamaeUGT	530	54
2	D.rerioPR	526	3	P.platessaUGT	530	54
2	D.rerioPR	526	4	T.nigroviridisPR	501	60
2	D.rerioPR	526	5	P.yokohamaeUGT	530	55
3	P.platessaUGT	530	4	T.nigroviridisPR	501	60
3	P.platessaUGT	530	5	P.yokohamaeUGT	530	91
4	T.nigroviridisPR	501	5	P.yokohamaeUGT	530	60

Accession numbers: D.rerioPR (NP_998587.1); P.platessaUGT (CAB51368.1); T.nigroviridisPR (CAG04937.1); P.yokohamaeUGT (BAC87829.1)

```
CLUSTAL W (1.83) multiple sequence alignment

P.platessaUGT         ------------------------------------MSGRVWFQMLGLVAWLCLLSLGPVQ 25
P.yokohamaeUGT        ------------------------------------MSGRVWFPSLGLVAWLCLLSLGPVQ 25
T.nigroviridisPR      ------------------------------------MRGSVGILTLGLLAWIGCFGPQPVQ 25
livUGTp               GMLRARVPGLFFSHSSSFFFSSKICFL-T-LETFKLKMPRLLAALCLQIYLCSFLG-PVE 57
D.rerioPR             ------------------------------------MKRTLFVPALGLFAFLCLFSSESVQ 25
                                                           :     .  * *  ::  :   .*:

P.platessaUGT         GGKVLVMPADGSHWLSLKILVKGLIHRGHDVVVLVPESSLFMHQSEDYKTEVYPVSFTTE 85
P.yokohamaeUGT        GGKVLVMPADGSHWLSLKILVKGLVHRGHDVVVLVPESSLFMHQSEDYKTEVYPVSFTME 85
T.nigroviridisPR      AGKVLVLPVDGSHWLSMKILVKELIQRGHDVLVLVPETSLLIKSSENYRTEIYQVPYSKE 85
livUGTp               GGKVLVMPVDGSHWLSMKILVEELSRRGHEMVVLVPETSVLIHGSDAYVARSFKVPYTKA 117
D.rerioPR             AGKVLVMPVDGSHWLSMKILVEEMSSRGHEMVVLVPETSILIGKSGNFTTKSFRVPYSFD 85
                      .*****:*.*******:****: :  ***:::*****:*:::  *  : :. : *.::

P.platessaUGT         EMDATHKQLKDGLFLKQPDWTEYYVNIMRFVNFTSIHLRGCENLLENQPLMSRMRGMGFD 145
P.yokohamaeUGT        EMDAVHKQLKDGLFLKQPDWTEYYVNIMRFVNFTSIHLRGCENLLQNQPLMSRLKGMGFD 145
T.nigroviridisPR      DLGGSFQALKDGLFLKPPSMADLFVNVERLMNFTTMQVTGCESLLRNQPLMTRLREQGFE 145
livUGTp               ELDESMNKL-KEGITKAPRISDLLENIIGLLSFTNMQVKGCEALLYNEPLMQNLREEHFD 176
D.rerioPR             ELNAHVDHIRKTAIEKAPRFIDIVGALGNLIQFTNMQVKACEGLLYDEPLMKSLRDMKFD 145
                      ::.   . : .  : * *   :    :  ::.**.::: .** ** ::***  ::   *:

P.platessaUGT         IVLTDPFFPCGALVGNIFSIPVVNFLRGLPCGLDMKVNKCPSPPSYIPVPYSGNTNIMTF 205
P.yokohamaeUGT        IVLTDPFFPCGALVGHIFSIPVVNFLRGLPCGLDMKVNKCPSPPSYIPVPYSGHTDIMTF 205
T.nigroviridisPR      VVLTDPFLPCGPIVSHLFNIPAVYFLHGLPCELDSKANQCPAPPSYIPTSFSGNSDVMTF 205
livUGTp               LMLTDPFLPCGPIIAEAFSLPAVYFLRGLPCGLDLEAAQCPSPPSYVPRFFTGNTDVMTF 236
D.rerioPR             ALLTDPFLPCGSVIADYFSIPAVYFLRGIPCRLDEAAAQCPSPPSFIPRFFTGYTDKMTF 205
                       :*****:***.::.. *.:*.* **:*:** **  . :**:***::*  ::* :: ***

P.platessaUGT         PQRVINMAMTVLESYQCSLLYGHYDEMVSKYVGNNMDYRTLLSHGALWLIRNEFTLDWAR 265
P.yokohamaeUGT        QQRVINMAMTVVESFQCSLLYSHYDEMVSKHLGNNMDYRTLLSNGALWLIRNEFSLDWPR 265
T.nigroviridisPR      PQRVKNMLMYLVQSYLCKVMYREFDRLVTRHMSDIQSYRELISRGAFWLLKYDFTFQHPK 265
livUGTp               SQRVKNVLMTGFESILCKIFFSSFDELTSRYLKKDVTFRDVLGHAAIWLYRYDFTFEYPR 296
D.rerioPR             PQRMINTFMTVFEKYLCHQLFASFDELATRYLKKDTSYAELLGHGAVWLLRYDFSFEYPK 265
                       **: *  *  .:. :*  ::  :*.:.:::: .   :  ::...*.** : :*::: .:

P.platessaUGT         PLLPNMVLIGGINCAEKKKNASLPADLEEFVQGSGDDGFIIFTLGSMLPDMPQEKAQHFL 325
P.yokohamaeUGT        PLLPNMVLIGGINCAEKKTKASLPADLEEFVQGSGDHGFIIFTLGSMLPDMPQEMAQHFL 325
T.nigroviridisPR      PVMPNTAFIGGINCAKK---APLPADLEEFVNGSEDHGFIVFSLGSMVENMPVEKAKQFF 322
livUGTp               PVMPNAVRIGGINCAKK---NPLPADLEEFVDGSGDHGFIVFTLGSFVSELPEFKAREFF 353
D.rerioPR             PQMPNMVQIGGINCAKR---APLTKELEEFVNGSGEHGFVVFTLGSMVSQLPEAKAREFF 322
                      * :** . *******::    .*. :*****:** :.**::*:***:: ::*   *:.*:
```

Figure 5-11. Comparison of liv/intUGTp with homologous proteins in other fish, showing scores and alignment of closely related sequences.

```
P.platessaUGT          DAFRQIPQRVVWRYAGDPPKGLPKNVRLMKWLPQKELLAHPKARLFLTHGGSHSVYEGIC 385
P.yokohamaeUGT         DAFRQIPQRVVWRYAGEPPKGLPKNVKLMKWLPQKDLLAHPKAKLFLTHGGSHSVFEGIC 385
T.nigroviridisPR       DAFAQIPQRVLWRYNGAVPENAPKNVKVMKWLPQNDLLAHPKAKVFMTHGGIHGIYEGIC 382
livUGTp                EAFRQIPQRVLWRYTGVIPKDIPENVKVMKWLPQNDLLAHPKAKVFITHGGAHGIYEGIC 412
D.rerioPR              EAFRQIPQRVLWRYTGPVPENAPKNVKLMKWLPQNDLLGHPKVRAFVTHGGSHGIYEGIC 382
                       :** ******:*** *  *:. *:**::******::**.***.: *:**** *.::****

P.platessaUGT          NAVPMLMFPLFAEQGDNGLRMVTRGAAETLNIYDVTSDNLLAALNKILKNKSYKEKITEM 445
P.yokohamaeUGT         NAVPMLMFPLFAEQGDNGLRMVTRGVAETLFIYDVTSDTLLATLNKILKNKSYKEKMTEL 445
T.nigroviridisPR       NGVPMLMFPLFGDQIDNVPRMIHRGVAETLSIYDVTSQKLVAALKKMVQDKSYKENMVTL 442
livUGTp                NGVPMVMIPLFGDQVDNVLRMVLRGVAESLTMFDLTSEQLLGALRKVLNNKRYKEKITQL 472
D.rerioPR              NGVPMVMLPLFGDQGDNAQRLVSRGVAESLTIYDVTSEKLLVALKKVINDKSYKEKMMKL 442
                       *.***:*:***.:* **  *:: **.**:* ::*:**: *: :*.*::::* ***::  :

P.platessaUGT          SQIHHDRPVAPLDLAVFWTEFVIRHKGASHLRVAAHELNWIQYHSLDVFGFILLILLTVL 505
P.yokohamaeUGT         SQIHHDRPVGPLDLAIFWTEFVIRHKGAAHLRVSAHDLNWIQYHSLDVFGFLLLILLTVL 505
T.nigroviridisPR       SQLNQDRPVAPLDLAVFWTEFVMRHQGAQHLRVPPHDLNWFQYHSLDIFCFLAVVLLTV- 501
livUGTp                SLIHKDRPIEPLDLAVFWTEFVMRHGSAEHLRPAAHHLNWVQYHSLDVIAFLLLVLSTVV 532
D.rerioPR              SAIHRDRPIEPLDLAVFWTEFVMRHKGAEHLRPAAHDLNWIQYHSLDVIGFLLLILLTVI 502
                       * :::***: *****:******:** .* *** ..*.***.******:: *: ::* **

P.platessaUGT          WATLKCCLFCTRRCCRRGTAKTKSE---------------------------------- 530
P.yokohamaeUGT         LVTLKCCLSCTRRCCRRGTAKTKSE---------------------------------- 530
T.nigroviridisPR       ------------------------------------------------------------
livUGTp                FIAVKTCALCFRKCFRRAQKSKKE-NGQ-MIRNGFGAVFN-RRWFIGVMSYCENLK-L-C 587
D.rerioPR              FVTVKSCMFCFRKCFKTSQKKKKA---------------------------------- 526


P.platessaUGT          --------------------------------
P.yokohamaeUGT         --------------------------------
T.nigroviridisPR       --------------------------------
livUGTp                SHHHVQFNIQGCQQLWFSHCSYGCYDVTKKKK 619
D.rerioPR              --------------------------------
```

Figure 5-11. (continued)

Highlighted area in livUGTp indicates UTRs.

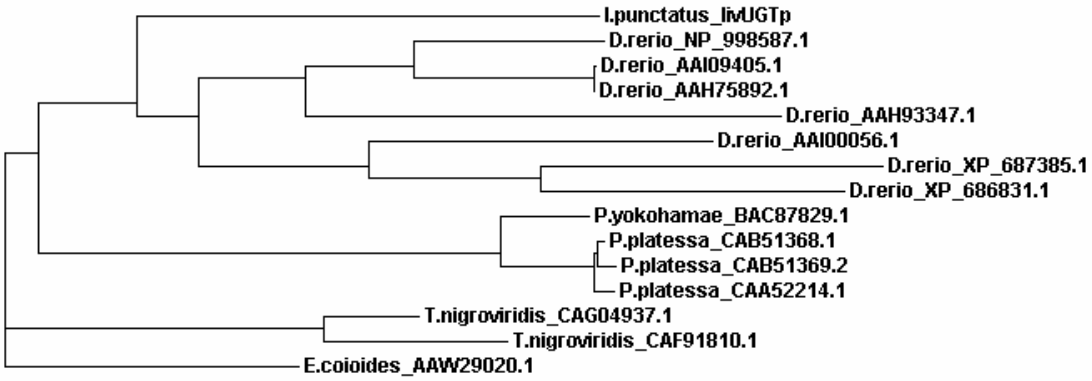

Figure 5-12. Phylogram for fish UGT proteins homologous to liv/intUGTp

Scores

SeqA	Name	Len(aa)	SeqB	Name	Len(aa)	Score
1	I.punctatus_livUGTp	522	2	F.catus_UGT1A1	533	51
1	I.punctatus_livUGTp	522	3	R.norvegicus1A2	533	51
1	I.punctatus_livUGTp	522	4	R.norvegicus1A1	535	50
1	I.punctatus_livUGTp	522	5	H.sapiensUGT1A1	533	48
1	I.punctatus_livUGTp	522	6	R.norvegicus1A6	531	51
2	F.catus_UGT1A1	533	3	R.norvegicus1A2	533	67
2	F.catus_UGT1A1	533	4	R.norvegicus1A1	535	76
2	F.catus_UGT1A1	533	5	H.sapiensUGT1A1	533	79
2	F.catus_UGT1A1	533	6	R.norvegicus1A6	531	67
3	R.norvegicus1A2	533	4	R.norvegicus1A1	535	70
3	R.norvegicus1A2	533	5	H.sapiensUGT1A1	533	66
3	R.norvegicus1A2	533	6	R.norvegicus1A6	531	88
4	R.norvegicus1A1	535	5	H.sapiensUGT1A1	533	78
4	R.norvegicus1A1	535	6	R.norvegicus1A6	531	70
5	H.sapiensUGT1A1	533	6	R.norvegicus1A6	531	67

Accession numbers: F.catusUGT1A1 (NP_001009359.1); R.norvegicusUGT1A2 (AAR95631.1); R.norvegicus1A1 (AAR95629.1); R.norvegicus1A6 (AAR95633.1); H.sapiensUGT1A1 (AAS99732.1)

```
F.catus_UGT1A1          MAARSRGPRPLVLS--LLLCALNPLLSQGGKLLLVPMDGSHWLSLFGVIQRLHQRGHDVV 58
H.sapiensUGT1A1         MAVESQGGRPLVLG--LLLCVLGPVVSHAGKILLIPVDGSHWLSMLGAIQQLQQRGHEIV 58
R.norvegicus1A1         MSVVCRSSCSLLLLPCLLLCVLGPSASHAGKLLVIPIDGSHWLSMLGVIQQLQQKGHEVV 60
R.norvegicus1A2         MDTGLCAPLRGLSGLLLLLCALP--WAEGGKVLVFPMEGSHWLSMRDVVRELHARGHQAV 58
R.norvegicus1A6         --MGLHVTLQGLAGLLLLLYALP--WAEGGKVLVFPMEGSHWLSMRDVVRELHARGHQAV 56
I.punctatus_livUGTp     -----MPRLLAALCLQIYLCSFLG-PVEGGKVLVMPVDGSHWLSMKILVEELSRRGHEMV 54
                                          : *  :     ..**:*:.*::******:   :..*  :**: *

F.catus_UGT1A1          VVAPEASVYIKEGAFYTLKSYPVPFRREDVEASFTGLGLGVFEKKPFLQRVVATYKRVKK 118
H.sapiensUGT1A1         VLAPDASLYIRDGAFYTLKTYPVPFQREDVKESFVSLGHNVFENDSFLQRVIKTYKKIKK 118
R.norvegicus1A1         VIAPEASIHIKEGSFYTMRKYPVPFQNENVTAAFVELGRSVFDQDPFLLRVVKTYNKVKR 120
R.norvegicus1A2         VLAPEVTVHMKGEDFFTLQTYAFPYTKEEYQREILGNAKKGFEPQHFVKTFFETMASIKK 118
R.norvegicus1A6         VLAPEVTVHIKEEDFFTLQTYPVPYTRQGFRQQMMRNIKVVFETGNYVKTFLETSEILKN 116
I.punctatus_livUGTp     VLVPETSVLIHGSDAYVARSFKVPYTKAELDESMNKLKEGIT-KAPRISDLLENIIGLLS 113
                        *:.*:.:: ::    :: :.: .*: .      :             :  .. .   :

F.catus_UGT1A1          DSALLLSACSHLLYNEELMASLAESGFDAMLTDPFLPCGPIVALRLALPVVFFLNSLPCG 178
H.sapiensUGT1A1         DSAMLLSGCSHLLHNKELMASLAESSFDVMLTDPFLPCSPIVAQYLSLPTVFFLHALPCS 178
R.norvegicus1A1         DSSMLLSGCSHLLHNAEFMASLEQSHFDALLTDPFLPCGSIVAQYLSLPAVYFLNALPCS 180
R.norvegicus1A2         FFDLYANSCAALLHNKTLIQQLNSSSFDVVLTDPVFPCGALLAKYLQIPAVFFLRSVPCG 178
R.norvegicus1A6         ISTVLLRSCMNLLHNGSLLQHLNSSSFDMVLTDPVIPCGAVLAKYLGIPTVFFLRYIPCG 176
I.punctatus_livUGTp     FTNMQVKGCEALLYNEPLMQNLREEHFDLMLTDPFLPCGPIIAEAFSLPAVYFLRGLPCG 173
                           :   .*  **:*  ::  * .. ** :****.:**..::*  : :*.*:**. :**.

F.catus_UGT1A1          LDFQGTRCPSPPSYVPRVLSLNSDHMTFLQRVKNMLILGSEGFLCNVVYSPYASLASEVL 238
H.sapiensUGT1A1         LEFEATQCPNPFSYVPRPLSSHSDHMTFLQRVKNMLIAFSQNFLCDVVYSPYATLASEFL 238
R.norvegicus1A1         LDLEATQCPAPLSYVPKSLSSNTDRMNFLQRVKNMIIALTENFLCRVVYSPYGSLATEIL 240
R.norvegicus1A2         IDYEATQCPKPSSYIPNLLTMLSDHMTFLQRVKNMLYPLTLKYICHLSITPYESLASELL 238
R.norvegicus1A6         IDSEATQCPKPSSYIPNLLTMLSDHMTFLQRVKNMLYPLALKYICHFSFTRYESLASELL 236
I.punctatus_livUGTp     LDLEAAQCPSPPSYVPRFFTGNTDVMTFSQRVKNVLMTGFESILCKIFFSSFDELTSRYL 233
                        :: :.::** * **:*. ::  :* *.* *****::       :* .  : :  *::. *
```

Figure 5-13. Alignment of liv/intUGTp (excluding UTRs) with selected mammalian UGT proteins, showing scores and multiple alignment of sequences, highlighting important regions and residues (see discussion)

```
F.catus_UGT1A1          QKDVTVQDLMGSASVWLFRSDFVKDYSRPIMPNMVFIGGINCAGKNPLSQEFEAYVNASG 298
H.sapiensUGT1A1         QREVTVQDLLSSASVWLFRSDFVKDYPRPIMPNMVFVGGINCLHQNPLSQEFEAYINASG 298
R.norvegicus1A1         QKEVTVKDLLSPASIWLMRNDFVKDYPRPIMPNMVFIGGINCLQKKALSQEFEAYVNASG 300
R.norvegicus1A2         QREMSLVEVLSHASVWLFRGDFVFDYPRPIMPNMVFIGGINCVIKKPLSQEFEAYVNASG 298
R.norvegicus1A6         QREVSLVEVLSHASVWLFRGDFVFDYPRPVMPNMVFIGGINCVIKKPLSQEFEAYVNASG 296
I.punctatus_livUGTp     KKDVTFRDVLGHAAIWLYRYDFTFEYPRPVMPNAVRIGGINCAKKNPLPADLEEFVDGSG 293
                        :::::. :::. *::** * **. :*.**:*** * :*****  ::.*. ::* :::.**

F.catus_UGT1A1          EHGIVVFSLGSMVSAIPKEKAMEIADALGKIPQTVLWRYTGTPPPNLAKNTILVKWLPQN 358
H.sapiensUGT1A1         EHGIVVFSLGSMVSEIPEKKAMAIADALGKIPQTVLWRYTGTRPSNLANNTILVKWLPQN 358
R.norvegicus1A1         EHGIVVFSLGSMVSEIPEKKAMEIAEALGRIPQTVLWRYTGTRPSNLAKNTILVKWLPQN 360
R.norvegicus1A2         EHGIVVFSLGSMVSEIPEKKAMEIAEALGRIPQTVLWRYTGTRPSNLAKNTILVKWLPQN 358
R.norvegicus1A6         EHGIVVFSLGSMVSEIPEKKAMEIAEALGRIPQTVLWRYTGTRPSNLAKNTILVKWLPQN 356
I.punctatus_livUGTp     DHGFIVFTLGSFVSELPEFKAREFFEAFRQIPQRVLWRYTGVIPKDIPENVKVMKWLPQN 352
                        :**::**:***:** :*: **  : :*: :*** *******. * ::.:*.:::*****
                                                                              <----
F.catus_UGT1A1          DLLGHPKARAFITHSGSHGIYEGICNGVPMVMLPLFGDQMDNAKRMETRGAGLTLNVLEM 418
H.sapiensUGT1A1         DLLGHPMTRAFITHAGSHGVYESICNGVPMVMMPLFGDQMDNAKRMETKGAGVTLNVLEM 418
R.norvegicus1A1         DLLGHPKARAFITHSGSHGIYEGICNGVPMVMMPLFGDQMDNAKRMETRGAGVTLNVLEM 420
R.norvegicus1A2         DLLGHPKARAFITHSGSHGIYEGICNGVPMVMMPLFGDQMDNAKRMETRGAGVTLNVLEM 418
R.norvegicus1A6         DLLGHPKARAFITHSGSHGIYEGICNGVPMVMMPLFGDQMDNAKRMETRGAGVTLNVLEM 416
I.punctatus_livUGTp     DLLAHPKAKVFITHGGAHGIYEGICNGVPMVMIPLFGDQVDNVLRMVLRGVAESLTMFDL 412
                        ***.** ::.****.*:**:**.*********:******:**. **  :*.. :*.:::: 
                        ---- UDPGA binding site ----------------->
F.catus_UGT1A1          TSEDLANGLKAVINDKSYKENIMRLSSLHKDRPIEPLDLAVFWVEFVMRHKGAPHLRPAA 478
H.sapiensUGT1A1         TSEDLENALKAVINDKSYKENIMRLSSLHKDRPVEPLDLAVFWVEFVMRHKGAPHLRPAA 478
R.norvegicus1A1         TADDLENALKTVINNKSYKENIMRLSSLHKDRPIEPLDLAVFWVEYVMRHKGAPHLRPAA 480
R.norvegicus1A2         TADDLENALKTVINNKSYKENIMRLSSLHKDRPIEPLDLAVFWVEYVMRHKGAPHLRPAA 478
R.norvegicus1A6         TADDLENALKTVINNKSYKENIMRLSSLHKDRPIEPLDLAVFWVEYVMRHKGAPHLRPAA 476
I.punctatus_livUGTp     TSEQLLGALRKVLNNKRYKEKITQLSLIHKDRPIEPLDLAVFWTEFVMRHGSAEHLRPAA 472
                        *:::* ..*: *:*:* ***:* :** :*****:*********.*:**** .* ******

F.catus_UGT1A1          HDLTWYQYHSVDVIGFLLAIVLGIVFITYKCCAFGCRKCFGRKGRVKKSHKSKTH 533
H.sapiensUGT1A1         HDLTWYQYHSLDVIGFLLAVVLTVAFITFKCCAYGYRKCLGKKGRVKKAHKSKTH 533
R.norvegicus1A1         HDLTWYQYHSLDVIGFLLAIVLTVVFIVYKSCAYGCRKCFGGKGRVKKSHKSKTH 535
R.norvegicus1A2         HDLTWYQYHSLDVIGFLLAIVLTVVFIVYKSCAYGCRKCFGGKGRVKKSHKSKTH 533
R.norvegicus1A6         HDLTWYQYHSLDVIGFLLAIVLTVVFIVYKSCAYGCRKCFGGKGRVKKSHKSKTH 531
I.punctatus_livUGTp     HHLNWVQYHSLDVIAFLLLVLSTVVFIAVKTCALCFRKCFR---RAQKSKKE--- 521
                        *.*.* ****:***.*** ::  :.**. * **   ***:    *.:*::*.
                              <- TM region ->
```

Figure 5-13. (continued)

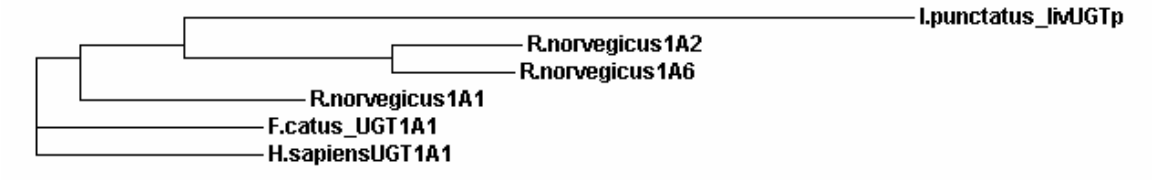

Figure 5-14. Phylogram for *I.punctatus* liv/intUGTp and selected mammalian UGT proteins

b. Distinct partial sequence found in intestine (I35R_C). The partial nucleotide sequence of I35R_C (combined overlapping sequences of I35R and I35R_PCR) was subjected to a blastN search (Table 5-10) and shown to have homology with other UGTs and unknown fish cDNAs. Multiple sequence alignment showed that livUGTn and I4_3R are similar with respect to each other, while I35R was markedly different (Figure 5-15).

Table 5-10. Results of blastn search for I35R_C

Sequences producing significant alignments:		Score (Bits)	E Value
gi|56324617|emb|CR646752.3|CNS0EY06	*Tetraodon nigroviridis* full-length DNA	91.7	2e-15
gi|56242288|emb|CR644097.2|CNS0EVYF	*Tetraodon nigroviridis* full-length DNA	91.7	2e-15
gi|34850459|dbj|AB120133.1|	*Pleuronectes yokohamae* UGT1B2 mRNA	69.9	9e-09
gi|71679708|gb|BC100055.1|	*Danio rerio* cDNA clone IMAGE:7284571, partial cd	60.0	8e-06
gi|46518141|emb|BX005348.9|	Zebrafish DNA sequence from clone...	60.0	8e-06
gi|46016516|emb|BX323548.11|	Zebrafish DNA sequence from clon...	60.0	8e-06
gi|68369305|ref|XM_682293.1|	PREDICTED: *Danio rerio* similar to UGT1, mRNA	60.0	8e-06
gi|68369293|ref|XM_681739.1|	PREDICTED: *Danio rerio* similar to UGT1, mRNA	60.0	8e-06

Scores

SeqA	Name	Len(nt)	SeqB	Name	Len(nt)	Score
1	livUGTn	1881	2	I35R_C	581	39

```
livUGTn         AGCTTTGATGAGCTCACCAGCAGATATCTCAAGAAGGATGTTACGTTCAGAGACGTCCTC 840
I35R_C          ---------------------------------------------------AAATTCCCAA 10
                                                                   * *   **

livUGTn         GGACATGCCGCGATTTGGCTTTATAGATATGACTTCACCTTTGAGTACCCGAGACCTGTA 900
I35R_C          AGACATTCCTGAAAATG---TCAAAGTGATGAAGTGGCTTCCGCAGAATGACCTCTTAGG 67
                  **** **   *  **   * * **  ****  *  * *  *   *       * *

livUGTn         ATGCCCAATGCGGTCAGAATTGGTGGCATCAACTGTGCCAAGAAGAATCCTCTGCCTGCC 960
I35R_C          TTTGTTTACACGTCCTCTAACCGTAATAAATAGACACCCGGTCCCCATTTTCTCTCTCAC 127
                 *     *  **  *   *   **   *   *     **       **  ***  **  *

livUGTn         GATCTGGAGGAGTTCGTGGACGGTTCTGGAGATCACGGCTTCATCGTGTTCACTTTGGGC 1020
I35R_C          ACACACATCTATCTATCACACAGGTCTATGATTATCGATTATACCGTA--CGTTTCCAGC 185
                          *  *     ** * **      *  **  *  * ***   *  **   **

livUGTn         TCCTTCGTGTCCGAGCTGCCGGAGTTCAAAGCCCG----GGAGTTTTTCGAGGCTTTTCG 1076
I35R_C          TAA--CACTACTTGGATACTTTGGTCAAAAACTCACACCGAAGGTCATTAACACA---CA 240
                *    *    *   * * *    **  *** * *     * ** *  *  *  *    *

livUGTn         GCAGATTCCTCAGAGGGTTCTGTGGCGATACACCGGGGTCATTCCCAAAGACATTCCTGA 1136
I35R_C          GTTCCTGTTTTAAACAGCGTTAAAATT-TAAATCTGAAAGATTCGAGGAAATATAATGGT 299
                *    *   * * *  *   *       ** * * *    ****    * * **    *

livUGTn         AAATGTCTA--AGTGATGAGGTGGCTTCCGCAGAACGACCTCTTA----GCACACCCCAA 1190
I35R_C          GCATAATAATAATTTCCTTTTTTCTTTCCTTTCATCGCCGTGTTAAAAAGCACACCCCAA 359
                  **    *  * *       *   ****    * ** * * ***    ***********

livUGTn         GGCTAAGGTGTTCATCACGCACGGAGGAGCCCATGGCATCTACGAGGGTATCTGTAACGG 1250
I35R_C          GGCTAAGGTGTTCATCACGCACGGAGGAACCCATGGCATCTACGAGGGTATCTGTAACGG 419
                ************************** ******************************

livUGTn         CGTGCCGATGGTGATGATCCCGCTGTTCGGAGATCAGGTAGACAACGTTCTACGCATGGT 1310
I35R_C          CGTGCCGATGGTGATGATCCCGCTGTTCGGAGATCAGGTAGACAACGTTCTACGCATGGT 479
                ************************************************************

livUGTn         GCTGCGTGGAGTCGCAGAGAGCCTGACCATGTTCGACCTGACCTCAGAGCAACTGCTGGG 1370
I35R_C          GCTGCGTGAAGTCGCAGAGAGCCTGACCATGTTCGACCTGACCTCAGAGCAACTGCTGGG 539
                ******** ***************************************************

livUGTn         GGCACTCAGGAAAGTCCTCAACAACAAGCGCTACAAAGAGAAGATAACACAGCTGTCTTT 1430
I35R_C          GGCACTCAGGAAAGTCCTCAACAACGAGCGCTAAAAAAAAAA------------------ 581
                ************************ ******* *** * **
```

Figure 5-15. Multiple sequence alignment between livUGTn and I35R_C.

Part of livUGTn sequence omitted for clarity.

Protein sequence analysis

a.liv/intUGTp. Further confirmation that the predicted livUGTp is a UGT came from a conserved domain search (Figure 5-16). The sequence was 100% aligned with UDPGT, and it was also closely related to glycosyltransferases and N-acetylglucosamine transferases.

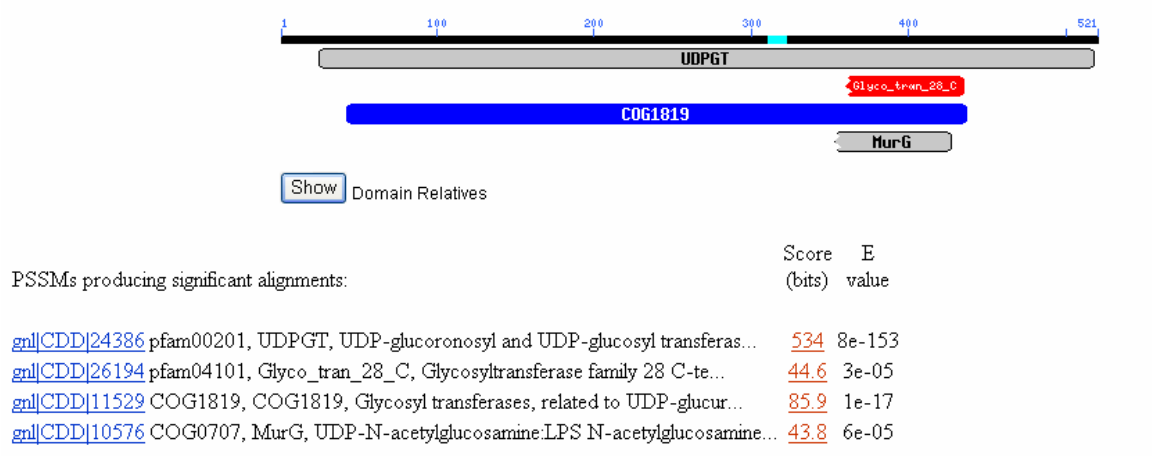

Figure 5-16. Results of NCBI conserved domain search

PSSM: position-specific scoring matrix

The protein displayed several areas of marked hydrophobicity, particularly at the C-terminal end, which presumably corresponds to the transmembrane region, which is followed by the positively charged cytoplasmic tail (Figure 5-17). Based upon the method developed by Kolaskar and Tongaonkar (1990), the Emboss program antigenic identified several potential antigenic sites. Maximum score position is denoted by the residues in bold and underlined format (Table 5-11).

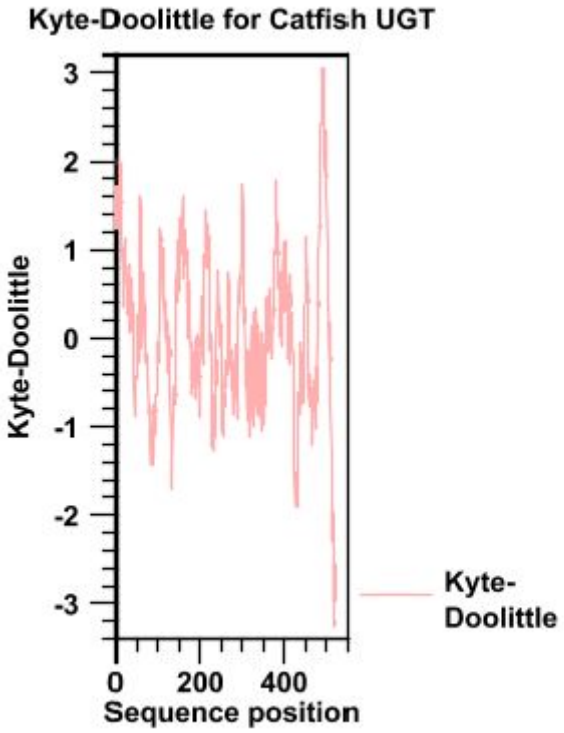

Figure 5-17. Kyte-Doolittle Hydrophobicity Plot for liv/intUGTp

Table 5-11. Potential antigenic sites on liv/intUGTp.

Sequence	Start	Length	Score
LLAALCLQ**I**YLCSFLGPV	4	18	1.236
AEHLRPAAHHLNWVQYHSLDVIAFLLLVL**S**TVVFIAVKTCALCFRKCFRR	466	50	1.224
DLMLTDPFLPCGPIIAEAFSLPA**V**YFLRGLPCGLDLEAAQCPSPPSYVPRF	141	51	1.180
EMVVL**V**PETSVLIHGSDAYVARSFKVPYTKA	52	31	1.175
GGKVL**V**MPVDGSH	23	13	1.174
ESILC**K**IFFSSF	214	12	1.154
IEPLD**L**AVFWTE	447	12	1.138
FRDVLG**H**AAIWLYRYD	239	16	1.127
VKGCE**A**LLYNE	119	11	1.123
VDNVLR**M**VLRGVAESL	393	16	1.12
LSM**K**ILVEEL	37	10	1.115

B. I35R_Cp. The predicted protein sequence for the partial cDNA obtained from intestine also exhibited homology with UGT proteins (Table 5-12). Conserved domain search showed that both sequences aligned with UDPGA-binding domains (Figure 5-18).

Table 5-12. Results of blastp search for I35R_Cp

Sequences producing significant alignments:	Score (Bits)	E Value
gi|47087385|ref|NP_998587.1| hypothetical protein LOC406731 [*Danio rerio*]	114	1e-24
gi|50370247|gb|AAH75892.1| Zgc:66393 protein [*Danio rerio*]	114	1e-24
gi|62531209|gb|AAH93347.1| Zgc:66393 protein [*Danio rerio*]	114	1e-24
gi|81097722|gb|AAI09405.1| Hypothetical protein LOC641488 [*Danio rerio*]	114	1e-24
gi|47205148|emb|CAG04937.1| unnamed protein product [*Tetraodon nigroviridis*]	113	4e-24
gi|47191630|emb|CAF92264.1| unnamed protein product [*Tetraodon nigroviridis*]	112	9e-24
gi|47198340|emb|CAF87158.1| unnamed protein product [*Tetraodon nigroviridis*]	112	9e-24
gi|47197196|emb|CAF89118.1| unnamed protein product [*Tetraodon nigroviridis*]	112	9e-24
gi|47210873|emb|CAF91810.1| unnamed protein product [*Tetraodon nigroviridis*]	111	2e-23
gi|56785765|gb|AAW29020.1| UGT [*Epinephelus coioides*]	108	1e-22
gi|975702|emb|CAA52214.1| UGT [*Pleuronectes platessa*]	105	1e-21
gi|71679709|gb|AAI00056.1| Unknown (protein for IMAGE:7284571)[*Danio rerio*]	104	2e-21
gi|68369306|ref|XP_687385.1| PREDICTED: similar to UGT1 family [*Danio rerio*]	104	2e-21
gi|68369294|ref|XP_686831.1| PREDICTED: similar to UGT1 family [*Danio rerio*]	104	2e-21
gi|5579028|emb|CAB51368.1| UGT [*Pleuronectes platessa*]	103	2e-21
gi|34850460|dbj|BAC87829.1| UGT [*Pleuronectes yokohamae*]	102	7e-21
gi|6272259|emb|CAB51369.2| UGT [*Pleuronectes platessa*]	102	9e-21
gi|2842546|dbj|BAA24692.1| UGT [*Felis catus*]	100	3e-20
gi|51260641|gb|AAH78732.1| Ugt1a7 protein [*Rattus norvegicus*]	99.0	8e-20
gi|40849836|gb|AAR95630.1| UGT1A11 [*Rattus norvegicus*]	99.0	8e-20
gi|40849840|gb|AAR95632.1| UGT1A4 [*Rattus norvegicus*]	99.0	8e-20
gi|40849848|gb|AAR95636.1| UGT1A9 [*Rattus norvegicus*]	99.0	8e-20
gi|40849846|gb|AAR95635.1| UGT1A8 [*Rattus norvegicus*]	99.0	8e-20
gi|79160160|gb|AAI07932.1| UGT1A6 [*Rattus norvegicus*]	99.0	8e-20
gi|40849842|gb|AAR95633.1| UGT1A6 [*Rattus norvegicus*]	99.0	8e-20
gi|40849838|gb|AAR95631.1| UGT1A2 [*Rattus norvegicus*]	99.0	8e-20
gi|18308176|gb|AAL67854.1| UGT1A7 [*Rattus norvegicus*]	99.0	8e-20
gi|18308170|gb|AAL67851.1| UGT1A8 [*Rattus norvegicus*]	99.0	8e-20
gi|18308168|gb|AAL67850.1| UGT1A5 [*Rattus norvegicus*]	99.0	8e-20
gi|18308174|gb|AAL67853.1| UGT1A6 [*Rattus norvegicus*]	99.0	8e-20
gi|207579|gb|AAA42312.1| bilirubin UGT [*Rattus norvegicus*]	99.0	8e-20
gi|136726|sp|P08430|UD16_RAT UGT 1-6 [*Rattus norvegicus*]	99.0	8e-20
gi|40849834|gb|AAR95629.1| UGT1A1 [*Rattus norvegicus*]	99.0	8e-20
gi|2501482|sp|Q64634|UD18_RAT UDP-glucuronosyltransferase 1-8...	99.0	8e-20
gi|2501481|sp|Q64633|UD17_RAT UDP-glucuronosyltransferase 1-7...	99.0	8e-20
gi|2501477|sp|Q64638|UD15_RAT UDP-glucuronosyltransferase 1-5...	99.0	8e-20
gi|2501475|sp|Q64637|UD13_RAT UDP-glucuronosyltransferase 1-3...	99.0	8e-20
gi|2507507|sp|P20720|UD12_RAT UDP-glucuronosyltransferase 1-2...	99.0	8e-20
gi|57163923|ref|NP_001009383.1| UGT1A [*Felis catus*]	98.6	1e-19
gi|57163903|ref|NP_001009359.1| UGT1A1 [*Felis catus*]	98.6	1e-19
gi|31324698|gb|AAP48597.1| UGT1A9 [*Mus musculus*]	98.6	1e-19
gi|31657196|gb|AAH53576.1| UGT1A10 protein [*Homo sapiens*]	98.6	1e-19

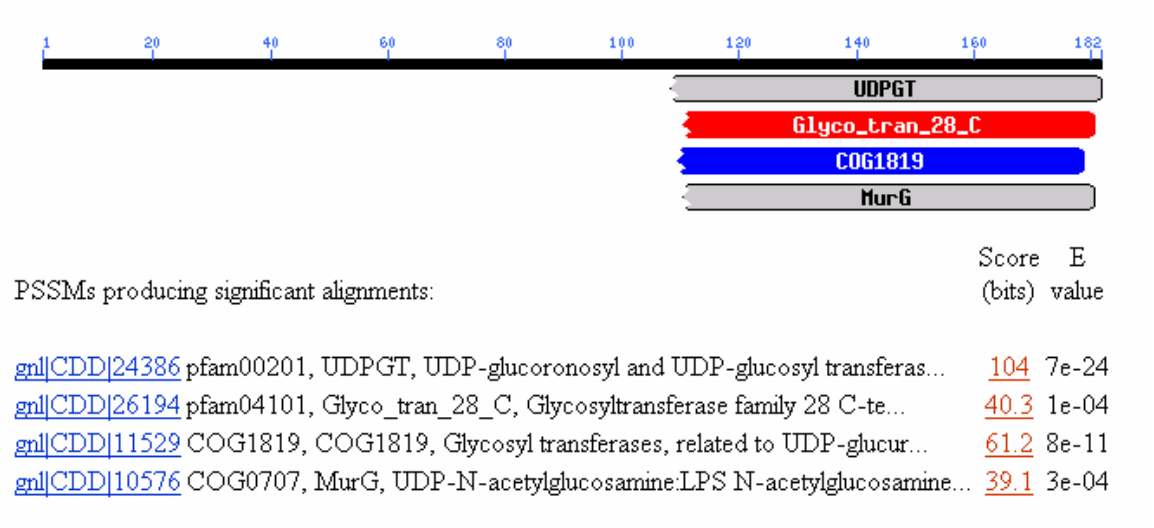

Figure 5-18. Results of NCBI conserved domain search for I35R_Cp

The protein sequences obtained from liver and intestine were aligned, showing a strongly conserved sequence for all three at residues 371-391 (relative to liv/intUGTn, Figure 5-19), which corresponds to the UDPGA binding site.

Scores

SeqA	Name	Len(aa)	SeqB	Name	Len(aa)	Score
1	livUGTp	627	2	I35R_Cp	133	60

```
livUGTp          GMLRARVPGLFFSHSSSFFFSSKICFL-T-LETFKLKMPRLLAALCLQIYLCSFLGPVEG 58
I35R_Cp          ------------------------------------------------------------

livUGTp          GKVLVMPVDGSHWLSMKILVEELSRRGHEMVVLVPETSVLIHGSDAYVARSFKVPYTKAE 118
I35R_Cp          ------------------------------------------------------------

livUGTp          LDESMNKLKEGITKAPRISDLLENIIGLLSFTNMQVKGCEALLYNEPLMQNLREEHFDLM 178
I35R_Cp          ------------------------------------------------------------

livUGTp          LTDPFLPCGPIIAEAFSLPAVYFLRGLPCGLDLEAAQCPSPPSYVPRFFTGNTDVMTFSQ 238
I35R_Cp          ------------------------------------------------------------

livUGTp          RVKNVLMTGFESILCKIFFSSFDELTSRYLKKDVTFRDVLGHAAIWLYRYDFTFEYPRPV 298
I35R_Cp          ------------------------------------------------------------

livUGTp          MPNAVRIGGINCAKKNPLPADLEEFVDGSGDHGFIVFTLGSFVSELPEFKAREFFEAFRQ 358
I35R_Cp          ----------------------------PANTTWILWSKTHTEGH----HTVPVLNSVKI 28
                                              ..:  :*:::     ..    ::  .::::.:

livUGTp          IPQRVLWRYTGVIPKDIPENVKVMKWLPQNDLLAHPKAKVFITHGGAHGIYEGICNGVPM 417
I35R_Cp          -----I-KIRGNI--MVHNNNFLFSFLSSPC-KAHPKAKVFITHGGTHGIYEGICNGVPM 79
                      : :  * *   : :*  :: :*..    **************:**************
                                          <----------- UDPGA binding site ---
livUGTp          VMIPLFGDQVDNVLRMVLRGVAESLTMFDLTSEQLLGALRKVLNNKRYKEKITQLSLIHK 477
I35R_Cp          VMIPLFGDQVDNVLRMVLREVAESLTMFDLTSEQLLGALRKVLNNER-KK---------- 128
                 :*:**************** ************************:* *:
                 ---------->
livUGTp          DRPIEPLDLAVFWTEFVMRHGSAEHLRPAAHHLNWVQYHSLDVIAFLLLVLSTVVFIAVK 537
I35R_Cp          ------------------------------------------------------------
                                                        <- TM region-->

livUGTp          TCALCFRKCFRRAQKSKKE-NGQ-MIRNGFGAVFN-RRWFIGVMSYCENLK-L-CSHHHV 592
I35R_Cp          ------------------------------------------------------------

livUGTp          QFNIQGCQQLWFSHCSYGCYDVTKKKK 619
I35R_Cp          ---------------------------
```

Figure 5-19. Alignment of predicted protein sequences from cloned catfish UGTs. Regions of interest and the starting and ending residue of the mature product are highlighted.

Cloning of entire UGT gene

The liver UGT gene was successfully amplified and cloned, using sets of primers that were complementary to both the untranslated regions (UTRs) upstream and downstream of the gene, as well as primers that annealed to the exact start and end of the translated portion of the gene (Figure 5-20). The same PCR conditions were used in an

attempt to amplify a product from intestinal cDNA, but this was successful only for the primers that annealed to the untranslated sequences (Figure 5-21).

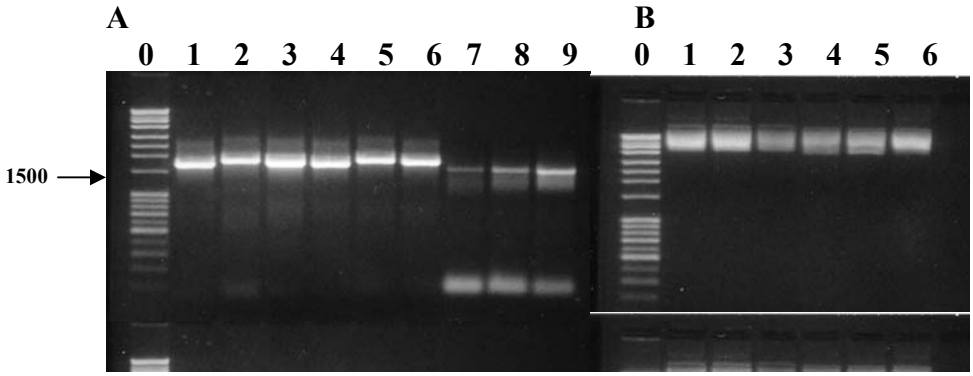

Figure 5-20. Cloning of livUGTn.

A. Amplification of UGT gene with (lanes 1-6) and without UTR (lanes 7-9), using various primer combinations and annealing temperatures. B. UTR insert (lanes 1-3) and UGT insert (lanes 4-6) cloned into p-GEM T-Easy vector, total size ~ 4500bp. 1kb ExactGene DNA ladder shown in first lane (0) of both pictures.

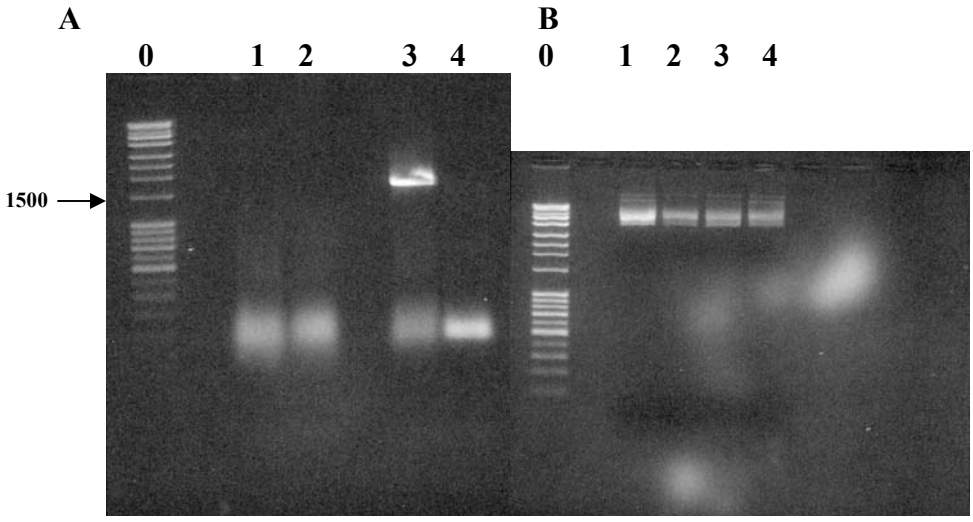

Figure 5-21. Cloning of intUGTn.

A. Amplification of UGT gene with (lane 3) and without UTR (lane 4); lanes 1 and 2 show unsuccessful amplification with degenerate primers. B. UTR insert (lanes 1-4) cloned into p-GEM T-Easy vector, total size ~ 4500bp. 1kb ExactGene DNA ladder shown in first lane (0) of both pictures.

The sequence of the DNA represented by these clones was compared to the UGT sequence deduced from the partial sequences of the various overlapping clones and amplicons (Table 5-13). There were minimal variations (99% homology), with the exception of a triple base change from AAA to TTT in all the clones at position 648.

Table 5-13. Results of ClustalW multiple sequence alignment analysis of the cloned UGTs and the original livUGTn

SeqA	Name	Len(nt)	SeqB	Name	Len(nt)	Score
1	livUGTn	1566	2	UTR1	1782	99
1	livUGTn	1566	3	UTR2	1799	99
1	livUGTn	1566	4	UTR3	1798	99
2	UTR1	1782	3	UTR2	1799	99
2	UTR1	1782	4	UTR3	1798	99
3	UTR2	1799	4	UTR3	1798	99

SeqA	Name	Len(nt)	SeqB	Name	Len(nt)	Score
1	UGT1	1569	2	UGT2	1569	99
1	UGT1	1569	3	UGT3	1569	99
1	UGT1	1569	4	livUGTn	1566	99
2	UGT2	1569	3	UGT3	1569	99
2	UGT2	1569	4	livUGTn	1566	99
3	UGT3	1569	4	livUGTn	1566	99

For full-sequences of these full-length UGT clones, refer to Appendix B.

Discussion

Multiplicity of UGT isoforms. At least two different UGT isoforms were identified from channel catfish liver (livUGTn) and intestine. One isoform (liv/intUGTn) was sequenced in its entirety and was cloned from both liver and intestine. Another isoform (I35R_C) was sequenced from intestine; amplification of this partial sequence towards its 5′- and 3′-ends was unsuccessful. However, the partial sequence obtained, particularly a 45-bp stretch at the known 5′-end of this sequence (which includes part of the UDPGA binding site) was significantly different from the sequence of the other isoform when both sequences were aligned.

The liv/intUGTn sequence appeared to be analogous to mammalian UGT1A1, or bilirubin UGT, while blastp searches for the predicted partial protein sequence of I35R_C resulted in better matches with the higher-numbered UGT isoforms such as UGT1A4, UGT1A7, UGT1A6. Of course, one cannot conclude anything further since these sequences are only partial, lacking the substrate-binding site which is responsible for the distinct specificity of the UGT isoform.

The presence of different UGT isoforms in catfish liver and intestine are probably one of the reasons for the disparate glucuronidation kinetics observed in these organs with substrates such as 3-hydroxybenzo[a]pyrene and polychlorinated biphenylols.

Characteristics of the predicted protein for livUGTn. As seen from Figure 5-13, the UGT isoform obtained from catfish shows several strongly conserved regions with mammals, even though 350 million years of evolution separate the two phyla. These indicate amino acid residues that are important for the function of the protein.

By drawing an analogy with mammalian UGTs, which have been extensively studied, several interesting features regarding the catfish UGT sequence were noted. Two

regions were clearly distinguished in the C-terminal domain, that is the UDPGA binding site at residues 347-394 (Mackenzie et al., 1997), and the transmembrane domain at residues 499-517. The cytoplasmic tail ends with the double lysine retrieval motif (-KSKKE); in mammals this is –KSKTH (Radominska-Pandya et al., 2005)

The UDPGA-binding region is highly conserved. The two basic residues K^{347} and K^{359} may form Schiff-base adducts with the uridinyl moiety as part of the process of transfer of glucuronic acid to the substrate (Radominska-Pandya et al., 1999). The histidine residue at 357 interacts with UDPGA while ^{366}His is required for catalysis in UGT1A6 (Battaglia et al., 1994). Further downstream, the 441-504 region is also highly conserved; it contains a ^{442}Lys and ^{443}Asp that help to maintain the active conformation of the enzyme (Iwano et al., 1999), as well as a ^{481}His that is one of 6 histidine residues important for the catalytic activity of human UGT1A6 (Battaglia et al., 1994).

The most variable amino acids for mammalian UGT sequences are located between amino acid residues 55-180. We observed, however, some strongly conserved regions even in this region, as well as further downstream (Table 5-14). One region of interest in UGT1A proteins is where a conserved hydrophobic region is thought to be the site of a buried α-helix containing an essential Phe that is critical for bilirubin glucuronidation (Ciotti et al., 1998). In the catfish UGT, there is an equivalent hydrophobic region VYF^{166}L (Fig 5-16). In mammalian steroid UGTs (UGT2B family), this region is disrupted by a Ser, thus providing further evidence that the catfish UGT is more likely a homolog of the mammalian UGT1 family.

Table 5-14. Conserved consecutive residues observed in catfish liver and mammalian UGTs (sequences shown in Figure 5-13). *X* indicates unconserved residue

Residue Start	Sequence	Importance	Reference
32	GS**H**WLSM	Contains His which is critical for activity	Battaglia et al., 1994
49	RG**H**	Conserved hydrophobic region; His required for optimal enzyme activity but not involved in catalysis	Battaglia et al., 1994 Senay et al., 1997
54	VVLVP	Important for enzyme function	Senay et al., 1997
144	LTDPF	Unknown	
199	M**T**F*X*QRVKN*X*L	Contains a phosphokinase site (T)	Basu et al., 2005
249	WL*X*R*X*DF	Unknown	
263	M**P**N*X*VI**GG**INC	Pro and Gly important for UGT1A1 activity and secondary structure	Ciotti et al., 1995
299	VFS/TLGS*X*VSEI/LP	Unknown	
324	IPQ*X*VLWRYTG	Unknown	
424	VL/INNK*X*YKE	Unknown	

A high degree of conservation (77%) was present for proline residues between catfish and the mammalian UGTs. The unique structure of this cyclic amino acid permits twists and kinks in the protein's tertiary structure. This indicates that overall, the three-dimensional structure of catfish liver UGTs is similar to its mammalian homologs.

On the other hand, there were some important differences. The Ile^{211} residue which is essential for activity in human UGT1A10 (Martineau et al., 2004), was replaced by a Leu in channel catfish (as in human UGT1A1, UGT1A3, UGT1A4, UGT1A6). The phenylalanine residues at positions 90 and 93 which have shown to be important for the catalytic activity of UGT1A10 towards phenols such as para-nitrophenol and 4-methylumbelliferone (Xiong et al., 2006), were absent in the catfish sequence as well as other fish sequences (Figure 5-22). Further upstream, the strongly conserved binding motif $Y^{73/72}$*XX*TK*X*YPVP that has been shown to be involved in the binding of phenols in

the case of mammalian UGT1A1 and UGT1A6 respectively (Senay et al., 1999) was discernible in the fish sequences, including catfish. The substitution of Ala for Thr at position 72 in catfish may provide additional evidence that the cloned UGT is not an analog of mammalian UGT1A7 and UGT1A10, since other studies have shown that mutation of this highly conserved residue led to a total inactivation of these isozymes, possibly due to the alteration of phosphorylation state of the enzyme (Basu et al., 2005).

```
                                  ..........                ..........
D.rerio_AAI09405.1            TSILIKKSGKYSTKTYPVSFTHDDLAENLKEIQNSALEK--APKLTDIVV 109
D.rerio_AAH75892.1            TSILIKKSGKYSTKTYPVSFTHDDLAENLKEIQNSALEK--APKLTDIVV 107
D.rerio_NP_998587.1           TSILIGKSGNFTTKSFRVPYSFDELNAHVDHIRKTAIEK--APRFIDIVG 110
D.rerio_AAH93347.1            ASLSMGPSEKTTTLTYPVNYTKAELHMVLEGNLTEILSTDFSTEVSKFFV 104
T.nigroviridis_CAG04937.1     TSLLIKSSENYRTEIYQVPYSKEDLGGSFQALKDGLFLK--PPSMADLFV 110
T.nigroviridis_CAF91810.1     TSLLIKSSENYRTEIYQVPYSKEDLDGSFQALKDGLFLK--PPSMADLFV 110
E.coioides_AAW29020.1         SSLLIHGSESYKTEIYQVSYTKAELDGKFAELQTGVSLK--PPAITDLFI 62
P.platessa_CAB51368.1         SSLFMHQSEDYKTEVYPVSFTTEEMDATHKQLKDGLFLK--QPDWTEYYV 110
P.platessa_CAB51369.2         SSLFMHQSEDYKTEVYPVSFTTEEMDATHKQLKDGLFLK--QPDWTEYYV 110
P.platessa_CAA52214.1         SSLFMHQSEDYETEVYPVSFTTEEMDATHKQLKDGLFLK--QPDWTEYYV 52
P.yokohamae_BAC87829.1        SSLFMHQSEDYKTEVYPVSFTMEEMDAVHKQLKDGLFLK--QPDWTEYYV 110
I.punctatus_livUGTp           TSVLIHGSDAYVARSFKVPYTKAELDESMNKLKEGIT-K--APRISDLLE 141
D.rerio_XP_687385.1           ISMRLGPGKHYITKKFPVKYDQKLFNEVLTEHVHEVTNPG-HSRLKTVTS 398
D.rerio_XP_686831.1           VSVLLGPGKHYVTRTFPVLYGKQQLDELQARNAQVMESKQ-LPLMEKIST 126
D.rerio_AAI00056.1            KNILIQSSELFRTETFPVKISKEQLSKSLKGFQQGVFTR--SPALMDVFV 113
                               .: :  .    :  : *      :
```

Figure 5-22. Multiple sequence alignment for fish sequences homologous to catfish UGT isolated from liver and intestine, showing regions where substrate binding of phenols is thought to occur for mammalian UGT1A isozymes.

Upstream highlighted eight residue-long sequence represents putative phenol binding site for UGT1A6 and UGT 1A1; downstream highlighted four residue-long sequence represents the phenol binding site for UGT1A10.

A potential phosphorylation site analogous to that observed for human UGT1A7 (Basu et al., 2005) may also be present at Thr^{200}; however other sites which have been shown to be phosphorylated, notably Ser^{432}, are absent in the cloned catfish UGT (but present in the fish sequences listed in Figure 5-10).

Limitations

3′-truncated UGT sequences. These were obtained for both liver and intestine. For example, the 3′ RACE performed in order to extend the UGT liver sequence resulted

in three bands (Figure 5-23). The 700bp and 300bp bands were cloned and sequenced and were found to be identical except for the fact that the 300bp product had a polyadenylated tail 400 bases upstream (in an adenine-rich region) of the polyadenylated tail belonging to the larger product. Cloning of the 1,200bp product was unsuccessful.

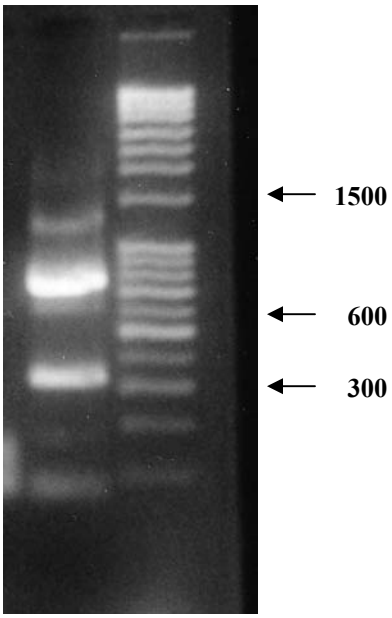

Figure 5-23. Results of 3′ RACE performed on liver, showing multiple products obtained.

In addition, it was also observed that further amplifying a PCR product obtained via RACE in order to increase the yield of this product, often resulted in the formation of smaller products. For example, the 3′ RACE performed in order to extend I4_degenerate resulted in two products which showed up as an intense 300bp band and a faint 700bp band (which was the expected product size) (Figure 5-24A). The gel piece containing the larger amplicon was purified and then subjected to an additional round of PCR (Figure 5-24B). The result were three bands: an expected one at 700bp (which was sequenced and corresponded to the sequence containing a full-length 3′ end (I4_3R)), and two smaller bands approximately 300 and 200bp in size. This could mean that there is some form of

degradation. Lacking any other explanation, it was tentatively concluded that these truncated UGT sequences were artifacts of the PCR reaction.

A

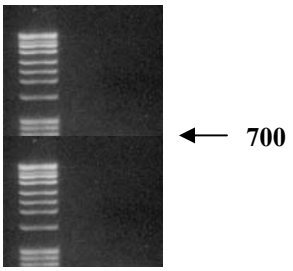

B

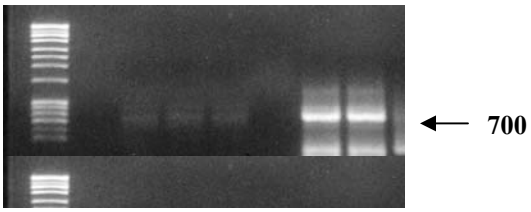

Figure 5-24. 3′ RACE for I4.

A. Inner PCR, B. Additional round of PCR (PCR reaction loaded in duplicate)

Quality of RNA. The fact that only two UGT isoforms were identified indicated some problem with the methodology. Catfish, like the phylogenetically related zebrafish, was expected to have multiple dissimilar UGT isoforms, particularly in liver. The fact that RACE failed to amplify the partial DNA sequences on several occasions led to the postulation that the RT reaction had been performed at a temperature that was too low (42°C, even though this is within the normal operating temperatures for the MMLV-RT enzyme), resulting in mRNA that was not folded correctly. In addition, it was noted that the RACE procedure omitted the heating step for 3 min at 70-85°C, prior to the actual reverse transcription, which helps to unfold the RNA. However, the heating step had been

used to generate cDNA in the initial PCR using the degenerate primers, which resulted in only two successful amplifications for the liver and one for the intestine (Figure 5-4). The RT reaction was reperformed at 50°C, but this did not seem to increase the number of amplicons. Thus, it was unlikely that the problem was in the reverse transcription step.

When the degenerate primers were rerun for cDNA originating from the intestine of another channel catfish (AT17), and cDNA from largemouth bass (*Micropterus salmoides*) liver, a larger number of amplicons (of expected sizes) were generated (Figure 5-25). In addition, the bands representing these various amplicons were more intense. The UGT cloned from catfish intestine derived from AT17 and not AT45. These findings indicate that the quality of the original RNA prepared from catfish AT45 intestine (and possibly liver) was not satisfactory. One reason for the difference between the RNA of both intestinal samples could have been due to the fact that while the intestinal RNA that was used originated from mucosa that had been scraped off the smooth muscle wall of the intestine, the AT17 intestinal RNA was derived from a tissue sample that was processed without separation of the mucosa from the underlying muscle. It is possible that the process of scraping the mucosa, even though this was done on ice and only lasted for a few minutes, caused the degradation of a significant proportion of the UGT mRNA population, resulting in the generation of a limited cDNA library. This may occur due to stimulation of the secretion of proteases, nucleases, and other hydrolytic enzymes. On one previous occasion, the process of scraping the catfish intestinal mucosa resulted in poor quality cDNA for a CYP450 cloning study. Subsequently, the CYP450 was successfully cloned from a sample that was derived from RNA originating from a transverse section of the intestine (Dr.David Barber, personal communication).

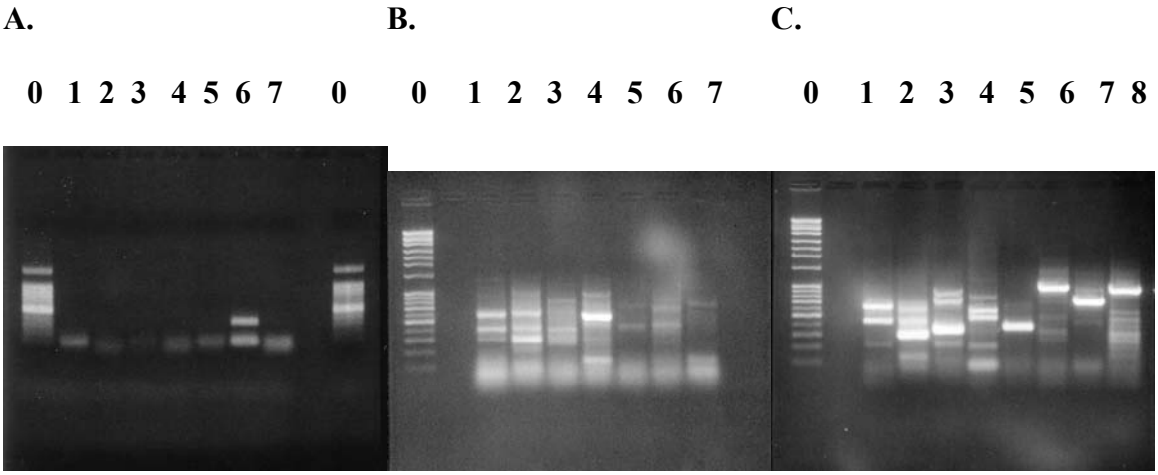

Figure 5-25. PCR amplification of UGT using degenerate primers.

In all cases, the same seven sets of primers were used under similar PCR conditions. cDNA templates were as follows: A, channel catfish AT45 intestine; B, channel catfish AT17 intestine; C, largemouth bass liver (lane 8 is similar to lane 6, but the PCR was run at a higher annealing temperature). Lane 0 represents 100kb ladder for (A) and 1kb ladder for (B) and (C).

Conclusions and recommendations

One full length UGT from catfish liver, together with an identical UGT from catfish intestine, was successfully cloned. A partial sequence of another UGT from catfish intestine was also cloned. By homology with mammalian UGTs, the full-length catfish UGT clone appeared to be analogous to UGT1A1 or UGT1A6. Expressing this gene into suitable cells (e.g. V79 or HEK cells) and characterizing the resulting protein should provide us with further information on glucuronidation in the catfish. Performing enzyme assays with UGT-selective probes, such as bilirubin (UGT1A1) and serotonin (UGT1A6) (Patten et al., 2001; Krishnaswami et al., 2003), would assist in such studies. As Table 5-11 shows, there are several potential antigenic sites on the predicted protein sequence that may be exploited to design specific anti-UGT antibodies which would

recognize such epitopes, in order to study the different levels of UGT protein in various tissues or in response to environmental stressors such as xenobiotic inducers or inhibitors. The availability of such isoform-selective antibodies is lacking, even for human UGTs (Miners et al., 2006).

Additional samples of catfish liver and intestinal RNA should be obtained, ensuring that the RNA is of optimal quality. After a number of isoforms have been isolated, real-time PCR could be performed using cDNA from catfish tissues such as brain, kidney, gills and skin to investigate the distribution of different UGT mRNAs in the channel catfish. Other studies can be performed on genomic DNA, in order to understand the gene locus for catfish UGT and whether differential splicing does indeed occur as in mammals. This would also be an opportunity to identify HNF-1 binding sites which reside within proximal upstream regulatory regions of human UGT genes (Gardner-Stephen et al., 2005) as well as the distal enhancer module which is the site of binding of nuclear receptors such as the glucocorticoid and the pregnane X receptor in mammalian UGTs (Sugatani et al., 2005).

CHAPTER 6
DETERMINATION OF PHYSIOLOGICAL UDPGA CONCENTRATIONS IN CHANNEL CATFISH LIVER AND INTESTINE

UDP-Glucuronic Acid (UDPGA)

When trying to determine K_m (or S_{50}) and V_{max} values for the substrate of interest in a bisubstrate system such as glucuronidation, one keeps the concentrations of co-substrate constant. This is done since, in theory, by using different concentrations of co-substrate one can get an infinite variety of values (*apparent values*) for the kinetic parameters. Thus, in order to obtain *true values* via the Michaelis-Menten equation, one has to determine kinetic parameters at saturating concentrations of co-substrate, assuming that these excess concentrations do not have any other effect on UGTs. Thus, for example, saturating concentrations of 0.2 mM UDPGA were used in our catfish intestine glucuronidation experiments (Chapter 4).

However, the use of excess concentrations of UDPGA present one with two problems. Are UDPGA concentrations saturating *in vivo*? How is the enzymatic efficiency affected, in view of the affinity (shown by K_m or S_{50}) of UGT(s) for UDPGA? If the physiological UDPGA concentrations are lower than the excess concentration used *in vitro* one may expect to observe a difference in kinetic parameters. While some studies have measured the physiological UDPGA level in tissues (mainly liver), most of this work has been limited to mammalian species such as humans and rats (Table 6-1).

The rate of glucuronidation of 3-OH-B[a]P was also found to be dependent on the endogenous level of UDPGA by Singh and co-workers (1986). This concept of UDPGA

supply as a rate-limiting factor has been observed in the glucuronidation of 7-hydroxycoumarin (Conway et al., 1988) and acetaminophen given together with retinol (which depletes UDPGA stores) (Bray and Rosengren 2001).

Table 6-1. UDPGA concentrations (μM) in liver and intestine of various species

Species	Liver	Small intestine	Reference
Human	279, 301 ± 119	19.3 ± 4.5	Cappiello et al., 1991, 2000
Human fetus	59.4 ± 11.3		Cappiello et al., 2000
Rat	200-500	121 ± 5 70 crypt cells 200 villus cells	Hjelle et al., 1985, Goon and Klaassen 1992, Yamamura et al., 2000, Dills et al., 1987[D], Pang et al., 1981, Hjelle 1986, Zhivkov et al., 1975 [D], Dubey and Singh 1988
Mouse	201 ± 17.6		Bray and Rosengren 2001
Guinea-pig	413 ± 3	322 – 580 79 ± 6 stomach 36 ± 3 colon	Zhivkov et al., 1975 [D], Singh et al., 1986
Pig Cat Rabbit	292 ± 24 153 182 ± 20		Zhivkov et al., 1975 [D]
Chicken Turkey Pigeon	51± 6 124 ± 26 78 ± 13		*Ibid*
Frog Newt	81 ± 11 73 ± 5		*Ibid*
Trout Carp	116 ± 8 21± 3		*Ibid*

[D] refers to a direct method of UDPGA measurement. All other references relied on indirect methods of UDPGA determination (see discussion).

Biphasic UDPGA kinetics have been demonstrated for 1-naphthol, morphine, 4-methylumbelliferone, and 3-hydroxybenzo[a]pyrene (Miners et al., 1988a,b; Tsoutsikos et al., 2004; Chapter 3). Whether this was due to the presence of multiple enzymes or an

allosteric effect by UDPGA on substrate binding (as proposed by Ethell and Wrighton 2004) is not known. Does the low-affinity component of the biphasic glucuronidation exist *in vivo*, or is it an *in vitro* artifact of the excess UDPGA concentrations?

In summary, the implication here is that the UGT activity obtained using saturating concentrations of UDPGA that are in excess of physiological concentrations in a certain tissue belonging to a specific species can render extrapolating *in vitro* data to *in vivo* situations potentially useless. One can overestimate the efficacy of glucuronidation of a xenobiotic because the maximal rate determined by conventional kinetic experiments may be greater than the maximal rate *in vivo*. In addition, compounds which are glucuronidated at rates ranging from the low nmol/min per mg to <1 pmol/min per mg may all be regarded as substrates in the presence of high concentrations of UDPGA (Miners et al., 2006).

Objective

To develop a reproducible method for the determination of UDPGA concentrations in channel catfish liver and intestine.

Method Development

Previous attempts to separate UDPGA by HPLC utilizing a C18 or a C4 column gave rise to results which were not reproducible. It was decided that, since UDPGA is acidic at physiological *p*H, an ion-exchange column would be used in order to separate this compound from other components of biological tissue that absorb at 260 nm (mainly nucleotides and nucleotide sugars).

Sample Digestion

The effect of boiling on UDPGA stability was investigated both with regards to heating time as well as the chemical nature of the solution in which the UDPGA was dissolved in. Boiling in water for 3 minutes resulted in a 12.7% loss of UDPGA (present as standard solution), compared to boiling in 0.25M H_2PO_4 for the same amount of time (7.7% loss). A final boiling time of 1 min was chosen since measurement of the temperature inside the glass tube showed that, within 15 seconds, the temperature of the water within the tube rose to 98°C when the tube was plunged into briskly boiling water. In addition, UDPGA loss when boiling in buffer for this period of time was minimal (Figure 6-1), and did not lead to appreciable decomposition of UDPGA to UDP and UMP (Bedford et al., 2003; Figure 6-2). Boiling of the liver sample for 1 minute in 0.30 M buffer, *p*H 4.3 resulted in less sample loss than boiling for 1 min or 3 min in 0.25 M buffer, *p*H 3.4 (Figure 6-3). Thus the final sample treatment conditions chosen were boiling for 1 minute in 0.30 M H_2PO_4 in H_2O, *p*H 4.3.

While liver samples were boiled in buffer as a 1 in 5 dilution (0.1 g liver with 0.4 mL buffer), intestinal samples were boiled as 2 in 5 (0.2 g with 0.3 mL), since UDPGA concentrations in intestine were expected to be significantly less than in liver.

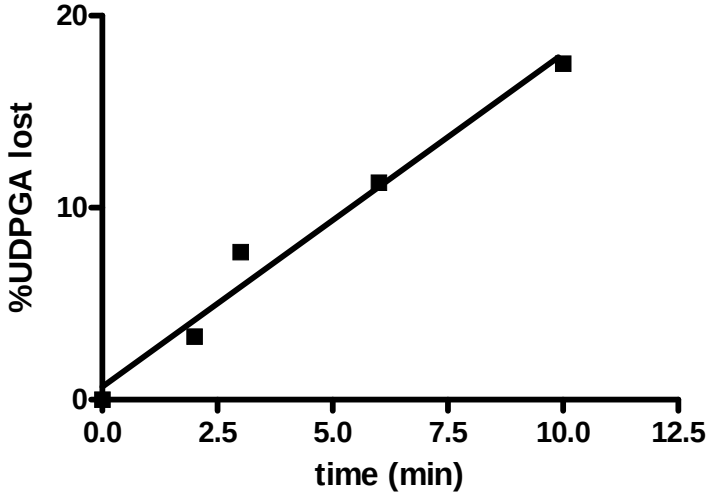

Figure 6-1. Heat-induced degradation of UDPGA (boiling in 0.25 M H_2PO_4 buffer)

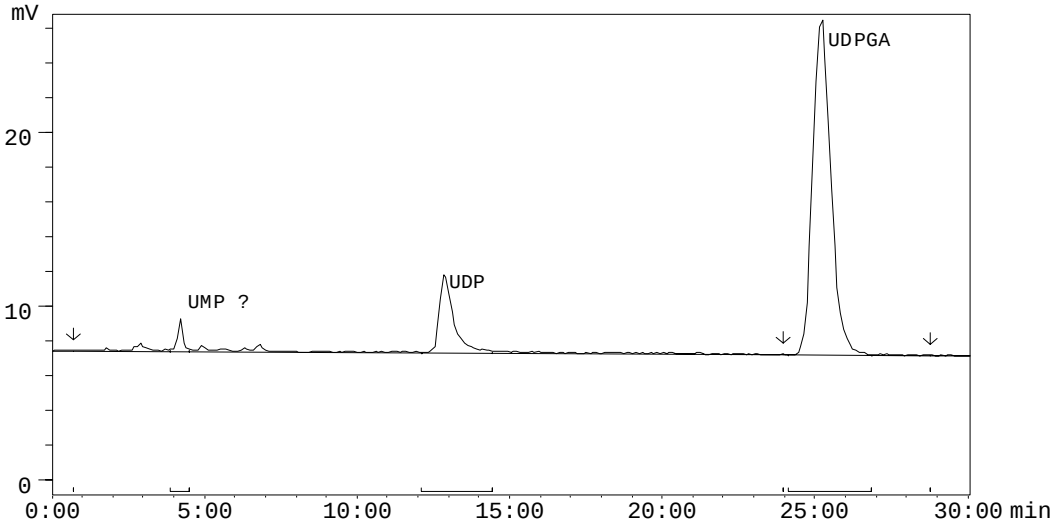

Figure 6-2. Decomposition of UDPGA to UDP and UMP after boiling in 0.25 M H_2PO_4 buffer for 10 minutes

A

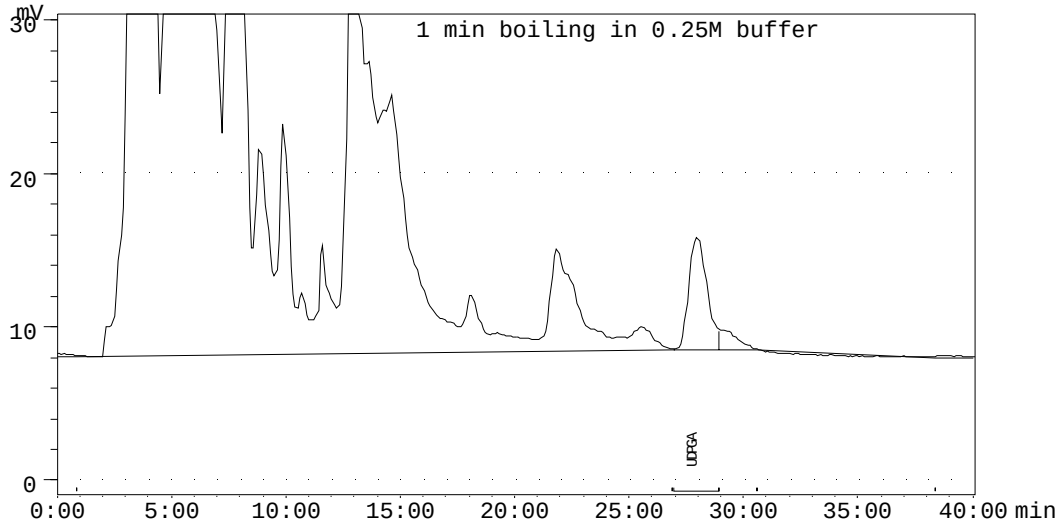

B

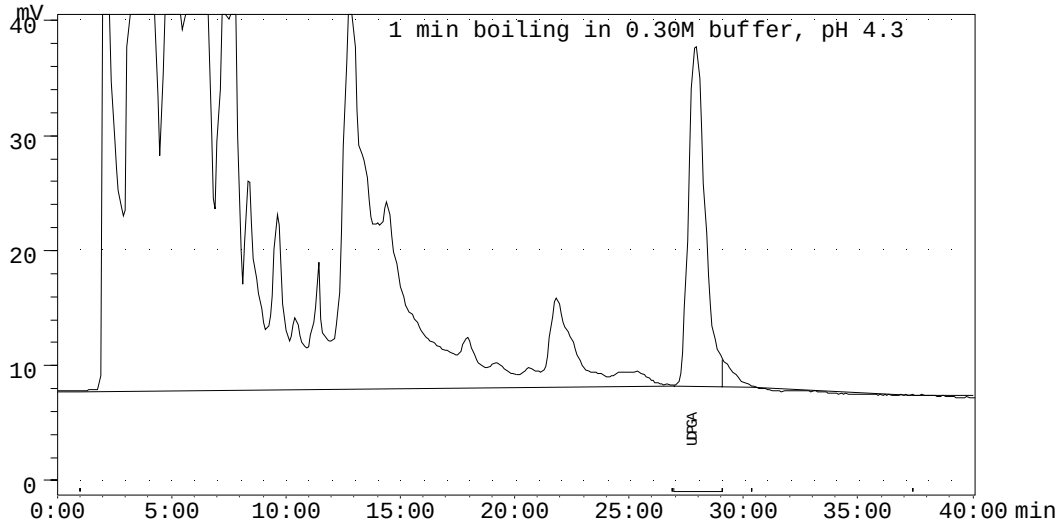

Figure 6-3. Effect of boiling liver tissue for 1 minute in two different concentrations of buffer. A, 0.25 M H_2PO_4, *p*H 3.4; B, 0.30 M H_2PO_4, *p*H 4.3

HPLC

A mobile phase consisting of 0.3 M $NH_4H_2PO_4$ in water (*p*H 3.1) was initially tried. UDPGA standards eluted at 16 min. However, this elution time was found to be

unsatisfactory when liver samples were tested, due to the proximity of various other peaks which led to a drifting baseline and inaccurate estimations of peak area. A decrease in buffer concentration to 0.25 M, with *p*H at 3.4, resulted in an increased retention time of 26 min. This is to be expected since the decreased concentration of $H_2PO_4^-$ ions results in decreased competition with the $UDPGA^-$ ions for the column bound NH_4^+. The net result was a well resolved peak corresponding to liver and intestinal UDPGA (Figures 6-4 and 6-5). The decreased retention time for UDPGA in the case of intestine may be due to differences in the sample matrix arising from the smaller dilution used in the initial homogenization step (p.120).

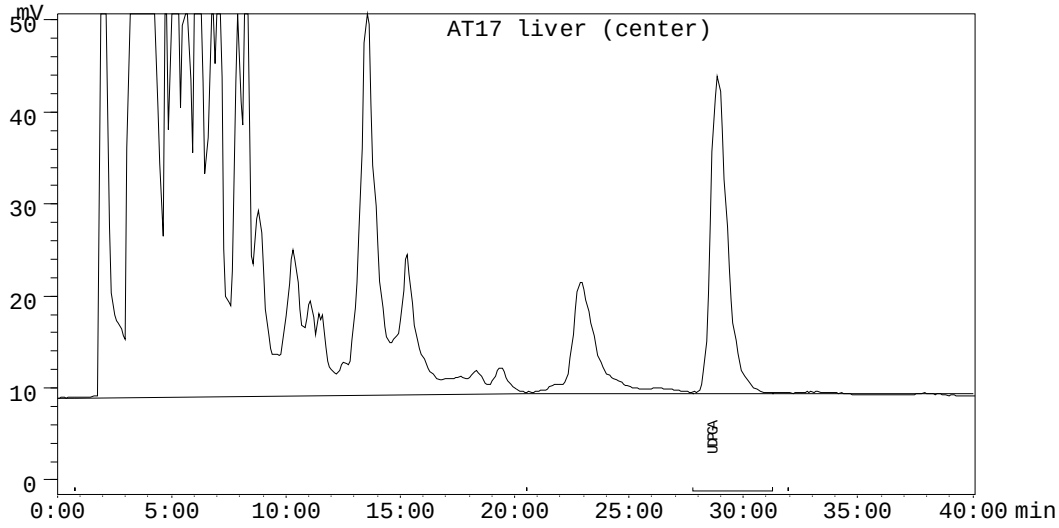

Figure 6-4. HPLC chromatogram for catfish AT17 liver. Center refers to region of liver from which the sample was taken.

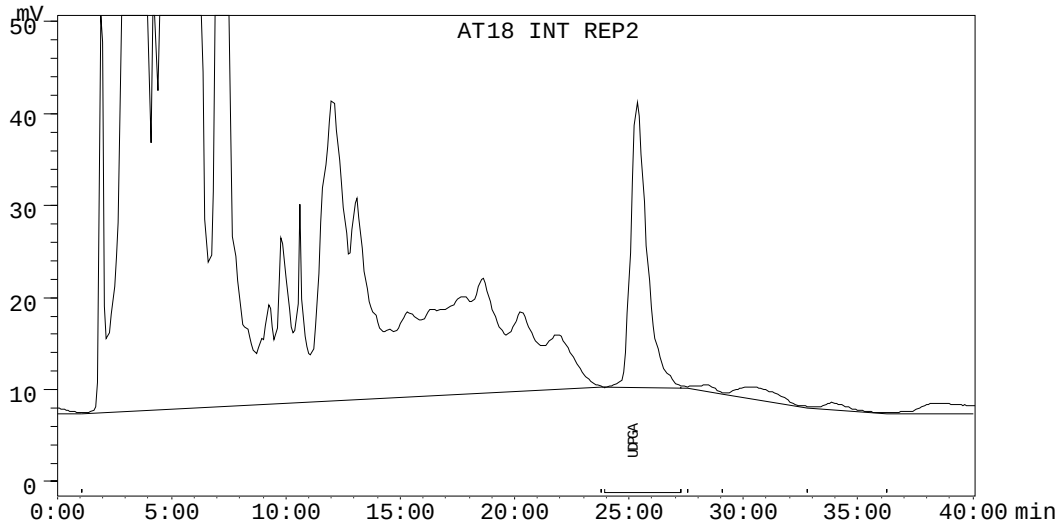

Figure 6-5. HPLC chromatogram for catfish AT18 intestine. Rep 2 refers to second sample taken from AT18 intestine.

Final Method

Liver tissue, 0.1 g, or 0.2 g intestinal mucosa were placed at the bottom of a small thick glass homogenizing tube (Thomas AA717). Using a rough tipped pestle attached to an electric drill, the tissue was homogenized for 10 seconds with 0.4 or 0.3 mL (liver or intestine respectively) of 0.3 M $NH_4H_2PO_4$. The tube in the homogenate was then placed in a briskly boiling water bath for 1 minute after which it was removed and placed on ice. The boiled mixture was briefly rehomogenized. The tubes were centrifuged, and the supernatant (still containing suspended matter) was transferred into a 1.5 mL microfuge tube and recentrifuged for 15 minutes at 16,000g. The supernatant was then filtered by spin-centrifugation (using 0.45 μM Spin-filters (Costar, Corning Inc., NY)) at 16,000g for 5 minutes. A sample, 50μL, was analyzed by HPLC (Model 2300 pump (ISCO, Lincoln, NE) with Dynamax UV absorbance detector (Rainin, Woburn, MA)).

HPLC conditions involved an isocratic system passing 0.25M $NH_4H_2PO_4$ (HPLC grade) in water (*p*H 3.4) at 1mL/min through a Zorbax SAX column (4.6mm i.d. x 250 mm, 5 μM) with UV detection at 260 nm. The elution times of some physiologically important chemicals, including UDPGA, are given in Table 6-2.

Table 6-2. Elution times of certain physiological substances (standards dissolved in mobile phase[1]) using the anion-exchange HPLC conditions described above.

Compound	Approximate elution time (min)
UDP-glucuronic acid	23
UDP-glucose	7
UDP	18
UDP-galacturonic acid	21
PAPS[1]	45

[1] The PAPS (3′-phosphoadenosine-5′-phosphosulfate, co-substrate for sulfonate conjugation) standard was dissolved in water in view of uncertainties regarding its heat lability and/or acid stability.

UDP-galacturonic acid, an epimer of UDPGA, could be resolved from UDPGA using this method (Figure 6-6). The usefulness of anion-exchange chromatography in separating these structurally related nucleotide sugars has been demonstrated elsewhere (Liljebjelke et al., 1995; Schlüpmann et al., 1994).

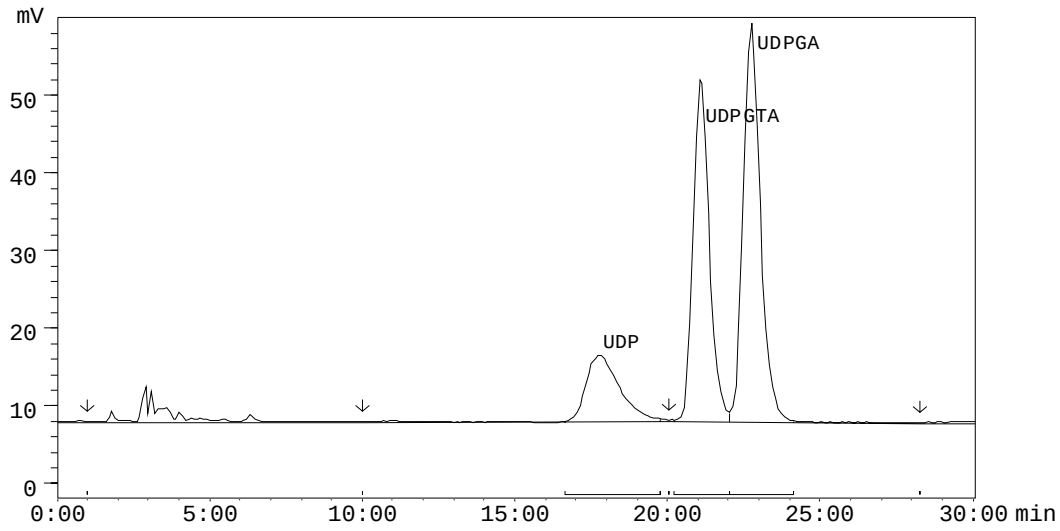

Figure 6-6. HPLC chromatogram of UDP, UDP-galacturonic acid (UDPGTA), and UDPGA standards.

Results

Several catfish liver and whole intestines were analyzed for UDPGA content using this method. The livers had been put in plastic tubes (with no buffer) immediately following sacrifice, and stored at -80°C. A paired t-test revealed that mean concentrations in liver were significantly higher than in intestine (p=0.008, Table 6-3 and Figure 6-7). Replicates showed less than 25% SD except for two fish (AT17 and AT18). Interestingly, the intestinal UDPGA values for one fish (AT17) were comparable to the hepatic UDPGA values of another fish (GS39).

Table 6-3. UDPGA concentrations in μM (duplicates for individual fish), in catfish liver and intestine.

Fish	Liver	Intestine
GS38	332, 326	ND[1]
GS39	252, 242	ND[1]
AT17	368, 397	235, 281
AT18	287, 355	174, 173
AT19	368, 376	87, 116
AT20	437, 426	87, 68
AT45	429, 458	59,71
Mean	**361 ± 68[2]**	**135 ± 81[2]**

[1] ND, not performed due to unavailability of tissue
[2] Standard deviation of the mean

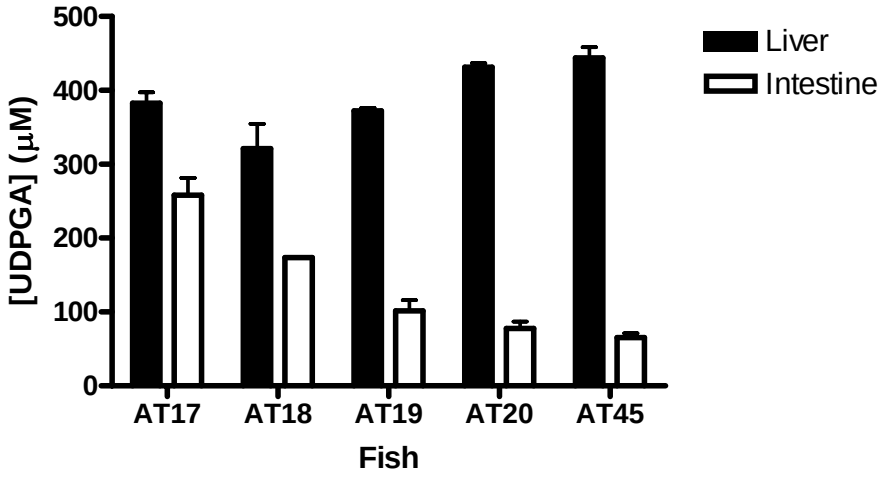

Figure 6-7. Comparison of hepatic and intestinal [UDPGA] in 4 individual channel catfish.

Discussion

Two major strategies have been used to study UDPGA concentrations in tissues. Indirect determination of UDPGA concentrations is based on the normally linear relationship between glucuronide formation and UDPGA concentration. The determination of glucuronide formation, whether via radiochemical detection (Schiller et al., 1982; Watkins and Klaasen, 1982; Hjelle et al., 1985; Cappiello et al., 1991), fluorometry (Singh et al., 1986) or reverse-phase HPLC (Yamamura et al., 2000), can then be used to down-extrapolate the UDPGA level via a standard curve. Since this method assumes that the linear relationship holds at low UDPGA physiological concentrations, determination of this co-substrate in tissues with lower levels (such as intestine) may be more subject to inaccuracies.

Reverse phase HPLC has been used to directly determine UDPGA concentrations in liver cell extracts (Aw and Jones, 1978; Dills et al., 1987; Alary et al., 1992) and whole tissue (Adachi et al., 1991; Suto et al., 2002). Imamura and co-workers (2003) used a reverse-phase system in order to determine both UDPGA and PAPS in cultured rat hepatocytes. While direct determination of UDPGA by HPLC is most desirable, the use of a C18 reverse-phase column was unsuccessful, due to the interference of other substances co-eluting with the UDPGA peak, as well as a drifting baseline. The use of an anion-exchange HPLC column dramatically improved resolution, sensitivity and reproducibility. Sub-micromolar concentrations of UDPGA standard, dissolved in ammonium phosphate buffer, could be detected.

Catfish liver UDPGA concentrations were similar to those previously reported for mammals such as humans, rats, and guinea pigs (Table 6-1). The results reported by Zhivkov and co-workers (1975) for other mammalian species, birds, amphibians and fish

are much lower than the catfish UDPGA levels measured with this method. Intestinal UDPGA concentrations in the catfish reported here are the first, to our knowledge, ever to have been reported for the intestine of any piscine species. These concentrations were in the same range as that reported for rats, but higher than humans and lower than guinea pigs. While some of these differences are species-related, another important contributor to the discrepancy is the different analytical techniques, some of which are inherently limited by an indirect measurement of UDPGA. Another possible source of variation may have been the dietary status of the individual animal, since UDPGA concentrations are decreased by fasting (Reinke et al., 1981). The only values measured in fish are those measured by Zhivkov and co-workers (1975), who homogenized liver tissue in perchloric acid in order to solubilize the nucleotides. This may have led to the lower values observed in trout and carp liver (Table 6-1) relative to catfish liver, since the rate of hydrolysis of UDPGA to UDP has been shown to be proportional to hydrogen ion concentration (Bedford et al., 2003).

Hepatic UDPGA concentrations were in the range of 329-444 μM. The UDPGA K_m values obtained for the hepatic glucuronidation were 247 μM and 697 μM for 4′-OHCB-72 and 4′-OHCB-35 respectively (Table 4-1). This means that, *in vivo*, at the saturating concentration of substrate used in the assay, and assuming that this UDPGA concentration range is typical of catfish populations, hepatic glucuronidation proceeds at a suboptimal rate for both 4′-OHCB-72 and 4′-OHCB-35. Of course, one must remember that the substrate concentrations used in the assay were not representative of environmental concentrations, and thus at smaller, more realistic OH-PCB levels, the UDPGA concentration is probably sufficient to efficiently glucuronidate 4′-OHCB-35.

Intestinal UDPGA concentrations appeared to have a larger range than in liver (65-258 μM). The decreased UDPGA concentrations (relative to liver) are reflected in the decreased UDPGA K_m of 27 μM reported for 4′-OHCB-69 (Table 4-1). The UGT isoforms in the intestine responsible for OH-PCB glucuronidation operate in a cellular environment with decreased UDPGA concentrations and thus appear to work optimally at lower concentrations of co-substrate.

The physiological hepatic levels of UDPGA are about 4 times lower than the 1.5 mM co-substrate concentrations utilized in the OH-PCB glucuronidation study in catfish (Chapter 4). In contrast, the physiological intestinal levels of UDPGA are around the same concentration as the amount used in the UGT assay (200 μM). This means that the V_{max} reported for hepatic OH-PCB glucuronidation in Chapter 4, probably represent overestimates that would not be achievable *in vivo*.

Conclusions and Recommendations

A method to directly determine UDPGA in tissue by anion-exchange chromatography was developed and used to study UDPGA concentrations in channel catfish liver and intestine. The method was sensitive, reproducible and displayed good resolution for UDPGA. The technique may be adapted to study other nucleotide sugars. The hepatic UDPGA levels determined by this technique were similar to those in other mammalian species and higher than two other fish species. This was the first time intestinal UDPGA concentrations in any piscine species were determined; the values were similar to rat, but significantly higher than in human small intestine.

Future studies should determine the UDPGA concentrations in a greater number of catfish, as well as in different tissues, including determination of the UDPGA

concentrations in the proximal and distal parts of the intestine. The effect of diet on the concentrations of this co-substrate in the experimental animals should also be taken into consideration. These studies should be performed in conjunction with experiments on glucuronidation kinetics, so as to better extrapolate *in vitro* findings to the *in vivo* situation.

APPENDIX A
SEQUENCES OF UGT PARTIAL CLONES AND AMPLICONS

The information given in parentheses after the title of each sequence provides data on the experiment which generated the sequence, together with photographic evidence. This includes Lab Book number and page, as well as the exact lane which shows the agarose gel-purified DNA.

A. 5' → 3' sequences of partial length clones for liver UGT

i. SEQUENCES OBTAINED BY DEGENERATE PRIMERS

>L1_DEGENERATE (LB XI, p. 86, lane 1)
GAGTTTGTGG ATGGCTCAGG AGATCACGGC TTCATCGTGT TCACTTTGGG CTCCTTCGTG
TCCGAGCTGC CGGAGTTCAA AGCCCGGGAG TTTTTCGAGG CTTTTCGGCA GATTCCTCAG
AGGGTTCTGT GGCGATACAC CGGGGTCATT CCCAAAGACA TTCCTGAAAA TGTCAAAGTG
ATGAAGTGGC TTCCGCAGAA TGACCTCTTA GCACACCCCA AGGCTAAGGT GTTCATCACG
CACGGAGGAA CCCATGGCAT CTACGAGGGT ATCTGTAACG GCGTGCCGAT GCTGATGTTT
CCTCTGTTT

>L2_DEGENERATE (LB XI, p. 86, lane 2)
GAGTTTGTGG ATGGCTCAGG AGATCACGGC TTCATCGTGT TCACTTTGGG CTCCTTCGTG
TCCGAGCTGC CGGAGTTCAA AGCCCGGGAG TTTTTCGAGG CTTTTCGGCA GATTCCTCAG
AGGGTTCTGT GGCGATACAC CGGGGTCATT CCCAAAGACA TTCCTGAAAA TGTCAAAGTG
ATGAAGTGGC TTCCGCAGAA TGACCTCTTA GCACACCCCA AGGCTAAGGT GTTCATCACG
CACGGAGGAA CCCATGGCAT CTACGAGGGT ATCTGTAACG GCGTGCCGAT GCTGATGTTC
CCTCTGTTT

>L3_DEGENERATE (LB XI, p. 86, lane 3)
GAGTTTGTGA AAGGCTCTGG AGATCACGGC TTCATCGTGT TCACTTTGGG CTCCTTCGTG
TCCGAGCTGC CGGAGTTCAA AGCCCGGGAG TTTTTCGAGG CTTTTCGGCA GATTCCTCAG
AGGGTTCTGT GGCGATACAC CGGGGTCATT CCCAAAGACA TTCCTGAAAA TGTCAAAGTG
ATGAAGTGGC TTCCGCAGAA CGACCTCTTA GCACACCCCA AGGCTAAGGT GTTCATCACG
CACGGAGGAG CCCATGGCAT CTACGAGGGT ATCTGTAACG GCGTGCCGAT GCTGATGTTC
CCGCTGTTT

>L4_DEGENERATE (LB XI, p. 86, lane 4)
GAGTTTGTCG AAGGCTCAGG AGATCACGGC TTCATCGTGT TCACTTTGGG CTCCTTCGTG
TCCGAGCTGC CGGAGTTCAA AGCCCGGGAG TTTTTCGAGG CTTTTCGGCA GATTCCTCAG
AGGGTTCTGT GGCGATACAC CGGGGTCATT CCCAAAGACA TTCCTGAAAA TGTCAAAGTG
ATGAAGTGGC TTCCGCAGAA CGACCTCTTA GCACACCCCA AGGCTAAGGT GTTCATCACG
CACGGAGGTG CCCATGGCAT CTACGAGGGT ATCTGTAACG GCGTGCCGAT GTTGATGTTC
CCGCTGTTT

>L5_DEGENERATE (LB XI, p. 86, lane 5)
GAGTTTGTGA AAGGCTCAGG AGATCACGGC TTCATCGTGT TCACTTTGGG CTCCTTCGTG
TCCGAGCTGC CGGAGTTCAA AGCCCGGGAG TTTTTCGAGG CTTTTCGGCA GATTCCTCAG
AGGGTTCTGT GGCGATACAC CGGGGTCATT CCCAAAGACA TTCCTGAAAA TGTCAAAGTG
ATGAAGTGGC TTCCGCAGAA CGACCTCTTA GCACACCCCA AGGCTAAGGT GTTCATCACG
CACGGAGGAG CCCATGGCAT CTACGAGGGT ATCTGTAACG GCGTGCCGAT GTTGATGTTC
CCGCTGTTT

>L6_DEGENERATE (LB XI, p. 86, lane 6)
GAGTTTGTGA ATGGCTCTGG AGATCACGGC TTCATCGTGT TCACTTTGGG CTCCTTCGTG
TCCGAGCTGC CGGAGTTCAA AGCCCGGGAG TTTTTCGAGG CTTTTCGGCA GATTCCTCAG
AGGGTTCTGT GGCGATACAC CGGGGTCATT CCCAAAGACA TTCCTGAAAA TGTCAAAGTG
ATGAAGTGGC TTCCGCAGAA TGACCTCTTA GCACACCCCA AGGCTAAGGT GTTCATCACG
CACGGAGGAA CCCATGGCAT CTACGAGGGT ATCTGTAACG GCGTGCCGAT GGTGATGATC
CCGCTGTTCG GAGATCAGGT AGACAACGTT CTACGCATGG TGCTGCGTGA AGTCGCAGAG
AGCCTGACCA TGTTCGACCT GACCTCAGAG CAACTGCTGG GGGCACTCAG GAAAGTCCTC
AACAACAAGC GCTACAAAGA GAAGATAACA CAGCTGTCTT TGATCCATAA AGACCGTCCG
ATCGAGCCGC TGGACTTGGC CGTGTTCTGG ACCGAGTTTG TGATGAGACA CGGAAGTGCC
GAGCACCTGA GACCGGCCGC TCACCACCTG AACTGGATTC AGTACCAC

>L7_DEGENERATE (LB XI, p. 86, lane 7)
GAGTTTGTGG AAGGCTCTGG AGATCACGGC TTCATCGTGT TCACTTTGGG CTCCTTCGTG
TCCGAGCTGC CGGAGTTCAA AGCCCGGGAG TTTTTCGAGG CTTTTCGGCA GATTCCTCAG
AGGGTTCTGT GGCGATACAC CGGGGTCATT CCCAAAGACA TTCCTGAAAA TGTCAAAGTG
ATGAAGTGGC TTCCGCAGAA CGACCTCTTA GCACACCCCA AGGCTAAGGT GTTCATCACG
CACGGAGGAG CCCATGGCAT CTACGAGGGT ATCTGTAACG GCGTGCCGAT GGTGATGATC
CCGCTGTTCG GAGATCAGGT AGACAACGTT CTACGCATGG TGCTGCGTGG AGTCGCAGAG
AGCCTGACCA TGTTCGACCT GACCTCAGAG CAACTGCTGG GGGCACTCAG GAAAGTCCTC
AACAACAAGC GCTACAAAGA GAAGATAACA CAGCTGTCTT TGATCCATAA AGACCGTCCG
ATCGAGCCGC TGGACTTGGC CGTGTTCTGG ACCGAGTTTG TGATGAGACA CGGAAGTGCC
GAGCACCTGA GACCGGCCGC TCACCACCTG AACTGGATCC AGTACCAC

ii. SEQUENCES OBTAINED BY 5′-RACE (1st round)

>UGT_L25R (LB XI, p. 139, lane 2)
AAAGCAAGAT ATTTTTCTCC AGCTTTGATG AGCTCACCAG CAGATATCTC AAGAAGGATG
TTACGTTCAG AGACGTCCTC GGACATGCCG CGATTTGGCT TTATAGATAT GACTTCACCT
TTGAGTACCC GAGACCTGTA ATGCCCAATG CGGTCAGAAT TGGTGGCATC AACTGTGCCA
AGAAGAATCC TCTGCCTGCC GATCTGGAGG AGTTCGTGGA CGGTTCTGGA GATCACGGCT
TCATCGTGTT CACTTTGGGC TCCTTCGTGT CCGAGCTGCC GGAGTTCAAA GCCCGGGAGT
TTTTCGAGGC TTTTCGGCAG ATTCCTCAGA GGGTTCTGTG GCGATACACC GGGGTCATTC
CCAAAGACAT TCCTGAAGAT GTCAAAGTGA TGAAGTGGCT TCCGCAGAAC GACCTCTTAG
CACACCCCAA GGCTAAGGTG TTCATCACGC AC

>UGT_L35R (LB XI, p. 139, lane 3)
AGCTCACCAG CAGATATCTC AAGAAGGATG TTACGTTCAG AGACGTCCTC GGACATGCCG
CGATTTGGCT TTATGGATAT GACTTCACCT TTGAGTACCC GAGACCTGTA ATGCCCAATG
CGGTCAGAAT TGGTGGCATC AACTGTGCCA AGAAGAATCC TCTGCCTGCC GATCTGGAGG
AGTTCGTGGA CGGTCCTGGA GATCACGGCT TCATCGTGTT CACTTTGGGC TCCTTCGTGT
CCGAGCTGCC GGAGTTCAAA GCCCGGGAGT TTTTCGAGGC TTTTCGGCAG ATTCCTCAGA
GGGTTCTGTG GCGATACACC GGGGTCATTC CCAAAGACAT TCCTGAAAAT GTCAAAGTGA
TGAAGTGGCT TCCGCAGAAC GACCTCTTAG CACACCCCAA GGCTAAGGTG TTCATCACGC
ACGGAGGAGC CCATGGCATC TACGAGGGTA TCTGT

iii. SEQUENCES OBTAINED BY 5'-RACE (2nd round) PCR products only, not cloned

>UGT_L25R_5R (LB XII, p.8, lanes 1-2; p.49, lanes 1-2)
(1 additional round of amplification)
GGAATGCTAA GAGCTCGAGT ACCGGGCCTG TTCTTCTCAC ATTCCTCCTC TTCTTTTTTT
CCTCCAAAAT CTGCTTCCTC TAGACGTAAT TAGAAACTTT TAAGCTAAAA ATGCCTCGTC
TTCTTGCAGC TCTCTGTCTC CAGATTTATC TTTGCAGCTT TTTAGGACCA GTGGAAGGAG
GGAAGGTCCT GGTGATGCCC GTGGACGGCA GCCACTGGCT CAGTATGAAG ATCTTGGTGG
AGGAATTGTC TCGGAGAGGA CATGAAATGG TGGTCCTGGT TCCCGAGACA AGCGTGTTGA
TCCATGGCTC TGACGCGTAC GCCGCTCGGA GCTTTAAGGT TCCGTACACC AAGGCTGACT
GGATGAAAGC ATGAATAAGT TGAAGGAGGG CATTACGAAA GCACCGCGGA TCTCTGACTT
ATTGGAGAAC ATCATCGGGC TCCTCAGCTT CACGAACATG CAGGTGAAAG GATGCGAGGG
CTGCTGTATA ACGAGCCTCT GATGCAGAAC CTGCGCGAGG AACACTTCGA TCTCATGCTC
ACCGATCCCT TCCTGCCTTG TGGCCCCATC ATCGCCGAGG CTTTCTCCCT CCCCGCCGTT
TATTTCCTGC GTGGGCTTCC CTGCGGATTG GATCTGGAAG CCGCTCAGTG CCCATCGCCT
CCGTCCTACG TCCCGCGCTT TTTCACAGGC AACACCGACG TCATGACGTT TTCTCAGAGG
GTCAAGAACG TGCTCATGAC GGGATTCGAG AGCATCCAAA GCAAGATATT TTTCTCCAGC
TTTGATGAGC TCACCAGCAG A

>UGT_L25R_5R (LB XII, p. 108, lanes 2 and 3)
AATGCTAAGA GCTCGAGTAC CGGGCCTGTT CTTCTCACAT TCCTCCTCCT TCTTTTTTTC
CTCCAAAATC TGCTTCCTCT AGACGTAATT AGAAACTTTT AAGCTAAAAA TGCCTCGTCT
TCTTGCAGCT CTCTGTCTCC AGATTTATCT TTGCAGCTTT TTAGGACCAG TGGAAGGAGG
GAAGGTCCTG GTGATGCCCG TGGACGGCAG CCACTGGCTC AGTATGAAGA TCTTGGTGGA
GGAATTGTCT CGGAGAGGAC ATGAAATGGT GGTCCTGGTT CCCGAGACAA GCGTGTTGAT
CCATGGCTCT GACGCGTACG CCGCTCGGAG CTTTAAGGTT CCGTACACCA AGGCTGAACT
GGATGAAAGC ATGAATAAGT TGAAGGAGGG CATTACGAAA GCACCGCGGA TCTCTGACTT
ATTGGAGAAC ATCATCGGGC TCCTCAGCTT CACGAACATG CAGGTGAAAG GATGCGAGGC
GCTGCTGTAT AACGAGCCTC TGATGCAGAA CCTGCGCGAG GAACACTTCG ATCTCATGCT
CACCGATCCC TTCCTGCCTT GTGGCCCCAT CATCGCCGAG GCTTTCTCCC TCCCCGCCGT
TTATTTCCTG CGTGGGCTTC CCTGCGGATT GGATCTGGAA GCCGCTTAGT GCCCATCGCC
TCCGTCCTAC GTCCCGCGCT TTTTCACAGG CAACACCGAC GTCATGACGT TTTCTCAGAG
GGTCAAGAAC GTGCTCATGA CGGGATTCGA GAGCATCCTT TGCAAAATAT TTTTCTCCAG
CTTTGATGAG CTCACCAGCA GA

iii. SEQUENCES OBTAINED BY 3′-RACE

>UGT_L25R_5A (LB XII, p. 13, lane 6)

GGGGTCATTC CCAAAGACAT TCCTGAAAAT GTCAAAGTGA TGAAGTGGCT TCCGCAGAAC
GACCTCTTAG CACACCCCAA GGCTAAGGTG TTCATCACGC ACGGAGGAGC CCATGGCATC
TACGAGGGTA TCTGTAACGG CGTGCCGATG GTGATGATCC CGCTGTTCGG AGATCAGGTA
GACAACGTTC TACGCATGGT GCTGCGTGAA GTCGCAGAGA GCCTGACCAT GTTCGACCTG
ACCTCAGAGC AACTGCTGGG GGCACTCAGG AAAGTCCTCA ACAACGAGCG CTAAAAAAAA
AAA

>UGT_L25R_5Av (LB XII, p. 47, lane 4)
GGGGTCATTC CCAAAGACAT TCCTGAAAAT GTCAAAGTGA TGAAGTGGCT TCCGCAGAAT
GACCTCTTAG CACACCCCAA GGCTAAGGTG TTCATCACGC ACGGAGGAAC CCATGGCATC
TACGAGGGTA TCTGTAACGG CGTGCCGATG GTGATGATCC CGCTGTTCGG AGATCAGGTA
GACAACGTTC TACGCATGGT GCTGCGTGAA GTCGCAGAGA GCCTGACCAT GTTCGACCTG
ACCTCAGAGC AACTGCTGGG GGCACTCAGG AAAGTCCTCA ACAACAAGCG CTAAAAAAAA
AAAA
>UGT_L25R_5Avi (LB XII, p. 47, lane 5)
GGGGTCATTC CCAAAGACAT TCCTGAAAAT GTCAAAGTGA TGAAGTGGCT TCCGCAGAAT
GACCTCTTAG CACACCCCAA GGCTAAGGTG TTCATCACGC ACGGAGGAAC CCATGGCATC
TACGAGGGTA TCTGTAACGG CGTGCCGATG GTGATGATCC CGCTGTTCGG AGATCAGGTA
GACAACGTTC TACGCATGGT GCTGCGTGAA GTCGCAGAGA GCCTGACCAT GTTCGACCTG
ACCTCAGAGC AACTGCTGGG GGCACTCAGG AAAGTCCTCA ACAACAAGCG CTACAAAGAA
AAAAAAAA

>UGT_L25R_4Bb (LB XII, p. 27, lane 9)
GGGGTCATTC CCAAAGACAT TCCTGAAAAT GTCTAAGTGA TGAGGTGGCT TCCGCAGAAC
GACCTCTTAG CACACCCCAA GGCTAAGGTG TTCATCACGC ACGGAGGAGC CCATGGCATC
TACGAGGGTA TCTGTAACGG CGTGCCGATG GTGATGATCC CGCTGTTCGG AGATCAGGTA
GACAACGTTC TACGCATGGT GCTGCGTGGA GTCGCAGAGA GCCTGACCAT GTTCGACCTG
ACCTCAGAGC AACTGCTGGG GGCACTCAGG AAAGTCCTCA ACAACAAGCG CTACAAAGAG
AAGATAACAC AGCTGTCTTT GATCCATAAA GACCGTCCGA TCGAGCCGCT GGACTTGGCC
GTGTTCTGGA CCGAGTTTGT GATGAGACAC GGAAGTGCCG AGCACCTGAG ACCGGCCGCT
CACCACCTCA ACTGGGTTCA GTACCACAGT CTCGATGTCA TCGCCTTCCT CCTGCTCGTT
CTATCCACCG TCGTTTTTAT CGCCGTCAAA ACCTGCGCGC TCTGTTTCAG GAAGTGTTTC
CGGAGGGCTC AGAAGAGCAA AAAGGAGTGA AACGGCCAGT GAATGATCAG GAATGGATTT
GGTGCCGTCT TTAATTAACG CCGATGGTTT ATCGGCGTGA TGTCATACTG TGAAAACCTG
AAATAGTTAT AGTGTTCTCA TCACCACGTT CAATTTAATA TTCAGGGGTG CCAGCAATTA
TGGTTTAGCC ATTGCAGTTA CGGTTGTTAT GATGTCACTA AAAAAAAAAA A

>UGT_L25R_4Bi (LB XII, p. 47, lane 1)
GGGGTCATTC CCAAAGACAT TCCTGAAAAT GTCAAAGTGA TGAAGTGGCT TCCGCAGAAT
GACCTCTTAG CACACCCCAA GGCTAAGGTG TTCATCACGC ACGGAGGAAC CCATGGCATC
TACGAGGGTA TCTGTAACGG CGTGCCGATG GTGATGATCC CGCTGTTCGG AGATCAGGTA
GACAACGTTC TACGCATGGT GCTGCGTGAA GTCGCAGAGA GCCTGACCAT GTTCGACCTG
ACCTCAGAGC AACTGCTGGG GGCACTCAGG AAAGTCCTCA ACAACAAGCG CTACAAAGAG
AAGATAACAC AGCTGTCTTT GATCCATAAA GACCGTCCGA TCGAGCCGCT GGACTTGGCC
GTGTTCTGGA CCGAGTTTGT GATGAGACAC GGAAGTGCCG AGCACCTGAG ACCGGCCGCT
CACCACCTCA ACTGGGTTCA GTACCACAGT CTCGATGTCA TCGCCTTCCT CCTGCTCGTT
CTATCCACCG TCGTTTTTAT CGCCGTCAAA ACCTGCGCGC TCTGTTTCAG GAAGTGTTTC
CGGAGGGCTC AGAAGAGCAA AAAGGAGTGA AACGGCCAGT GAATGATCAG GAATGGATTT
GGTGCCGTCT TTAATTAACG CCGATGGTTT ATCGGCGTGA TGTCATACTG TGAAAACCTG
AAATAGTTAT AGTGTTCTCA TCACCACGTT CAATTTAATA TTCAGGGGTG CCAGCAATTA
TGGTTTAGCC ATTGCAGTTA CGGTTGTTAT GATGTCACAA AAAAAAAAAA

>UGT_L25R_4Bii (LB XII, p. 47, lane 2)
GGGGTCATTC CCAAAGACAT TCCTGAAAAT GTCAAGGTGA TGAAGTGGCT TCCGCAGAAT
GACCTCTTAG CACACCCCAA GGCTAAGGTG TTCATCACGC ACGGAGGAGC CCATGGCATC
TACGAGGGTA TCTGTAACGG CGTGCCGATG GTGATGATCC CGCTGTTCGG AGATCAGGTA
GACAACGTTC TACGCATGGT GCTGCGTGAA GTCGCAGAGA GCCTGACCAT GTTCGACCTG
ACCTCAGAGC AACTGCTGGG GGCACTCAGG AAAGTCCTCA ACAACAAGCG CTACAAAGAG
AAGATAACAC AGCTGTCTTT GATCCATAAA GACCGTCCGA TCGAGCCGCT GGACTTGGCC
GTGTTCTGGA CCGAGTTTGT GATGAGACAC GGAAGTGCCG AGCACCTGAG ACCGGCCGCT
CACCACCTCA ACTGGGTTCA GTACCACAGT CTCGATGTCA TCGCCTTCCT CCTGCTCGTT
CTATCCACCG TCGTTTTTAT CGCCGTCAAA ACCTGCGCGC TCTGTTTCAG GAAGTGTTTC
CGGAGGGCTC AGAAGAGCAA AAAGGAGTGA AACGGCCAGT GAATGATCAG GAATGGATTT
GGTGCCGTCT TTAATTAACG CCGATGGTTT ATCGGCGTGA TGTCATACTG TGAAAACCTG
AAATAGTTAT AGTGTTCTCA TCACCACGTT CAATTTAATA TTCAGGGGTG CCAGCAATTA
TGGTTTAGCC ATTGCAGTTA CGGTTGTTAT GATGTCACTA AAAAAAAAAA AA

>UGT_L25R_4Biii (LB XII, p. 47, lane 3)
GGGGTCATTC CCAAAGACAT TCCTGAAAAT GTCAAAGTGA TGAAGTGGCT TCCGCAGAAT
GACCTCTTAG CACACCCCAA GGCTAAGGTG TTCATCACGC ACGGAGGAAC CCATGGCATC
TACGAGGGTA TCTGTAACGG CGTGCCGATG GTGATGATCC CGCTGTTCGG AGATCAGGTA
GACAACGTTC TACGCATGGT GCTGCGTGAA GTCGCAGAGA GCCTGACCAT GTTCGACCTG
ACCTCAGAGC AACTGCTGGG GGCACTCAGG AAAGTCCTCA ACAACAAGCG CTACAAAGAG
AAGATAACAC AGCTGTCTTT GATCCATAAA GACCGTCCGA TCGAGCCGCT GGACTTGGCC
GTGTTCTGGA CCGAGTTTGT GATGAGACAC GGAAGTGCCG AGCACCTGAG ACCGGCCGCT
CACCACCTCA ACTGGGTTCA GTACCACAGT CTCGATGTCA TCGCCTTCCT CCTGCTCGTT
CTATCCACCG TCGTTTTTAT CGCCGTCAAA ACCTGCGTGC TCTGTTTCAG GAAGTGTTTC
CGGAGGGCTC AGAAGAGCAA AAAGGAGTGA AACGGCCAGT GAATGATCAG GAATGGATTT
GGTGCCGTCT TTAATTAACG CCGATGGTTT ATCGGCGTGA TGTCATACTG TGAAAACCTG
AAATAGTTAT AGTGTTCTCA TCACCACGTT CAATTTAATA TTCAGGGGTG CCAGCAATTA
TGGTTTAGCC ATTGCAGTTA CGGTTGTTAT GATGTCACGA AAAAAAAAAA A

B. 5'→3' sequences of partial length clones for intestinal UGT

i. SEQUENCES OBTAINED BY DEGENERATE PRIMERS

>UGT_I1 DEGENERATE (LB XI, p. 91, lane 1)
GAGTTTGTGG ATGGCTCAGG AGATCACGGC TTCATCGTGT TCACTTTGGG CTCCTTCGTG
TCCGAGCTGC CGGAGTTCAA AGCCCGGGAG TTTTTCGAGG CTTTTCGGCA GATTCCTCAG
AGGGTTCTGT GGCGATACAC CGGGGTCATT CCCAAAGACA TTCCTGAAAA TGTCAAAGTG
ATGAAGTGGC TTCCGCAGAA CGACCTCTTA GCACACCCCA AGGCTAAGGT GTTCATCACG
CACGGAGGTG CCCATGGCAT CTACGAGGGT ATCTGTAACG GCGTGCCGAT GTTGATGTTC
CCACTGTTT

>UGT_I2 DEGENERATE (LB XI, p. 91, lane 2)
GAGTTTGTGA ATGGCTCAGG AGATCACGGC TTCATCGTGT TCACTTTGGG CTCCTTCGTG
TCCGAGCTGC CGGAGTTCAA AGCCCGGGAG TTTTTCGAGG CTTTTCGGCA GATTCCTCAG
AGGGTTCTGT GGCGATACAC CGGGGTCATT CCCAAAGACA TTCCTGAAAA TGTCAAAGTG
ATGAAGTGGC TTCCGCAGAA TGACCTCTTA GCACACCCCA AGGCTAAGGT GTTCATCACG
CACGGAGGAA CCCATGGCAT CTACGAGGGT ATCTGTAACG GCGTGCCGAT GCTGATGTTC
CCACTGTTT

>UGT_I3 DEGENERATE (LB XI, p. 91, lane 3)
CTAGTGATTG AGTTTGTGGA TGGCTCTGGA GATCACGGCT TCATCGTGTT CACTTTGGGC
TCCTTCGTGT CCGAGCTGCC GGAGTTCAAA GCCCGGGAGT TTTTCGAGGC TTTTCGGCAG
ATTCCTCAGA GGGTTCTGTG GCGATACACC GGGGTCATTC CCAAAGACAT TCCTGAAAAT
GTCAAAGTGA TGAAGTGGCT TCCGCAGAAC GACCTCTTAG CACACCCCAA GGCTAAGGTG
TTCATCACGC ACGGAGGAGC CCATGGCATC TACGAGGGTA TCTGTAACGG CGTGCCGATG
TTGATGTTCC CTCTGTTT

>UGT_I4 DEGENERATE (LB XI, p. 91, lane 4)
GAGTTTGTGG AAGGCTCAGG AGATCACGGC TTCATCGTGT TCACTTTGAG CTCCTTCGTG
TCCGAGCTGC CGGAGTTCAA AGCCCGGGAG TTTTTCGAGG CTTTTCGGCA GATTCCTCAG
AGGGTTCTGT GGCGATACAC CGGGGTCATT CCCAAAGACA TTCCTGAAAA TGTCAAAGTG
ATGAAGTGGC TTCCGCAGAA CGACCTCTTA GCACACCCCA AGGCTAAGGT GTTCATCACG
CACGGAGGTG CCCATGGCAT CTACGAGGGT ATCTGTAACG GCGTGCCGAT GTTGATGTTC
CCACTGTTT

ii. SEQUENCES OBTAINED BY 5′-RACE

>UGT_I15R (LB XI, p. 139, lane 5)
AAATTCCCAA GGACATTCCT GAAAATGTCA AAGTGATGAA GTGGCTTCCG CAGAATGACC
TCTTAGGTTT GTTTACACGT CCTCTAACCG TAATAAATAG ACACCCGGTC CCCATTTCTC
TCACACACAC ACACATCTAT CTATCACGCA GGTCTATGAT TATCGATTAT ACCGTACGTT
TCCAGCTAAC ACTACTTGGA TACTTTGGTC AAAAACTCAC ACCGAAGGTC ATTAACACAC
AGTTCCTGTT TTAAACAGCG TTAAAATTTA AATCTGAAAG ATTCGAGGAA ATATAATGGT
GCATAATAAT AATTTCCTTT TTTCTTTCCT TTCATCGCCG TGTTAAAAAG CACACCCCAA
GGCTAAGGTG TTCATCACGC ACGGAGGAAC CCATGGCATC TACGAGGGTA TCTGT

>UGT_I25R (LB XI, p. 139, lane 6)
AAATTCCCAA AGACATTCCT GAAAATGTCA AAGTGATGAA GTGGCTTCCG CAGAATGACC
TCTTAGGTTT GTTTACACGT CCTCTAACCG TAATAAATAG ACACCCGGTC CCCATTTTCT
CTCACACACA CACACATCTA TCTATCACAC AGGTCTATGA TTATCGATTA TACCGTACGT
TTCCAGCTAA CACTACTTGG ATACTTTGGT CAAAAACTCA CACCGAAGGT CATTAACACA
CAGTTCCTGT TTTAAACAGC GTTAAAATTT AAATCTGAAA GATTCGAGGA AATATAATGG
TGCATAATAA TAATTTCCTT TTTTCTTTCC TTTCATCGCC GTGTTAAAAA GCACACCCCA
AGGCTAAGGT GTTCATCACG CACGGAGGAA CCCATGGCAT CTACGAGGGT ATCTGT

>UGT_I35R (LB XI, p. 139, lane 7)
AAATTCCCAA AGACATTCCT GAAAATGTCA AAGTGATGAA GTGGCTTCCG CAGAATGACC
TCTTAGGTTT GTTTACACGT CCTCTAACCG TAATAAATAG ACACCCGGTC CCCATTTTCT
CTCTCACACA CACACATCTA TCTATCACAC AGGTCTATGA TTATCGATTA TACCGTACGT
TTCCAGCTAA CACTACTTGG ATACTTTGGT CAAAAACTCA CACCGAAGGT CATTAACACA
CAGTTCCTGT TTTAAACAGC GTTAAAATTT AAATCTGAAA GATTCGAGGA AATATAATGG
TGCATAATAA TAATTTCCTT TTTTCTTTCC TTTCATCGCC GTGTTAAAAA GCACACCCCA
AGGCTAAGGT GTTCATCACG CACGGAGGAA CCCATGGCAT CTACGAGGGT ATCTGT

iii. SEQUENCES OBTAINED BY 3'-RACE

>UGT_I4_6A (LB XII, p. 27, lane 5)
CCCAAGGCTA AGGTGTTCAT CACGCACGGA GGAGCCCATG GCATCTACGA GGGTATCTGT
AACGGCGTGC CGATGGTGAT GATCCCGCTG TTCGGAGATC AGGTAGACAA CGTTCTACGC
ATGGTGCTGC GTGAAGTCGC AGAGAGCCTG ACCATGTTCG ACCTGACCTC AGAGCAACTG
CTGGGGGCAC TCAGGAAAGT CCTCAACAAC GAGCGCCAAA AAAAAAAAAA

>UGT_I46Aix (LB XII, p. 47, lane 6)
CCCAAGGCTA AGGTGTTCAT CACGCACGGA GGAGCCCATG GCATCTACGA GGGTATCTGT
AACGGCGTGC CGATGGTGAT GATCCCGCTG TTCGGAGATC AGGTAGACAA CGTTCTACGC
ATGGTGCTGC GTGAAGTCGC AGAGAGCCTG ACCATGTTCG ACCTGACCTC AGAGCAACTG
CTGGGGGCAC TCAGGAAAGT CCTCAACAAC GAGCGCTAAA AAAAA

>UGT_I46Ax (LB XII, p. 47, lane 7)
CCCAAGGCTA AGGTGTTCAT CACGCACGGA GGAGCCCATG GCATCTACGA GGGTATCTGT
AACGGCGTGC CGATGGTGAT GATCCCGCTG TTCGGAGATC AGGTAGACAA CGTTCTACGC
ATGGTGCTGC GTGAAGTCGC AGAGAGCCTG ACCATGTTCG ACCTGACCTC AGAGCAACTG
CTGGGGGCAC TCAGGAAAGT CCTCAACAAC GAGCGCTAAA AAAAAAAA

The following sequences were all sequenced directly from the PCR product and were not cloned
>I4_3R (LB XII, p.128, lower lanes 4-5; p.142, lane 1)
CACGCACGGA GGAACCCATG GCATCTACGA GGGTATCTGT AACGGCGTGC CGATGGTGAT
GATCCCGCTG TTCGGAGATC AGGTAGACAA CGTTCTACGC ATGGTGCTGC GTGAAGTCGC
AGAGAGCCTG ACCATGTTCG ACCTGACCTC AGAGCAACTG CTGGGGGCAC TCAGGAAAGT
CCTCAACAAC AAGCGCTACA AAGAGAAGAT AACACAGCTG TCTTTGATCC ATAAAGACCG
TCCGATCGAG CCGCTGGACT TGGCCGTGTT CTGGACCGAG TTTGTGATGA GACACGGAAG
TGCCGAGCAC CTGAGACCGG CCGCTCACCA CCTCAACTGG GTTCAGTACC ACAGTCTCGA
TGTCATCGCC TTCCTCCTGC TCGTTCTATC CACCGTCGTT TTTATCGCCG TCAAAACCTG
CGTGCTCTGT TTCAGGAAGT GTTTCCGGAG GGCTCAGAAG AGCAAAAAGG AGTGAAACGG
CCAGTGAATG ATCAGGAATG GATTTGGTGC CGTCTTTAAT TAACGCCGAT GGTTTATCGG
CGTGATGTCA TACTGTGAAA ACCTGAAATA GTTATAGTGT TCTCATCACC ACGTTCAATT
TAATATTCAG GGGTGCCAGC AATTATGGTT TAGCCATTGC AGTTACGGTT GTTATGATGT
CACGAAAAAA AAAAA

>I35R_PCR (LB XII, p.126, band 6, lane 6)
AGCCCATGGC ATCTACGAGG GTATCTGTAA CGGCGTGCCG ATGGTGATGA TCCCGCTGTT
CGGAGATCAG GTAGACAACG TTCTACGCAT GGTGCTGCGT GAAGTCGCAG AGAGCCTGAC
CATGTTCGAC CTGACCTCAG AGCAACTGCT GGGGGCACTC AGGAAAGTCC TCAACAACGA
GCGCTAAAAA AAAAA

>I35R_PCR2 (LB XII, p.126, band 6A, lane 6; p.130, lanes 3-4)
CCATGGCATC TACGAGGGTA TCTGTAACGG CGTGCCGATG GTGATGATCC CGCTGTTCGG
AGATCAGGTA GACAACGTTC TACGCATGGT GCTGCGTGAA GTCGCAGAGA GCCTGACCAT
GTTCGACCTG ACCTCAGAGC AACTGCTGGG GGCACTCAGG AAAGTCCTCA ACAACGAGCG
CTAAAAAAAA AA

APPENDIX B

SEQUENCES FOR UGT FULL-LENGTH CLONES FROM CATFISH LIVER

A. UGT clones with UTRs at either end (highlighted area indicates start and stop codons)

>UTR1

```
1    CTGCTTCCTC TAGACGTAAT TAGAAACTTT TAAGCTAAAA ATGCTTCGTC TTCTTGCAGC
61   TCTCTGTCTC CAGATTTATC TTTGCAGCTT TTTAGGACCA GTGGAAGGAG GGAAGGTCCT
121  GGTGATGCCC GTGGACGGCA GCCACTGGCT CAGTATGAAG ATCTTGGTGG AGGAATTGTC
181  TCGGAGAGGA CATGAAATGG TGGTCCTGGT TCCCGAGACA AGCGTGTTGA TCCATGGCTC
241  TGACGCGTAC GCCGCTCGGA GCTTTAAGGT TCCGTACACC AAGGCTGAAC TGGATGAAAG
301  CATGAATAAG TTGAAGGAGG GCATTACGAA AGCACCGCGG ATCTCTGACT TATTGGAGAA
361  CATCATCGGG CTCCTCAGCT TCACGAACAT GCAGGTGAAA GGATGCGAGG CGCTGCTGTA
421  TAACGAGCCT CTGATGCAGA ACCTGCGCGA GGAACACTTC GATCTCATGC TCACCGATCC
481  CTTCCTGCCT TGTGGCCCCA TCATCGCCGA GGCTTTCTCC CTCCCCGCCG TTTATTTCCT
541  GCGTGGGCTT CCCTGCGGAT TGGATCTGGA AGCCACTCAG TGCCCATCGC CTCCGTCCTA
601  CGTCCCGCGC TTTTTCACAG GCAACACCGA CGTCATGACG TTTTCTCAGA GGGTCAAGAA
661  CGTGCTCATG ACGGGATTCG AGAGCATCCT TTGCAAAATA TTTTTCTCCA GCTTTGATGA
721  GCTCACCAGC AGATATCTCA AGAAGGATGT TACGTTCAGA GACGTCCTCG GACATGCCGC
781  GATTTGGCTT TATAGATATG ACTTCACCTT TGAGTACCCG AGACCTGTAA TGCCCAATGC
841  GGTCAGAATT GGTGGCATCA ACTGTGCCAA GAAGAATCCT CTGCCTGCCG ATCTGGAGGA
901  GTTCGTGGAC GGTTCTGGAG ATCACGGCTT CATCGTGTTC ACTTTGGGCT CCTTCGTGTC
961  CGAGCTGCCG GAGTTCAAAG CCCGGGAGTT TTTCGAGGCT TTTCGGCAGA TTCCTCAGAG
1021 GGTTCTGTGG CGATACACCG GGGTCATTCC CAAAGACATT CCTGAAAATG TCAAAGTGAT
1081 GAAGTGGCTT CCGCAGAACG ACCTCTTAGC ACACCCAAGG CTAAGGTGTT CATCACGCAC
1141 GGAGGAGCCC ATGGCATCTA CGAGGGTATC TGTAACGGCG TGCCGATGGT GATGATCCCG
1201 CTGTTCGGAG ATCAGGTAGA CAGCGTTCTA CGCATGGTGC TGCGTGGAGT CGCAGAGAGC
1261 CTGACCATGT TCGACCTGAC CTCAGAGCAA CTGCTGGGGG CACTCAGGAA AGTCCTCAAC
1321 AACAAGCGCT ACAAAGAGAA GATAACACAG CTGTCTTTGA TCCATAAAGA CCGTCCGATC
1381 GAGCCGCTGG ACTTGGCCGT GTTCTGGACC GAGTTTGTGA TGAGACACGG AAGTGCCGAG
1441 CACCTGAGAC CGGCCGCTCA CCACCTCAAC TGGGTTCAGT ACCACAGTCT CGATGTCATC
1501 GCCTTCCTCC TGCTCGTTCT ATCCACCGTC GTTTTTATCG CCGTCAAAAC CTGCGCGCTC
1561 TGTTTCAGGA AGTGTTTCCG GAGGGCTCAG AAGAGCAAAA AGGAGTGAAA CGGCCAGTGA
1621 ATGATCAGGA ATGGATTTGG TGCCGTCTTT AATTAACGCC GATGGTTTAT CGGCGTGATG
1681 TCATACTGTG AAAACCTGAA ATAGTTATAG TGTTCTCATC ACCACGTTCA ATTTAATATT
1741 CAGGGGTGCC AGCAATTATG GTTTAGCCAT TGCAGTTACG GT
```

>UTR2

```
1     CTGCTTCCTC TAGACGTAAT TAGAAACTTT TAAGCTAAAA ATGCCTCGTC TTCTTGCAGC
61    TCTCTGTCTC CAGATTTATC TTTGCAGCTT TTTAGGACCA GTGGAAGGAG GGAAGGTCCT
121   GGTGATGCCC GAGGACGGCA GCCACTGGCT CAGTATGAAG ATCTTGGTGG AGGAATTGTC
181   TCGGAGAGGA CATGAAATGG TGGTCCTGGT TCCCGAGACA AGCGTGTTGA TCCATGGCTC
241   TGACGCGTAC GTCGCTCGGA GCTTTAAGGT TCCGTACACC AAGGCTGAAC TGGATGAAAG
301   CATGAATAAG TTGAAGGAGG GCATTACGAA AGCACCGCGG ATCTCTGACT TATTGGAGAA
361   CATCATCGGG CTCCTCAGCT TCACGAACAT GCAGGTGAAA GGATGCGAGG CGCTGCTGTA
421   TAACGAGCCT CTGATGCAGA ACCTGCGCGA GGAACACTTC GATCTCATGC TCACCGATCC
481   CTTCCTGCCT TGTGGCCCCA TCATCGCCGA GGCTTTCTCC CTCCCCGCCG TTTATTTCCT
541   GCGTGGGCTT CCCTGCGGAT TGGATCTGGA AGCCGCTCAG TGCCCATCGC CTCCGTCCTA
601   CGTCCCGCGC TTTTTCACAG GCAACACCGA CGTCATGACG TTTTCTCAGA GGGTCAAGAA
661   CGTGCTCATG ACGGGATTCG AGAGCATCCT TTGCAAAATA TTTTTCTCCA GCTTTGATGA
721   GCTCACCAGC AGATATCTCA AGAAGGATGT TACGTTCAGA GACGTCCTCG GACATGCCGC
781   AATTTGGCTT TATAGATATG ACTTCACCTT TGAGTACCCG AGACCTGTAA TGCCCAATGC
841   GGTCAGAATT GGTGGCATCA ACTGTGCCAA GAAGAATCCT CTGCCTGCCG ATCTGGAGGA
901   GTTCGTGGAC GGTTCTGGAG ATCACGGCTT CATCGTGTTC ACTTTGGGCT CCTTCGTGTC
961   CGAGCTGCCG GAGTTCAAAG CCCGGGAGTT TTTCGAGGCT TTTCGGCAGA TTCCTCAGAG
1021  GGTTCTGTGG CGATACACCG GGGTCATTCC CAAAGACATT CCTGAAAATG TCAAAGTGAT
1081  GAAGTGGCTT CCGCAGAATG TCCTCTTAGC ACACCCCAAG GCTAAGGTGT TCATCACGCA
1141  CGGAGGAACC CATGGCATCT ACGAGGGTAT CTGTAACGGC GTGCCGATGG TGATGATCCC
1201  GCTGTTCGGA GATCAGGTAG ACAACGTTCT ACGCATGGTG CTGCGTGAAG TCGCAGAGAG
1261  CCTGACCATG TTCGACCTGA CCTCAGAGCA ACTGCTGGGG GCACTCAGGA AAGTCCTCAA
1321  CAACAAGCGC TACAAAGAGA GGATAACACA GCTGTCTTTG ATCCATAAAG ACCGTCCGAT
1381  CGAGCCGCTG GACTTGGCCG TGTTCTGGAC CGAGTTTGTG ATGAGACACG GAAGTGCCGA
1441  GCACCTGAGA CCGGCCGCTC ACCACCTCAA CTGGGTTCAG TACCACAGTC TCGATGTCAT
1501  CGCCTTCCTC CTGCTCGTTC TATCCACCGT CGTTTTTATC GCCGTCAAAA CCTGCGCGCT
1561  CTGTTTCAGG AAGTGTTTCC GGAGGGCTCA GAAGAGCAAA AAAGAGTGAA ACGGCCAGTG
1621  AATGATCAGG AATGGATTTG GTGCCGTCTT TAATTAACGC CGATGGTTTA TCGGCGTGAT
1681  GTCATACTGT GAAAACCTGA AATAGTTATA GTGTTCTCAT CACCACGTTC AATTTAATAT
1741  TCAGGGGTGC CAGCAATTAT GGTTTAGCCA TTGCAGTTAC GGTTGTTATG ATGTCACTA
```

>UTR3

```
1     CTGCTTCCTC TAGACGTAAT TAGAAACTTT TAAGCTAAAA ATGCCTCGTC TTCTTGCAGC
61    TCTCTGTCTC CAGATTTATC TTTGCAGCTT TTTAGGACCA GTGGAAGGAG GGAAGGTCCT
121   GGTGATGCCC GTGGACGGCA GCCACTGGCT CAGTATGAAG ATCTTGGTGG AGGAATTGTC
181   TCGGAGAGGA CATGAAATGG TGGTCCTGGT TCCCGAGACA AGCGTGTTGA TCCATGGCTC
241   TGACGCGTAC GTCGCTCGGA GCTTTAAGGT TCCGTACACC AAGGCTGAAC TGGATGAAAG
301   CATGAATAAG TTGAAGGAGG GCATTACGAA AGCACCGCGG ATCTCTGACT TATTGGAGAA
361   CATCATCGGG CTCCTCAGCT TCACGAACAT GCAGGTGAAA GGATGCGAGG CGCTGCTGTA
421   TAACGAGCCT CTGATGCAGA ACCTGCGCGA GGAACACTTC GATCTCATGC TCACCGATCC
481   CTTCCTGCCT TGTGGCCCCA TCATCGCCGA GGCTTTCTCC CTCCCCGCCG TTTATTTCCT
541   GCGTGGGCTT CCCTGCGGAT TGGATCTGGA AGCCGCTCAG TGCCCATCGC CTCCGTCCTA
601   CGTCCCGCGC TTTTTCACAG GCAACACCGA CGTCATGACG TTTTCTCAGA GGGTCAAGAA
661   CGTGCTCATG ACGGGATTCG AGAGCATCCT TTGCAAAATA TTTTTCTCCA GCTTTGATGA
721   GCTCACCAGC AGATATCTCA AGAAGGATGT TACGTTCAGA GACGTCCTCG GACATGCCGC
781   AATTTGGCTT TATAGATATG ACTTCACCTT TGAGTACCCG AGACCTGTAA TGCCCAATGC
841   GGTCAGAATT GGTGGCATCA ACTGTGCCAA GAAGAATCCT CTGCCTGCCG ATCTGGAGGA
901   GTTCGTGGAC GGTTCTGGAG ATCACGGCTT CATCGTGTTC ACTTTGGCTC CTTCGTGTCC
961   GAGCTGCCGG AGTTCAAAGC CCGGGAGTTT TTCGAGGCTT TTCGGCAGAT TCCTCAGAGG
1021  GTTCTGTGGC GATACACCGG GGTCATTCCC AAAGACATTC CTGAAAATGT CAAAGTGATG
1081  AAGTGGCTTC CGCAGAATGA CCTCTTAGCA CACCCCAAGG CTAAGGTGTT CATCACGCAC
1141  GGAGGAACCC ATGGCATCTA CGAGGGTATC TGTAACGGCG TGCCGATGGT GATGATCCCG
1201  CTGTTCGGAG ATCAGGTAGA CAACGTTCTA CGCATGGTGC TGCGTGAAGT CGCAGAGAGC
1261  CTGACCATGT TCGACCTGAC CTCAGAGCAA CTGCTGGGGG CACTCAGGAA AGTCCTCAAC
1321  AACAAGCGCT ACAAAGAGAA GATAACACAG CTGTCTTTGA TCCATAAAGA CCGTCCGATC
1381  GAGCCGCTGG ACTTGGCCGT GTTCTGGACC GAGTTTGTGA TGAGACACGG AAGTGCCGAG
1441  CACCTGAGAC CGGCCGCTCA CCACCTCAAC TGGGTTCAGT ACCACAGTCT CGATGTCATC
1501  GCCTTCCTCC TGCTCGTTCT ATCCACCGTC GTTTTTATCG CCGTCAAAAC CTGCGCGCTC
1561  TGTTTCAGGA AGTGTTTCCG GAGGGCTCAG AAGAGCAAAA AGGAGTGAAA CGGCCAGTGA
1621  ATGATCAGGA ATGGATTTGG TGCCGTCTTT AATTAACGCC GATGGTTTAT CGGCGTGATG
1681  TCATACTGTG AAAACCTGAA ATAGTTATAG TGTTCTCATC ACCACGTTCA ATTTAATATT
1741  CAGGGGTGCC AGCAATTATG GTTTAGCCAT TGCAGTTACG GTTGTTATGA TGTCACTA
```

As explained in Chapter 5, the full-length intestinal UGT clones were identical in sequence to the UTR sequences shown above for liver.

B. UGT clones comprising translated portion of gene

>UGT1

```
1     ATGCCTCGTC TTCTTGCAGC TCTCTGTCTC CAGATTTATC TTTGCAGCTT
51    TTTAGGACCA GTGGAAGGAG GGAAGGTCCT GGTGATGCCC GTGGACGGCA
101   GCCACTGGCT CAGTATGAAG ATCTTGGTGG AGGAATTGTC TCGGAGAGGA
151   CATGAAATGG TGGTCCTGGT TCCCGAGACA AGCGTGTTGA TCCATGGCTC
201   TGACGCGTAC GTCGCTCGGA GCTTTAAGGT TCCGTACACC AAGGCTGAAC
251   TGGATGAAAG CATGAATAAG TTGAAGGAGG GCATTACGAA AGCACCGCGG
301   ATCTCTGACT TATTGGAGAA CATCATCGGG CTCCTCAGCT TCACGAACAT
351   GCAGGTGAAA GGATGCGAGG CGCTGCTGTA TAACGAGCCT CTGATGCAGA
401   ACCTGCGCGA GGAACACTTC GATCTCATGC TCACCGATCC CTTCCTGCCT
451   TGTGGCCCCA TCATCGCCGA GGCTTTCTCC CTCCCCGCCG TTTATTTCCT
501   GCGTGGGCTT CCCTGCGGAT TGGATCTGGA AGCCGCTCAG TGCCCATCGC
551   CTCCGTCCTA CGTCCCGCGC TTTTTCACAG GCAACACCGA CGTCATGACG
601   TTTTCTCAGA GGGTCAAGAA CGTGCTCATG ACGGGATTCG AGAGCATCCT
651   TTGCAAAATA TTTTTCTCCA GCTTTGATGA GCTCACCAGC AGATATCTCA
701   AGAAGGATGT TACGTTCAGA GACGTCCTCG GACATGCCGC AATTTGGCTT
751   TATAGATATG GCTTCACCTT TGAGTACCCG AGACCTGTAA TGCCCAATGC
801   GGTCAGAATT GGTGGCATCA ACTGTGCCAA GAAGAATCCT CTGCCTGCCG
851   ATCTGGAGGA GTTCGTGGAC GGTTCTGGAG ATCACGGCTT CATCGTGTTC
901   ACTTTGGGCT CCTTCGTGTC CGAGCTGCCG GAGTTCAAAG CCCGGGAGTT
951   TTTCGAGGCT TTTCGGCAGA TTCCTCAGAG GGTTCTGTGG CGATACACCG
1001  GGGTCATTCC CAAAGACATT CCTGAAAATG TCAAAGTGAT GAAGTGGCTT
1051  CCGCAGAATG ACCTCTTAGC ACACCCCAAG GCTAAGGTGT TCATCACGCA
1101  CGGAGGAACC CATGGCATCT ACGAGGGTAT CTGTAACGGC GTGCCGATGG
1151  TGATGATCCC GCTGTTCGGA GATCAGGTAG ACAACGTTCT ACGCATGGTG
1201  CTGCGTGAAG TCGCAGAGAG CCTGACCATG TTCGACCTGA CCTCAGAGCA
1251  ACTGCTGGGG GCACTCAGGA AAGTCCTCAA CAACAAGCGC TACAAAGAGA
1301  AGATAACACA GCTGTCTTTG ATCCATAAAG ACCGTCCGAT CGAGCCGCTG
1351  GACTTGGCCG TGTTCTGGAC CGAGTTTGTG ATGAGACACG GAAGTGCCGA
1401  GCACCTGAGA CCGGCCGCTC ACCACCTCAA CTGGGTTCAG TACCACAGTC
1451  TCGATGTCAT CGCCTTCCTC CTGCTCGTTC TATCCACCGT CGTTTTTATC
1501  GCCGTCAAAA CCTGCGCGCT CTGTTTCAGG AAGTGTTTCC GGAGGGCTCA
1551  GAAGAGCAAA AAGGAGTGA
```

>UGT2

```
   1  ATGCCTCGTC TTCTTGCAGC TCTCTGTCTC CAGATTTATC TTTGCAGCTT
  51  TTTAGGACCA GTGGAAGGAG GGAAGGTCCT GGTGATGCCC GTGGACGGCA
 101  GCCACTGGCT CAGTATGAAG ATCTTGGTGG AGGAATTGTC TCGGAGAGGA
 151  CATGAAATGG TGGTCCTGGT TCCCGAGACA AGCGTGTTGA CCCATGGCTC
 201  TGACGCGTAC GTCGCTCGGA GCTTTAAGGT TCCGTACACC AAGGCTGAAC
 251  TGGATGAAAG CATGAATAAG TTGAAGGAGG GCATTACGAA GGCACCGCGG
 301  ATCTCTGACT TATTGGAGAA CATCATCGGG CTCCTCAGCT TCACGAACAT
 351  GCAGGTGAAA GGATGCGAGG CGCTGCTGTA TAACGAGCCT CTGATGCAGA
 401  ACCTGCGCGA GGAACACTTC GATCTCATGC TCACCGATCC CTTCCTGCCT
 451  TGTGGCCCCA TCATCGCCGA GGCTTTCTCC CTCCCCGCCG TTTATTTCCT
 501  GCGTGGGCCT CCCTGCGGAT TGGATCTGGA AGCCGCTCAG TGCCCATCGC
 551  CTCCGTCCTA CGTCCCGCGC TTTTTCACAG GCAACACCGA CGTCATGACG
 601  TTTTCTCAGA GGGTCAAGAA CGTGCTCATG ACGGGATTCG AGAGCATCCT
 651  TTGCAAAATA TTTTTCTCCA GCTTTGATGA GCTCACCAGC AGATATCTCA
 701  AGAAGGATGT TACGTTCAGA GACGTCCTCG GACATGCCGC AATTTGGCTT
 751  TATAGATATG ACTTCACCTT TGAGTACCCG AGACCTGTAA TGCCCAATGC
 801  GGTCAGAATT GGTGGCATCA ACTGTGCCAA GAAGAATCCT CTGCCTGCCG
 851  ATCTGGAGGA GTTCGTGGAC GGTTCTGGAG ATCACGGCTT CATCGTGTTC
 901  ACTTTGGGCT CCTTCGTGTC CGAGCTGCCG GAGTTCAAAG CCCGGGAGTT
 951  TTTCGAGGCT TTTCGGCAGA TTCCTCAGAG GGTTCTGTGG CGATACACCG
1001  GGGTCATTCC CAAAGACATT CCTGAAAATG TCAAAGTGAT GAAGTGGCTT
1051  CCGCAGAATG ACCTCTTAGC ACACCCCAAG GCTAAGGTGT TCATCACGCA
1101  CGGAGGAACC CATGGCATCT ACGAGGGTAT CTGTAACGGC GTGCCGATGG
1151  TGATGATCCC GCTGTTCGGA GATCAGGTAG ACAACGTTCT ACGCATGGTG
1201  CTGCGTGAAG TCGCAGAGAG CCTGACCATG TTCGACCTGA CCTCAGAGCA
1251  ACTGCTGGGG GCACTCAGGA AAGTCCTCAA CAACAAGCGC TACAAAGAGA
1301  AGATAACACA GCTGTCTTTG ATCCATAAAG ACCGTCCGAT CGAGCCGCTG
1351  GACTTGGCCG TGTTCTGGAC CGAGTTTGTG ATGAGACACG GAAGTGCCGA
1401  GCACCTGAGA CCGGCCGCTC ACCACCTCAA CTGGGTTCAG TACCACAGTC
1451  TCGATGTCAT CGCCTTCCTC CTGCTCGTTC TATCCACCGT CGTTTTTATC
1501  GCCGTCAAAA CCTGCGCGCT CTGTTTCAGG AAGTGTTTCC GGAGGGCTCA
1551  GAAGAGCAAA AAGGAGTGA
```

>UGT3

```
   1  ATGCCTCGTC TTCTTGCAGC TCTCTGTCTC CAGATTTATC TTTGCAGCTT
  51  TTTAGGACCA GTGGAAGGAG GGAAGGTCCT GGTGATGCCC GTGGACGGCA
 101  GCCACTGGCT CAGTATGAAG ATCTTGGTGG AGGAATTGTC TCGGAGAGGA
 151  CATGAAATGG TGGTCCTGGT TCCCGAGACA AGCGTGTTGA TCCATGGCTC
 201  TGACGCGTAC GCCGCTCGGA GCTTTAAGGT TCCGTACACC AAGGCTGAAC
 251  TGGATGAAAG CATGAATAAG TTGAAGGAGG GCATTACGAA AGCACCGCGG
 301  ATCTCTGACT TATTGGAGAA CATCATCGGG CTCCTCAGCT TCACGAACAT
 351  GCAGGTGAAA GGATGCGAGG CGCTGCTGTA TAACGAGCCT CTGATGCAGA
 401  ACCTGCGCGA GGAACACTTC GATCTCATGC TCACCGATCC CTTCCTGCCT
 451  TGTGGCCCCA TCATCGCCGA GGCTTTCTCC CTCCCCGCCG TTTATTTCCT
 501  GCGTGGGCTT CCCTGCGGAT TGGATCTGGA AGCCACTCAG TGCCCATCGC
 551  CTCCGTCCTA CGTCCCACGC TTTTTCACAG GCAACACCGA CGTCATGACG
 601  TTTTCTCAGA GGGTCAAGAA CGTGCTCATG ACGGGATTCG AGAGCATCCT
 651  TTGCAAAATA TTTTTCTCCA GCTTTGATGA GCTCACCAGC AGATATCTCA
 701  AGAAGGATGT TACGTTCAGA GACGTCCTCG GACATGCCGC GATTTGGCTT
 751  TATAGATATG ACTTCACCTT TGAGTACCCG AGACCTGTAA TGCCCAATGC
 801  GGTCAGAATT GGTGGCATCA ACTGTGCCAA GAAGAATCCT CTGCCTGCCG
 851  ATCTGGAGGA GTTCGTGGAC GGTTCTGGAG ATCACGGCTT CATCGTGTTC
 901  ACTTTGGGCT CCTTCGTGTC CGAGCTGCCG GAGTTCAAAG CCCGGGAGTT
 951  TTTCGAGGCT TTTCGGCAGA TTCCTCAGAG GGTTCTGTGG CGATACACCG
1001  GGGTCATTCC CAAAGACATT CCTGAAAATG TCAAAGTGAT GAAGTGGCTT
1051  CCGCAGAACG ACCTCTTAGC ACACCCCAAG GCTAAGGTGT TCATCACGCA
1101  CGGAGGAGCC CATGGCATCT ACGAGGGTAT CTGTAACGGC GTGCCGATGG
1151  TGATGATCCC GCTGTTCGGA GATCAGGTAG ACAACGTTCT ACGCATGGTG
1201  CTGCGTGGAG TCGCAGAGAG CCTGACCATG TTCGACCTGA CCTCAGAGCA
1251  ACTGCTGGGG GCACTCAGGA AAGTCCTCAA CAACAAGCGC TACAAAGAGA
1301  AGATAACACA GCTGTCTTTG ATCCATAAAG ACCGTCCGAT CGAGCCGCTG
1351  GACTTGGCCG TGTTCTGGAC CGAGTTTGTG ATGAGACACG GAAGTGCCGA
1401  GCACCTGAGA CCGGCCGCTC ACCACCTCAA CTGGGTTCAG TACCACAGTC
1451  TCGATGTCAT CGCCTTCCTC CTGCTCGTTC TATCCACCGT CGTTTTTATC
1501  GCCGTCAAAA CCTGCGCGCT CTGTTTCAGG AAGTGTTTCC GGAGGGCTCA
1551  GAAGAGCAAA AAGGAGTGA
```

LIST OF REFERENCES

Adachi Y, Kamisako T, and Yamashita T (1991) The effects of temporary occlusion of the superior mesenteric vein or splenic vein on biliary bilirubin and bile acid excretion in rats. *J Lab Clin Med* **118:**261-268.

Adolfsson-Erici M, Pettersson M, Parkkonen J, and Sturve J (2002) Triclosan, a commonly used bactericide found in human milk and in the aquatic environment in Sweden. *Chemosphere* **46:**1485-1489.

Alary J, Cravedi J, Baradat M, and Carrera G (1992) Mechanism of cadmium-decreased glucuronidation in the rat. *Biochem Pharmacol* **44:**2139-2147.

Altschul, SF, Madden TL, Schäffer AA, Zhang J, Zhang Z, Miller W, and Lipman DJ (1997) Gapped BLAST and PSI-BLAST: a new generation of protein database search programs. *Nucleic Acids Res* **25:**3389-3402.

Arulmozhiraja S, Shiraishi F, Okumura T, Iida M, Takigami H, Edmonds JS, and Morita M (2005) Structural requirements for the interaction of 91 hydroxylated polychlorinated biphenyls with estrogen and thyroid hormone receptors. *Toxicol Sci* **84:**49-62.

Aw TY and Jones DP (1978) Direct determination of UDP-glucuronic acid in cell extracts by high-performance liquid chromatography. *Anal Biochem* **127:**32-26.

Barnett AC, Tsvetanov S, Gamage N, Martin JL, Duggleby RG and McManus M (2004) Active site mutations and substrate inhibition in human sulfotransferase 1A1 and 1A3. *J Biol Chem* **279:**18799-805.

Basu NK, Kovarova M, Garza A, Kubota S, Saha T, Mitra PS, Banerjee R, Rivera J, and Owens IS (2005) Phosphorylation of a UGT-glucuronosyltransferase regulates substrate specificity. *Proc Natl Acad Sci USA* **102:**6285-6290.

Battaglia E, Pritchard M, Ouzzine M, Fournel-Gigleux S, Radominska A, Siest G, and Magdalou J (1994) Chemical modification of human UDP-glucuronosyltransferase UGT1*6 by diethyl pyrocarbonate: possible involvement of a histidine residue in the catalytic process. *Arch Biochem Biophys* **309:**266-72.

Bauer U, Amaro AR, and Robertson LW (1995) A new strategy for the synthesis of polychlorinated biphenyl metabolites. *Chem Res Toxicol* **8:** 92-95.

Bedford CT, Hickman AD, and Logan CJ (2003) Structure-activity studies of glucose transfer: Determination of the spontaneous rates of hydrolysis of uridine 5′-diphospho-α-D-glucose (UDPG) and uridine 5′-diphospho-α-D-glucuronic acid (UDPGA). *Biorganic Medicinal Chem* **11:**2339-2345.

Bergman Å, Klasson-Wehler E, and Kuroki K (1994) Selective retention of hydroxylated PCB metabolites in blood. *Environ Health Perspect* **102:**464-469.

Bidwell LM, McManus ME, Gaedigk A, Kakuta Y, Negishi M, Pedersen L, and Martin JL (1999) Crystal structure of human catecholamine sulfotransferase. *J Mol Biol* **293:**521-530.

Bray BJ and Rosengren RJ (2001) Retinol potentiates acetaminophen-induced hepatotoxicity in the mouse: Mechanistic studies. *Toxicol Appl Pharmacol* **173:**129-136.

Buhl AE, Waldon DJ, Baker CA, and Johnson GA (1990) Minoxidil sulfate is the active metabolite that stimulates hair follicles. *J Invest Dermatol* **95:**553-7.

Cappiello M, Giuliani L, and Pacifici GM (1991) Distribution of UDP-glucuronosyl-transferase and its endogenous substrate uridine 5'-diphosphoglucuronic acid in human tissues. *Eur J Clin Pharmacol* **41:**345-350.

Cappiello M, Giuliani L, Rane A, and Pacifici GM (2000) Uridine 5'-diphosphoglucuronic acid (UDPGlcUA) in human fetal liver, kidney and placenta. *Eur J Drug Metab Pharmacokinet* **25:**161-163.

Cheek AO, Kow K, and McLachlan JA (1999) Potential mechanism of thyroid disruption in humans: Interaction of organochlorine compounds with thyroid receptor, transthyretin, and thyroid-binding globulin. *Environ Health Perspec* **107:**273-278.

Ciotti M, Yeatman M, Sokol RJ, and Owens IS (1995) Altered coding for a strictly conserved di-glycine in the major bilirubin UDP-glucuronosyltransferase of a Crigler-Najjar type I patient *J Biol Chem* **270:**3284-3291.

Ciotti M, Cho JW, George J, and Owens IS (1998) Required buried α-helical structure in the bilirubin UDP-glucuronosyltransferase, UGT1A1, contains a nonreplaceable phenylalanine. *Biochemistry* **37:**11018-11025.

Clarke DJ, George SG, and Burchell B (1992a) Multiplicity of UDP-glucuronosyltransferases in fish. Identification and characterization of a phenol-UDP-glucuronosyltransferase from the liver of a marine teleost, *Pleuronectes platessa*. *Biochem J* **284:**417-423.

Clarke DJ, Burchell B, and George SG (1992b) Functional and immunochemical comparison of hepatic UDP-glucuronosyltransferases in a piscine and mammalian species. *Comp Biochem Physiol B* **102:**425-432.

Clarke DJ, Burchell B, and George SG (1992c) Differential expression and induction of UDP-glucuronosyltransferase isoforms in hepatic and extrahepatic tissues of a fish, Pleuronectes platessa: Immunochemical and functional characterization. *Toxicol Appl Pharmacol* **115:**130-136.

Conway JG, Kuffman FC, Tsukuda T, and Thurman RG (1988) Glucuronidation of 7-hydroxycoumarin in periportal and pericentral regions of the lobule in livers from untreated and 3-methylcholanthrene-treated rats. *Mol Pharmacol* **33:**111-119.

Daidoji T, Gozu H, Iwano H, Inoue H, and Yokota H (2005) UDP-glucuronosyltransferase isoforms catalyzing glucuronidation of hydroxy-polychlorinated biphenyls in rat. *Drug Metab Dispos* **33:**1466-1476.

Dajani R, Cleasby A, Neu M, Wonacott AJ, Jhoti H, Hood AM, Modi S, Hersey A, Taskinen J, Cooke RM, Manchee GR, and Coughtrie MW (1999) X-ray crystal structure of human dopamine sulfotransferase, SULT1A3. Molecular modeling and quantitative structure-activity relationship analysis demonstrate a molecular basis for sulfotransferase substrate specificity. *J Biol Chem* **274:**37862-8.

DePierre JW, Andersson G, and Dallner G (1987) In *The Liver: Biology and Pathobiology* (Arias IM, Jakoby WB, Popper H, Schachter D and Shafritz DA eds) pp 165-187, Raven Press, New York, NY.

Dills RL, Howell SR, and Klaassen CD (1987). Hepatic UDP-glucose and UDP-glucuronic acid synthesis rates in rats during a reduced energy state. *Drug Metab Disp* **15:**281-288.

Dubey RK and Singh J (1988) Localization and characterization of drug-metabolizing enzymes along the villus-crypt surface of the rat small intestine--II. Conjugases. *Biochem Pharmacol* **37:**177-84.

Duffel MW and Jakoby WB (1981) On the mechanism of aryl sulfotransferase. *J Biol Chem* **256:**11123-11127.

Ethell BT and Wrighton SA (2004) The effect of uridine 5´diphosphoglcuuronic acid (UDPGA) on glucuronidation kinetics: Investigations into allosterism with UDP-glucuronosyltransferases. Poster presentation. International Workshop on Glucuronidation, Dundee, Scotland. Sep 5-8, 2004.

Ethell BT, Ekins S, Wang J, and Burchell B (2002) Quantitative structure activity relationships for the glucuronidation of simple phenols by expressed human UGT1A6 and UGT1A9. *Drug Metab Dispos* **30:**734-738.

Fängström B, Athanasiadou M, Grandjean P, Weihe P, and Bergman Å (2002) Hydroxylated PCB metabolites and PCBs in serum from pregnant Faroese women. *Environ Health Perspect* **110:**895-899.

Gaido KW, Maness SC, McDonnell DP, Dehal SS, Kupfer D and Safe S (2000) Interaction of methoxychlor and related compounds with estrogen receptor α and β, and androgen receptor: Structure-activity studies. *Mol Pharmacol* **58:**852-858.

Gamage NU, Duggleby RG, Barnett AC, Tresillian M, Latham CF, Liyou NE, McManus ME and Martin JL (2003) Structure of a human carcinogen-converting enzyme, SULT1A1. Structural and kinetic implications of substrate inhibition. *J Biol Chem* **278:**7655-7662.

Gamage NU, Tsvetanov S, Duggleby RG, McManus ME and Martin JL (2005) The structure of human SULT1A1 crystallized with estradiol. *J Biol Chem* **280:**41482-41486.

Gardner-Stephen DA, Gregory PA, and Mackenzie PI (2005) Identification and characterization of functional hepatocyte nuclear factor 1 – binding sites in UDP-glucuronosyltransferase genes. *Methods Enzymol* **400:**22-46.

Gaworecki KM, Rice CD, and van den Hurk P (2004) Induction of phenol-type sulfotransferase and glucuronosyltransferase in channel catfish and mummichog. *Mar Environ Res* **58:**525-528.

George SG and Leaver M (2002) Allelic variations in the plaice UGT1B1 gene. *Mar Environ Res* **54:**259-262.

George SG and Taylor B (2002) Molecular evidence for multiple UDP-glucuronosyltransferase gene families in fish. *Mar Environ Res* **54:**253-257.

George SG, Groman D, Brown S, and Holmes K (1992) Studies of a fatal pollutant – induced hyperbilirubinaemia in spawning Atlantic salmon. *Mar Environ Res* **34:**81-86.

George SG, Leaver MJ, and Wright J (1998) Structural studies of a UDP-glucuronosyltransferase gene from the plaice (*Pleuronectes platessa*). *Mar Environ Res* **46:**33-35.

Glatt H (2000) Sulfotransferases in the bioactivation of xenobiotics. *Chem-Biol Interact* **129:**141-170.

Glatt HR (2002) Sulphotransferases, in *Enzyme Systems That Metabolise Drugs and Other Xenobiotics* (Costas I ed) pp 353-439, John Wiley and Sons, London, England

Glatt H, Pauly K, Czich A, Falany JL, and Falany CN (1995) Activation of benzylic alcohols to mutagens by rat and human SULTs expressed in *E.coli*. *Eur J Pharmacol* **293:**173-181.

Gong QH, Cho JW, Huang T, Potter C, Gholami N, Basu NK, Kubota S, Carvalho S, Pennington MW, Owens IS, and Popescu NC (2001) Thirteen UDPglucuronosyltransferase genes are encoded at the human UGT1 gene locus. *Pharmacogenetics* **11:**357-368.

Goon D and Klaassen CD (1992) Effects of microsomal enzyme inducers upon UDP-glucuronic acid concentration and UDP-glucuronosyltransferase activity in the rat intestine and liver. *Toxicol Appl Pharmacol* **115:**253-60.

Gschaidmeier H and Bock KW (1994) Radiation inactivation analysis of microsomal UDP-glucuronosyltransferases catalysing mono- and diglucuronide formation of 3,6-dihydroxybenzo(a)pyrene and 3,6-dihydroxychrysene. *Biochem Pharmacol* **48:**1545-9.

Guvenius DM, Aronnson A, Ekmar-Ordeberg G, Bergman Å, and Norén K (1992) Human prenatal and postnatal exposure to polybrominated diphenyl ethers, polychlorinated biphenyls, polychlorobiphenylols, and pentachlorophenol. *Environ Health Perspect* **111:**1235-1241.

Hjelle JJ (1986) Hepatic UDP-glucuronic acid regulation during acetaminophen biotransformation in rats. *J Pharmacol Exp Ther* **237:**75-756.

Hjelle JJ, Hazelton GA, and Klaassen CD (1985) Acetaminophen decreases adenosine 3'-phosphosulfate and uridine diphosphoglucuronic acid in rat liver. *Drug Metab Disp* **13:**35-41.

Hoekstra PF, Letcher RJ, O'Hara TM, Backus SM, Solomon KR, and Muir DCG (2003) Hydroxylated and methylsulfone-containing metabolites of polychlorinated biphenyls in the plasma and blubber of bowhead whales (*Balaena mysticetus*). *Environ Toxicol Chem* **22:**2650-2658.

Houston JB and Kenworthy KE (2000) In vitro-in vivo scaling of CYP kinetic data not consistent with the classical Michaelis-Menten model. *Drug Metab Dispos* **28:**246-254.

Hovander L, Malmberg T, Athanasiadou M, Athanassiadis I, Rahm S, Bergman Å, and Klasson-Wehler E (2002) Identification of hydroxylated PCB metabolites and other phenolic halogenated pollutants in human blood plasma. *Arch Environ Contam Toxicol* **42:**105-117.

Hu Y and Kupfer D (2002) Enantioselective metabolism of the endocrine disruptor pesticide methoxychlor by human cytochromes P450 (P450s): major differences in selective enantiomer formation by various P450 isoforms. *Drug Metab Dispos* **30:**1329-1336.

Ichikawa S, Sakiyama H, Suzuki G, Hidari KI, and Hirabayashi Y (1996) Expression cloning of a cDNA for human ceramide glucosyltransferase that catalyzes the first glycosylation step of glycosphingolipid synthesis. *Proc Natl Acad Sci USA* **93:**4638-4643.

Imamura M, Kumagai T, Sugihara N, and Furuno K (2003) High-performace liquid chromatographic assay of 3′-phosphoadenosine 5′-phosphosulfate (PAPS) and UDP-glcuuronic acid (UDPGA) in culture hepatic cell extracts. *J Health Sci* **49:**395-400.

Iwano H, Yokota H, Ohgiya S, and Yuasa A (1999) The significance of amino acid residue Asp446 for enzymatic stability of rat UDP-glucuronosyltransferase UGT1A6. *Arch Biochem Biophys* **363:**116-120.

James MO (2001) Polychlorinated biphenyls: metabolism and metabolites, in *PCBs. Recent Advances in the Environmental Toxicology and Health Effects* (Robertson LW and Hansen LG eds) pp 35-45, The University Press of Kentucky, Lexington, KY.

James MO, Altman AH, Morris K, Kleinow KM and Tong Z (1997) Dietary modulation of phase 1 and phase 2 activities with benzo[*a*]pyrene and related compounds in the intestine but not in the liver of the channel catfish, *Ictalurus punctatus. Drug Metab Dispos* **25:**346-354.

James MO, Tong Z, Rowland-Faux L, Venugopal CS and Kleinow KM (2001) Intestinal bioavailability and biotransformation of 3-hydroxybenzo[a]pyrene in an isolated perfused preparation from channel catfish, *Ictalurus punctatus*. *Drug Metab Dispos* **29:**721-728.

James MO and Rowland-Faux L (2003) Hydroxylated polychlorinated biphenyls as poor substrates but good inhibitors of the glucuronidation and sulfonation of hydroxylated benzo[a]pyrene metabolites. *Fresenius Environ Bull* **12:**227-231.

Jarman WM, Simon M, Norstrom RJ, Burns SA, Bacon CA, Simonelt BRT and Risebrough RW (1992) Global distribution of Tris(4-chlorophenyl)methanol in high trophic level birds and mammals. *Environ Sci Technol* **26:**1770-1774.

Kakuta Y, Pedersen LG, Carter CW, Negishi M, and Pedersen LC (1997) Crystal structure of estrogen sulphotransferase. *Nature Structr Biol* **11:**904-908.

Kester MH, Bulduk S, Tibboel D, Meinl W, Glatt H, Falany CN, Coughtrie MW, Bergman A, Safe SH, Kuiper GG, Schuur AG, Brouwer A and Visser TJ (2000) Potent inhibition of estrogen sulfotransferase by hydroxylated PCB metabolites: a novel pathway explaining the estrogenic activity of PCBs. *Endocrinology* **141:**1897-1900.

Kim KH (1991) Quantitative structure-activity relationships of the metabolism of drugs by uridine diphosphate glucuronosyltransferase. *J Pharm Sci* **80:**966-970.

King CD, Rios GR, Green MD, and Tephly TR (2000) UDP-glucuronosyltransferases. *Curr Drug Metab* **1:**143-161.

Korach KS, Sarver P, Chae K, McLachlan JA, and McKinney JD (1988) Estrogen receptor-binding activity of polychlorinated hydroxybiphenyls: Conformationally restricted structural probes. *Mol Pharmacol* **33:**120-126.

Kolaskar AS and Tongaonkar PC (1990) A semi-empirical method for prediction of antigenic determinants on protein antigens. *FEBS Letters* **276:**172-174.

Krishnaswamy S, Duan SX, von Moltke LL, Greenblatt DJ, and Court MH (2003) Validation of serotonin (5-hydroxytryptamine) as an *in vitro* substrate probe for human UDP-glucuronosyltransferase (UGT) 1A6. *Drug Metab Dispos* 31:133-139.

Kucklick JR, Struntz WDJ, Becker PR, York GW, O'Hara TM, and Bohonowych JE (2002) Persistent organochlorine pollutants in ringed seals and polar bears collected from northern Alaska. *Sci Total Environ* **287:**45-59.

Lans MC, Klasson-Wehler E, Willemsen M, Meussen E, Safe S, and Brouwer A (1993) Structure-dependent, competitive interaction of hydroxy-polychlorobiphenyls, -dibenzo-p-dioxins and –dibenzofurans with human transthyretin. *Chem Biol Interact* **88:**7-21.

Lehmler H-J and Robertson LW (2001). Synthesis of hydroxylated PCB metabolites with the Suzuki-coupling. *Chemosphere* **45:** 1119-1127.

Letcher RJ, Norstrom RJ, Lin S, Ramsay MA and Bandiera SM (1996) Immunoquantitation and microsomal monooxygenase activities of hepatic cytochromes P450 1A and P450 2B and chlorinated contaminant levels in polar bear *(Ursus maritimus*). *Toxicol Appl Pharmacol* **137:**127-140.

Li H, Drouillard KG, Bennett E, Haffner GD, and Letcher RJ (2003) Plasma-associated halogenated and phenolic contaminants in benthic and pelagic fish species from the Detroit river. *Environ Sci Technol* **37:**832-839.

Lilienblum W, Platt KL, Schirmer G, Oesch F and Bock KW (1987) Regioselectivity of rat liver microsomal UDP-glucuronosyltransferase activities toward phenols of benzo(a)pyrene and dibenz(a,h)anthracene. *Mol Pharmacol* **32:**173-177

Liljebjelke K, Adolphson R, Baker K, Doong RL, and Mohnen D (1995) Enzymatic synthesis and purification of uridine diphosphate [^{14}C]galacturonic acid: A substrate for pectin biosynthesis. *Anal Biochem* **225:**296-304.

Lin JH and Wong BK (2002) Complexities of glucuronidation affecting in vitro-in vivo extrapolation. *Curr Drug Metab* **3:**623-646.

Ma B, Shou M and Schrag ML (2003) Solvent effect on cDNA-expressed human sulfotransferase (SULT) activities in vitro. *Drug Metab Dispos* **31:**1300-1305.

Mackenzie PI, Owens IS, Burchell B, Bock KW, Bairoch A, Belanger A, Fournel-Gigleux S, Green M, Hum DW, Iyanagi T, Lancet D, Louisot P, Magdalou J, Chowdury JR, Ritter JK, Schachter H, Tephly TR, Tipton KF, and Nebert DW (1997) The UDP glycosyltransferase gene superfamily: recommended nomenclature update based on evolutionary divergence. *Pharmacogenetics* **7:**255-269.

Mackenzie PI, Bock KW, Burchell B, Guillemette C, Ikushiro S, Iyanagi T, Miners JO, Owens IS and Nebert DW (2005) Nomenclature update for the mammalian UDP glycosyltransferase (UGT) gene superfamily. *Pharmacogenetics and Genomics* **15:**677-685.

Macrides TA, Faktor DA, Kakafatis N, and Amiet G (1994) Enzymic sulfonation of bile salts. Partial purification and characterization of an enzyme from the liver of the shark *Heterodontus portusjacksoni* that catalyzes the sulfation of the shark bile steroid 5β-scymnol. *Comp Biochem Physiol* **1078:**461-469.

Maervoet J, Covaci A, Schepens P, Sandau CD, and Letcher RJ (2004) A reassessment of the nomenclature of polychlorinated biphenyl (PCB) metabolites. *Environ Health Perspect* **112:**291-294.

Marchler-Bauer A and Bryant SH (2004) CD-Search: protein domain annotations on the fly. *Nucleic Acids Res* **32:**W327-331.

Maruyama K and Sugano S (1994) Oligo-capping: a simple method to replace the cap structure of eukaryotic mRNAs with oligoribonucleotides. *Gene* **138:**171-174.

Meech R and Mackenzie PI (1997) UDP-glucuronosyltransferase, the role of the amino terminus in diemrization. *J Biol Chem* **272:**26913-26917.

Meerman JHN, Sterneborg HMJ and Mulder GJ (1983) Use of pentachlorophenol as long-term inhibitor of sulfation of phenols and hydroxamic acids in the rat in vivo. *Biochem Pharmacol* **32:**1587-1593.

Meerts IA, Lilienthal H, Hoving S, van den Berg JH, Weijers BM, Bergman Å, Koeman JH, and Brouwer A (2004) Developmental exposure to 4-hydroxy-2,3,3´,4´,5-pentachlorobiphenyl (4-OH-CB107): Long-term effects on brain development, behavior, and brain stem auditory evoked potentials in rats. *Toxicol Sci* **82:**207-218.

Miller TL (1978) Interaction of hydroxychlorobiphenyls-polychlorinated biphenyl metabolites-with the human erythrocyte membrane. *J Environ Pathol Toxicol* **1:**459-474.

Miners JO, Lillywhite KJ and Birkett DJ (1988a) Kinetic and inhibitor studies of 4-methylumbelliferone and 1-naphthol glucuronidation in human liver microsomes. *Biochem Pharmacol* **37:**665-671.

Miners JO, Lillywhite KJ and Birkett DJ (1988b) In vitro evidence for the involvement of at least two forms of human liver UDP-glucuronosyl transferase in morphine 3-glucuronidation. *Biochem Pharmacol* **37:**2839-2845.

Miners JO, Knights KM, Houston B, and Mackenzie PI (2006) In vitro-in vivo correlation for drugs and other compounds eliminated by glucuronidation in humans: Pitfalls and promises. *Biochem Pharmacol* **71:**1531-1539.

Minh TB, Watanabe M, Tanabe S, Yamada T, Hata J and Watanabe S (2000) Occurrence of tris(4-chlorophenyl)methane, tris(4-chlorophenyl)methanol and some other persistent organochlorine in Japanese human adipose tissue. *Environ Health Perspect* **108:**599-603

Mulder GJ and Jakoby WB (1990) Sulfation. In: *Conjugation Reactions in Drug Metabolism*. (Mulder GJ, ed). London: Taylor and Francis, 137-138.

Mulder GJ and van Doorn AB (1975) A rapid NAD^+ linked assay for microsomal uridine diphosphate glucuronyltransferase of rat liver and some observations on substrate specificity of the enzyme. *Biochem J* **151:**131-140.

Nakagawa Y, Tayama S, Moore G, and Moldeus P (1993) Cytotoxic effect of biphenyl and hydroxybiphenyls on isolated rat hepatocytes. *Biochem Pharmacol* **45:**1959-1965.

Pang KS, Koster H, Halsema ICM, Scholtens E, and Mulder GJ (1981) Aberrant pharmacokinetics of harmol in the perfused rat liver preparation: sulfate and glucuronide conjugations. *J Pharmacol Exp Ther* **219:**134-40.

Patten CJ, Code EL, Dehal SS, Gange PV, and Crespi CL (2001) Analysis of UGT enzyme levels in human liver microsomesusing form specific anti-peptide antibodies, probe substrate activities and recombinant UGT enzymes. *Drug Metab Rev* **33:**165.

Pedersen LC, Petrotchenko EV, and Negishi M (2000) Crystal structure of SULT2A3, human hydroxysteroid sulfotransferase. *FEBS Lett* **475:**61-64.

Pedersen LC, Petrotchenko E, Shevtsov S, and Negishi M (2002) Crystal structure of the human estrogen sulfotransferase-PAPS complex: evidence for catalytic role of Ser^{137} in the sulfuryl transfer reaction. *J Biol Chem* **277:**17928-32.

Radominska-Pandya A, Czernik PJ, Little JM Battaglia E, and Mackenzie PI (1999) Structural and functional studies of UDP-glucuronosyltransferases. *Drug Metab Rev* **31:**817-899.

Radominska-Pandya A, Ouzzine M, Fournel-Gigleux S, and Magdalou J (2005) Structure of UDP-glucuronosyltransferases in membranes. *Methods Enzymol* **400:**116-147.

Reinke LA, Belinsky SA, Evans RK, Kauffman FC, and Thurman RG (1981) Conjugation of p-nitrophenol in the perfused liver: the effect of substrate concentration and carbohydrate reserves. *J Pharmacol Exp Ther* **217:**863-870.

Ribeiro O, Kirkby CA, Hirom PC and Millburn P (1986) Reactive intermediates from 3-hydroxybenzo[a]pyrene and its glucuronide. *Carcinogenesis* **7:**481-484.

Ritter JK, Chen F, Sheen YY, Tran HM, Kimura S, Yeatman MT, and Owens IS (1992) A novel complex locus UGT1 encodes human bilirubin, phenol, and other UDP-glucuronosyltransferase isozymes with identical carboxyl termini. *J Biol Chem* **267:**3257-3261.

Sacco JC and James MO (2004) Glucuronidation in the polar bear (*Ursus maritimus*). *Mar Environ Res* **58:**475-479.

Safe S (2001) Hydroxylated polychlorinated biphenyls (PCBs) and organochlorine pesticides as potential endocrine disruptors. In: *The Handbook of Environmental Chemistry Vol. 3, Part L. Endocrine Disruptors, Part I* (Metzler M, ed). Berlin, Germany: Springer-Verlag, 155-167.

Sandau CD and Norstrom RJ (1998) Analysis of hydroxylated metabolites of PCBs (OH-PCBs) in polar bear plasma and human whole blood, in *Proceedings of the Second Biennial International Conference on Chemical Measurement and Monitoring of the Environment*, *11-14 May 1998*, pp 405-410 Ottawa, Canada.

Sandau CD, Meerts IA, Letcher RJ, Mcalees AJ, Chittim B, Brouwer A and Norstrom RJ (2000) Identification of 4-hydroxyheptachlorostyrene in polar bear plasma and its binding affinity to transthyretin: A metabolite of octachlorostyrene? *Environ Sci Technol* **34:**3871-3877.

Sandau CD, Ayotte P, Dewailly E, Duffe J and Norstrom RJ (2002) Pentachlorophenol and hydroxylated polychlorinated biphenyl metabolites in umbilical cord blood plasma of neonates from coastal populations in Quebec. *Environ Health Perspect* **110:**411-417.

Schiller CM, Dieringer CS, Twine ME, and Jeffcoat AR (1982) Determination of tissue UDP-glucuronic acid levels by high-pressure liquid chromatography. *Anal Biochem* **127:**68-72.

Schlüpmann H, Bacic A, and Read SM (1994) Uridine diphosphate glucose metabolism and callose synthesis in cultured pollen tubes of *Nicotiana alata* Link et Otto. *Plant Physiol* **105:**659-670.

Schrader TJ and Cooke GM (2002) Interaction between tris(4-chlorophenyl)methanol and the human androgen receptor in vitro. *Toxicol Lett* **136:**19-24.

Schuur AG, Legger FF, van Meeteren ME, Moonen MJH, van Leeuwen-Bol I, Bergman Å, Visser TJ, and Brouwer A (1998) In vitro inhibition of thyroid hormone sulfonation by hydroxylated metabolites of halogenated aromatic hydrocarbons. *Chem Res Toxicol* **11:**1075-1081.

Senay C, Ouzzine M, Battaglia E, Pless D, Cano V, Burchell B, Radominska A, Magdalou J, and Fournel-Gigleux S (1997) Arginine 52 and histidine 54 located in a conserved amino-terminal hydrophobic region (LX2-R52-G-H54-X3-V-L) are important amino acids for the functional and structural integrity of the human liver UDP-glucuronosyltransferase UGT1*6. *Mol Pharmacol* **51:**406-13.

Shaefer B (1995) Revolution in rapid amplification of cDNA ends: new strategies for polymerase chain reaction cloning of full-length cDNA ends. *Analytical Biochem* **227:**255-273.

Sharma R, and Kodavanti PRS (2002) In vitro effects of polychlorinated biphenyls and hydroxy metabolites on nitric oxide synthases in rat brain. *Toxicol Appl Pharmacol* **178:**127-136.

Shevtsov S, Petrotchenko EV, Pedersen LC and Negishi M (2003) Crystallographic analysis of a hydroxylated polychlorinated biphenyl (OH-PCB) bound to the catalytic estrogen binding site of human estrogen sulfotransferase. *Environ Health Perspect* **111:** 884-888.

Shiraishi F, Okumura T, Nomachi M, Serizawa S, Nishikawa J, Edmonds JS, Shiraishi H, and Morita M (2003) Estrogenic and thyroid hormone activity of a series of hydroxy-polychlorinated biphenyls. *Chemosphere* **52:**33-42.

Singh J, Dubey RK, and Atal CK (1986) Piperine-mediated inhibition of glucuronidation activity in isolated epithelial cells of the guinea-pig small intestine: evidence that piperine lowers the endogenous UDP-glucuronic acid content. *J Pharmacol Exp Ther* **236:**488-93.

Sinjari T, Klasson-Wehler E, Hovander L, and Darnerud PO (1998) Hydroxylated polychlorinated biphenyls: distribution in the pregnant mouse. *Xenobiotica* **28:**31-40.

Sjödin A, Hagmar L, Klasson-Wehler E, Björk J, and Bergman Å (2000) Influence of the consumption of fatty Baltic Sea fish on plasma levels of halogenated environmental contaminants in Latvian and Swedish men. *Environ Health Perspect* **108:**1035-1041.

Strassburg CP, Nguyen N, Manns MP, and Tukey RH (1998) Polymorphic expression of the UDP-glucuronosyltransferase UGT1A gene locus in human gastric epithelium. *Mol Pharmacol* **54:**647-654.

Sugatani J, Sueyoshi T, Negishi M, and Miwa M (2005) Regulation of the human UGT1A1 gene by nuclear receptors constitutive active/androstane receptor, pregnane X receptor, and glucocorticoid receptor. *Methods Enzymol* **400:**92-104.

Suto K, Fuse A, Igarashi Y, and Kimura W (2002) Significance of altered bilirubin subfractions in bile following hepatectomy. *J Surg Res* **106:**62-69.

Tampal N, Lehmler H-J, Espandiari P, Malmberg T, and Robertson LW (2002) Glucuronidation of hydroxylated polychlorinated biphenyls (PCBs). *Chem Res Toxicol* **15:**1259-1266.

Tong Z and James MO (2000) Purification and characterization of hepatic and intestinal phenol sulfotransferase with high affinity for benzo[a]pyrene phenols from channel catfish, *Ictalurus punctatus*. *Arch Biochem Biophys* **376:**409-419.

Tsoutsikos P, Miners JO, Stapleton A, Thomas A, Sallustio BC, and Knights KM (2004) Evidence that unsaturated fatty acids are potent inhibitors of renal UDP-glucuronosyltransferases (UGT): kinetic studies using human kidney cortical microsomes and recombinant UGT1A9 and UGT2B7. *Biochem Pharmacol* **67:**191-199.

Tukey RH and Strassburg CP (2000) Human UDP-glucuronosyltransferases: Metabolism, expression, and disease. *Annu Rev Pharmacol Toxicol* **40:**581-616.

van den Hurk P and James MO (2000) Sulfation and glucuronidation of benzo[*a*]pyrene-7,8-dihydrodiol in intestinal mucosa of channel catfish (*Ictalurus punctatus*). *Mar Environ Res* **50:**11-15.

van den Hurk P, Kubiczak GA, Lehmler H-J, and James MO (2002) Hydroxylated polychlorinated biphenyls as inhibitors of the sulfation and glucuronidation of 3-hydroxybenzo[a]pyrene. *Environ Health Perspect* **110:**343-348.

Venkatachalam KV, Llanos DE, Karami KJ, and Malinovskii VA (2004) Isolation, partial purification and characterization of a novel petromyzonol sulfotransferase from *Petromyzon marinus* (lamprey) larval liver. *J Lipid Res* **45:**486-495.

Vondráček J, Machala M, Bryja V, Chramostová K, Krčmář P, Dietrich C, Hampl A, and Kozubík A (2005) Aryl hydrocarbon receptor-activating polychlorinated biphenyls and their hydroxylated metabolites induce cell proliferation in contact-inhibited rat liver epithelial cells. *Toxicol Sci*. **83:**53-63

Wang D (2005) The uridine diphosphate glucuronosyltransferases: quantitative structure-activity relationships for hydroxyl polychlorinated biphenyl substrates. *Arch Toxicol* **79:**554-560.

Wang L-Q, Falany CN, and James MO (2004) Triclosan as a substrate and inhibitor of 3`-phosphoadenosine 5`-phosphosulfate-sulfotransferase and UDP-glucuronosyl transferase in human liver fractions. *Drug Metab Dispos* **32:**1162-1169.

Wang L-Q, Lehmler H-J, Robertson LW, Falany CN, and James MO (2005) *In vitro* inhibition of human hepatic and cDNA-expressed sulfotransferase activity with 3-hydroxybenzo[a]pyrene by polychlorobiphenylols. *Environ Health Perspect* **113:**680-687.

Wang L-Q, Lehmler H-J, Robertson LW, and James MO (2006) Polychlorobiphenylols are selective inhibitors of human phenol sulfotransferase 1A1 with 4-nitrophenol as a substrate. *Chem-Biol Interact* **159:**235-246.

Watkins JB and Klaassen CD (1982). Determination of hepatic uridine 5′-diphosphoglucuronic acid concentration by conjugation with diethylstilbestrol. *J Pharmacol Methods* **7:**145-151.

Wells PG, Mackenzie PI, Roy Chowdhury J, Guillemette C, Gregory PA, Ishii Y, Hansen AJ, Kessler FK, Kim PM, Roy Chowdhury N, and Ritter JK (2004) Glucuronidation and the UDP-glucuronosyltransferases in health and disease. *Drug Metab Dispos* **32:**281-290.

Xiong Y, Bernardi D, Bratton S, Ward MD, Battaglia E, Finel M, Drake RR, Radominska-Pandya A (2006) Phenylalanine 90 and 93 are localized within the phenol binding site of human UDP-glucuronosyltransferase 1A10 as determined by photoaffinity labeling, mass spectrometry, and site-directed mutagenesis. *Biochemistry* **45:**2322-2332.

Yin H, Bennett G, and Jones JP (1994) Mechanistic studies of uridine diphosphate glucuronosyltransferase. *Chem-Biol Interact* **90:**47.

Yamamura N, Imura-Miyoshi K, and Naganuma H (2000) Panipenum, a carbapenem antibiotic, increases the level of hepatic UDP-glucuronic acid in rats. *Drug Metab Dispos* **28:**1484-1486.

Yoshimura H, Ida S, Oguri K, and Tsukamoto H (1973) Biochemical basis for analgesic activity of morphine-6-glucuronide. I. Penetration of morphine-6-glucuronide in the brain of rats. *Biochem Pharmacol* **22:**1423-30.

Yoshimura T, Tanaka S, and Horie T (1992) Species difference and tissue distribution of uridine diphosphateglucuronosyltransferase activities towards E6080, 1-naphthol and 4-hydroxybiphenyl. *J Pharmacobiodyn* **15:**387-393.

Zhang H, Varlamova O, Vargas FM, Falany CN, Leyh TS, and Varmalova O (1998) Sulfuryl transfer: the catalytic mechanism of human estrogen sulfotransferase, *J Biol Chem* **273:**10888-10892.

Zhivkov V, Tosheva R and Zhivkova Y (1975) Concentration of uridine diphosphate sugars in various tissues of vertebrates. *Comp Biochem Physiol* **51:**421-424.

BIOGRAPHICAL SKETCH

James Sacco was born on October 30th, 1971, in the small island nation of Malta in the middle of the Mediterranean Sea. He graduated as a pharmacist from the University of Malta in 1992 and obtained a M.Phil. in pharmaceutical science from the same institution in 1998. While in Malta he was a volunteer in several environmental groups acting as youth secretary, public relations officer and newsletter editor for Nature Trust (Malta). From 2001 to 2006 he enrolled in the Ph.D. program at the Department of Medicinal Chemistry at the University of Florida where he conducted research on the enzymological, analytical, and molecular biological aspects of the biotransformation of xenobiotics by organisms such as polar bears and channel catfish. During this period he presented his work at several international conferences and has published several papers on the topic. He was a three-time finalist in the College of Pharmacy Annual Research Showcase, and the recipient of an International Student Award in 2006. He currently resides in Madison, Wisconsin, with his two cats.